University of Pavia

Department of Earth and Environmental Sciences

Primary Agroindustry: energy from PMFCs (Plant Microbial Fuel Cells) to power sensors

Ilaria Brugellis

Supervisor:
Silvia Assini
University of Pavia

Co-supervisor:
Cinzia Calvio
University of Pavia

XXXVIII PhD Series - Academic year 2025/2026

This work is part of the project NODES which has received funding from the MUR – M4C2 1.5 of PNRR funded by the European Union - NextGenerationEU (Grant agreement no. ECS00000036). The funding source was not involved in study design, in the collection, analysis and interpretation of data, as well as in the decision to submit the articles for publication.

“If everything on earth were governed by reason, nothing would ever come to pass. Without you there would be no events; and yet events must happen. So here I am, unwillingly occupied with bringing them about, performing irrational acts under order.”

- Fëdor Michajlovič Dostoevskij, *The Brothers Karamazov*

Table of Contents

Summary

This doctoral research investigates Plant Microbial Fuel Cells (PMFCs) as an emerging bioelectrochemical technology for sustainable electricity production, with a particular focus on the role of plant functional traits, system configuration, and biological and material factors influencing electrical performance. PMFCs exploit the natural interactions between plant roots and electrochemically active microorganisms in the rhizosphere, enabling the conversion of organic compounds derived from rhizodeposition into bioelectricity.

The research was conducted within the framework of the NODES project and developed over three years through an integrated experimental approach combining literature review, indoor laboratory experimentation, and outdoor field trials. The first part of the study provides a comprehensive botanical analysis of plant species used in PMFCs, addressing nomenclatural issues and evaluating the influence of plant life forms and root system architectures on bioelectrical performance. This analysis highlights the importance of accurate species identification and plant trait selection for reproducibility and technological optimization.

Subsequent experimental work focused on the development and testing of innovative PMFC configurations under controlled indoor conditions. A novel prototype was designed in which the plant compartment was physically separated from the microbial fuel cell, allowing nutrient transfer via plant-derived leachate while improving system maintenance and experimental control. The effects of carbon pellet stratification, membrane presence, and biological additives such as urea and *Trichoderma* spp. were evaluated. Results demonstrated that carbon pellet layering significantly affects electrical performance, with simpler configurations often yielding higher and more stable outputs. Biological treatments influenced system behavior, highlighting the need for optimized concentrations and further investigation into microbial–plant interactions.

Finally, outdoor PMFC experiments assessed the influence of plant functional traits under realistic environmental conditions. Native plant species characterized by different life forms and root architectures were compared, revealing that plant selection plays a critical role in determining electrical performance and system stability. Overall, this research contributes to the understanding of PMFC functioning by integrating botanical, ecological, and engineering perspectives, as support for the development of sustainable, nature-based bioelectrochemical energy systems.

Introduction

The intensive exploitation of conventional non-renewable energy sources to meet the rapidly increasing global energy demand has significantly contributed to the current energy and environmental crisis. Fossil fuel depletion, together with their well-documented impacts on climate change, greenhouse gas emissions, and air pollution, highlights the urgent need to identify alternative, environmentally friendly energy solutions [1,2]. The transition toward clean energy sources (such as solar, wind, bioenergy, and bioelectricity) is essential not only to reduce carbon footprints but also to enhance energy security and economic resilience [3].

In recent decades, growing electricity consumption has intensified interest in renewable, reliable, and environmentally friendly energy technologies. Achieving a sustainable energy transition requires innovative approaches that integrate economic development with environmental responsibility [4]. Among renewable energy sources, bioenergy already represents a major share of global renewable consumption, and its role is expected to increase substantially to meet international climate targets, including the 1.5 °C scenario outlined by the International Renewable Energy Agency [5]. However, this transition cannot rely solely on conventional biomass use and requires the development of integrated, decentralized, and resource-efficient technologies.

In this context, Microbial Fuel Cells (MFCs) have emerged as a promising bioelectrochemical technology capable of converting chemical energy stored in organic matter into electricity through the metabolic activity of electrochemically active microorganisms. Beyond energy generation, MFCs offer additional benefits, including organic matter degradation, wastewater treatment, contaminant removal, and potential applications in bioremediation and biosensing. These multifunctional characteristics make MFCs attractive candidates for low-impact and decentralized energy systems.

Operation and features of MFCs

MFCs can be constructed using a wide range of materials and stratification designs, resulting in diverse configurations. Functionally, they are comparable to electrochemical batteries and can be engineered so that proton transport occurs either vertically or horizontally, depending on cell architecture.

MFCs generate bioelectricity through redox reactions mediated by electrogenic bacteria. They typically consist of two main compartments: an anode chamber containing the anode electrode and anolyte, and a cathode chamber containing the cathode electrode and catholyte. The two compartments are separated by an ion exchange membrane that facilitates proton transfer while maintaining electrochemical separation [6].

Under anaerobic conditions in the anode chamber, specific microorganisms act as biological catalysts, oxidizing organic compounds and producing electrons and protons [7]. The electrons are transferred to the anode and flow through an external circuit toward the cathode, generating an electric current, while protons migrate through the membrane to the cathode compartment [8].

In the cathode compartment, oxygen acts as the terminal electron acceptor, completing the electrochemical circuit by reacting with electrons and protons to form water. It is essential that the anode chamber remains strictly anaerobic, as the presence of oxygen would interfere with microbial metabolism and inhibit effective electricity generation [9]. The electrical potential difference established between the anode and cathode compartments drives electron flow through the external circuit, enabling the production of usable electrical current.

The term *organic substrate* refers to the mixture of organic compounds contained in the material used as fuel. Although substrate composition varies depending on the type of organic waste employed, its oxidation consistently results in the release of electrons and protons that fuel the bioelectrochemical process.

When glucose is used as the substrate, the reactions occurring within the two compartments can be described as follows. Anodic and cathodic reactions are represented respectively in **Equations (1.1)** and **(1.2)**, while **Equation (1.3)** summarizes the overall process occurring in MFCs [10].

Anode:

$C_6H_{12}O_6 + 6H_2O \rightarrow 6CO_2 + 24H^+ + 24e^-$ - **Equation (1.1)**

Cathode:

$24H^+ + 24e^- + 6O_2 \rightarrow 12H_2O$ - **Equation (1.2)**

Overall reaction:

$C_6H_{12}O_6 + 6O_2 \rightarrow 6CO_2 + 6H_2O$ + Electrical energy - **Equation (1.3)**

Thanks to their ability to simultaneously generate electricity and promote the degradation of organic contaminants, MFCs represent a promising technological approach for wastewater treatment, offering both environmental and energy-related benefits. However, the performance of these systems is influenced by multiple interacting factors, including cell design, electrode materials and active surface area, microbial community composition, and the type of substrate employed. In addition, operational parameters such as pH and solution conductivity play a critical role, together with electron transfer efficiency, membrane proton exchange effectiveness, oxygen availability, and the continuous supply of water [11].

Plant Microbial Fuel Cells

Plant Microbial Fuel Cells (PMFCs) represent an evolution of conventional MFCs and are currently receiving increasing scientific attention as an innovative energy-harvesting biotechnology [12]. PMFCs integrate living plants into the bioelectrochemical system, allowing continuous substrate supply through rhizodeposition processes. Organic compounds released by plant roots—such as exudates, mucilage, and sloughed-off root cells—serve as electron donors for electrochemically active bacteria inhabiting the rhizosphere. This integration overcomes one of the main limitations of traditional MFCs, namely the progressive depletion of organic substrates and the resulting decline in electrical output over time [3].

PMFCs exploit the natural coupling between plant photosynthesis, root exudation, and microbial metabolism to sustain electricity generation. During photosynthesis, plants convert carbon dioxide and water into glucose, part of which is later released into the soil as rhizodeposits. These compounds are metabolized by electrochemically active bacteria under anaerobic conditions at the anode, leading to electron release and current generation. The rhizosphere thus represents a highly active bioelectrochemical interface, where microbial activity can be an order of magnitude higher than in bulk soil [13,14].

Factors affecting PMFCs performance

The performance of PMFCs is governed by a complex interaction between natural and engineered factors. Among natural factors, plant species play a pivotal role, as differences in photosynthetic activity and rhizodeposition rate, directly influence substrate availability for electrochemically active microorganisms [15].

Microbial community composition and diversity in the rhizosphere further affect electron transfer mechanisms and redox efficiency at the anode [16].

Microbial diversity within PMFCs varies substantially depending on plant species, substrate characteristics, and environmental conditions. Because these factors strongly influence which microbial populations develop, it is challenging to control the exact microbial community or the specific electron-transfer pathways active in the system. Different plant species release distinct profiles of root exudates into the rhizosphere, while substrates differ in nutrient content and pH. Overall, the composition and diversity of microorganisms in the rhizosphere are primarily determined by plant species and subspecies, root–soil interactions, substrate properties, and the specific PMFC configuration [3].

Environmental conditions, including soil moisture, temperature, pH, nutrient availability, and irrigation regimes, strongly regulate both plant physiology and microbial metabolism [17], thereby impacting electrical output and system stability. In parallel, engineered factors such as electrode materials and surface area, cell configuration, presence or absence of membranes, use of additives, and overall system design critically influence internal resistance, proton transport, and overall power generation efficiency.

Despite their conceptual appeal, PMFCs remain at an early stage of technological development. Their performance is influenced by numerous interacting factors, including plant species, microbial community composition, environmental conditions, electrode materials and design, system configuration, and the availability of nutrients and water. Challenges related to low power output, scalability, long-term durability, and economic feasibility still limit large-scale implementation [3].

Application of PMFC

PMFCs offer a wide range of potential applications due to their ability to generate electricity in a continuous and environmentally responsible manner. Their most promising use lies in powering low-energy devices, such as remote environmental sensors and distributed monitoring systems, particularly in off-grid or hard-to-access areas [18,19,20]. PMFCs are also being explored as biosensing platforms, where electrical signals can be correlated with environmental or biological changes [21,22]. Additionally, PMFC technology shows strong potential in wastewater treatment and bioremediation [23], as microbial metabolism can simultaneously support electricity generation and the degradation of organic or inorganic contaminants. This multifunctionality positions PMFCs as a promising nature-based solution capable of integrating renewable energy production with sustainable waste management and environmental remediation strategies.

These applications are particularly relevant in the context of decentralized energy systems and align with the United Nations Sustainable Development Goals, especially SDG 7 (Affordable and Clean Energy) and SDG 11 (Sustainable Cities and Communities).

Scope and Objectives of the Research

Within the framework of the NODES project, this doctoral research aimed to investigate PMFC performance through the development and testing of innovative system configurations under both indoor and outdoor conditions. A novel PMFC prototype was designed in which the plant compartment is physically separated from the microbial fuel cell, allowing controlled nutrient transfer via drainage water while facilitating system maintenance and experimental manipulation.

The research activities were carried out over a three-year period and focused on:

1. A comprehensive literature review on PMFC technology, plant functional traits, and nomenclatural constraints (**Chapter 1**);
2. Evaluation of PMFCs electrical performance under different system configurations: carbon pellets layering and urea treatment (**Chapter 2**);
3. Evaluation of PMFCs electrical performance under different system configurations: membrane presence, and *Trichoderma* treatment (**Chapter 3**);
4. Assessment of PMFC performance in outdoor environments using plant species with distinct functional traits (**Chapter 4**).

A description of the novel PMFC prototype developed, general MFCs assembly and several functional PMFCs comfiguration supplying devices (LED light strips and environmental monitoring sensors) is provided in **Appendix A**.

Overall, this research objectives were to contribute to a better understanding of the biological, ecological, and engineering factors that govern PMFCs efficiency, with the aim of supporting the development of renewable bioelectrochemical energy systems.

References

[1] S. Maddalwar, K.K. Nayak, M. Kumar, L. Singh, Plant microbial fuel cell: opportunities, challenges, and prospects, *Bioresour. Technol.* 341 (2021) 125772, https://doi.org/10.1016/j.biortech.2021.125772

[2] S. Mohyudin, R. Farooq, F. Jubeen, T. Rasheed, M. Fatima, F. Sher, Microbial fuel cells a state-of-the-art technology for wastewater treatment and bioelectricity generation, *Environ. Res. 204* (2022) 112387, https://doi.org/10.1016/j.envres.2021.112387.

[3] P. L. Chong, J. H. Chuah, C. O. Chow, P. K. Ng, Plant microbial fuel cells: A comprehensive review of influential factors, innovative configurations, diverse applications, persistent challenges, and promising prospects, *International Journal of Green Energy*, 22(3) (2025) 599-648.

[4] R. Chakma, M. K. Hossain, P. Paramasivam, R. Bousbih, M. Amami, G. I. Toki, R. Haldhar, A. K. Karmaker, Recent Applications, Challenges, and Future Prospects of Microbial Fuel Cells: A Review, *Global Challenges* (2025) 2500004.

[5] IRENA (2024). World Energy Transitions Outlook 2024: 1.5°C Pathway, International Renewable Energy Agency, Abu Dhabi.

[6] S. Shah, V. Venkatramanan, R. Prasad, Microbial Fuel Cell: Sustainable Green Technology for Bioelectricity Generation and Wastewater Treatment, in S. Shah, V. Venkatramanan, R. Prasad, *Sustainable Green Technologies for Environmental Management* (2019) 199–218. Springer Singapore. https://doi.org/10.1007/978-981-13-2772-8_10.

[7] G. Antonopoulou, K. Stamatelatou, S. Bebelis, G. Lyberatos, Electricity generation from synthetic substrates and cheese whey using a two chamber microbial fuel cell, *Biochemical Engineering Journal* 50 (2010) 10–15 https://doi.org/10.1016/j.bej.2010.02.008.

[8] M. Rahimnejad, G. Najafpour, A. A. Ghoreyshi, M. Rahimnejad, G. Najafpour, A. A. Ghoreyshi, Effect of Mass Transfer on Performance of Microbial Fuel Cell, in Mass Transfer in Chemical Engineering Processes, *Intech* 5 (2011): 233-250, https://doi.org/10.5772/19675.

[9] Y. Sharma, B. Li, The variation of power generation with organic substrates in single-chamber microbial fuel cells (SCMFCs), *Bioresource Technology* 101(6) (2010) 1844–1850, https://doi.org/10.1016/j.biortech.2009.10.040.

[10] R. Di Lorenzo, M. Grassi, S. Assini, M. Granata, M. Barcella, P. Malcovati, Electrical Energy Harvesting from Pot Plants, In B. Andò, F. Baldini, C. Di Natale, V. Ferrari, V. Marletta, G. Marrazza, V. Militello, G. Miolo, M. Rossi, L. Scalise, P. Siciliano, *Sensors* (2019) 545–550, Springer International Publishing, https://doi.org/10.1007/978-3-030-04324-7_65.

[11] B. E., Logan, J. M. Regan, Microbial Fuel Cells—Challenges and Applications, *Environ. Science & Technology* 40(17) (2006) 5172–5180. https://doi.org/10.1021/es0627592.

[12] P.N. Prasad, S. Kalla, Plant-microbial fuel cells - a bibliometric analysis, *Process Biochem* 111 (2021) 250–260, https://doi.org/10.1016/j.procbio.2021.10.001.

[13] M. Rahimnejad, A. Adhami, S. Darvari, A. Zirepour, S. E Oh, Microbial fuel cell as new technology for bioelectricity generation: A review, *Alexandria Engineering Journal* 54(3) (2015) 745-756.

[14] D.P.B.T.B. Strik, H.V.M. Hamelers Bert, J.F.H. Snel, C.J.N. Buisman, Green electricity production with living plants and bacteria in a fuel cell, Int. J. *Energy Res.* 32 (2008) 870–876, https://doi.org/10.1002/er.1397.

[15] W. Apollon, A. I. Luna-Maldonado, S. K. Kamaraj, J. A. Vidales-Contreras, H. Rodríguez-Fuentes, J. F. Gómez-Leyva, J. Aranda-Ruíz, Progress and recent trends in photosynthetic assisted microbial fuel cells: a review, *Biomass and Bioenergy* 148 (2021) 106028.

[16] R.A. Timmers, M. Rothballer, D.P.B.T.B. Strik, M. Engel, S. Schulz, M. Schloter, A. Hartmann, B. Hamelers, C. Buisman, Microbial community structure elucidates performance of Glyceria maxima plant microbial fuel cell, *Appl. Microbiol. Biotechnol.* 94 (2012) 537–548. https://link.springer.com/article/10. 1007/s00253-012-3894-6.

[17] M. El Gamal, H. A. Mousa, M. H. El-Naas, R. Zacharia, S. Judd, Bio-regeneration of activated carbon: A comprehensive review, *Separation and Purification Technology* 197 (2018) 345–359, https://doi.org/10.1016/j.seppur.2018.01.015.

[18] P. L. Chong, A. K. Singh, F. Y. Kong, Renewable energy from living plants to power IoT sensor for remote sensing, *ADBU Journal of Engineering Technology* 11 (1) (2022) https://journals.dbuniversity.ac.in/ojs/ index.php/AJET/article/view/3613.

[19] C. P. Silvia Ganesan, L. Chen, N. Kong, N. Ng, M. Reyasudin, IoT-enabled smart weather stations: Innovations, challenges, and future directions, *Malaysian Journal of Science and Advanced Technology (*2024) 180–90, doi:10.56532/mjsat.v4i2.293.

[20] S. Singh, Environmental energy harvesting techniques to power standalone IoT-equipped sensor and its application in 5G communication, *Emerging Science Journal* 4 (2021) 116–26, doi:10.28991/esj-2021-SP1-08.

[21] D. Brunelli, P. Tosato, M. Rossi, Flora health wireless monitoring with plant-microbial fuel cell, *Procedia Engineering* 168 (2016) 1646–50, doi:10.1016/j.proeng.2016.11.481.

[22] D. Brunelli, P. Tosato, M. Rossi, Microbial fuel cell as a biosensor and a power source for flora health monitoring, *IEEE Sensors* (2016), doi:10.1109/icsens.2016.7808831.

[23] F.T. Kabutey, Q. Zhao, L. Wei, J. Ding, P. Antwi, F.K. Quashie, W. Wang, An overview of plant microbial fuel cells (PMFCs): configurations and applications, *Renew. Sustain. Energy Rev.* 110 (2019) 402–414, https://doi.org/10.1016/j.rser.2019.05.016.

Chapter 1

Plant Microbial Fuel Cells in a botanical perspective: Nomenclatural constraints and new insights on plant traits potentially affecting bioelectrical performance

Ilaria Brugellis, Marco Grassi, Piero Malcovati, Silvia Assini

Abstract

Plant microbial fuel cells represent an innovative type of microbial fuel cell technology, utilizing plant rhizodeposition to fuel electrochemically active bacteria on the anode surface, thereby generating bioelectricity. This study delves into some botanical aspects of plant species employed in PMFCs and Constructed Wetland PMFCs, aiming to investigate whether their bioelectrical performance is influenced by Raunkiær life forms and root architecture. Our study involved 40 plant species described in 38 documents. In some cases, nomenclature issues prevented the interpretation of actual species used in the experiments. The bioelectrical performance of PMFCs appeared to be significantly affected by both life forms and root architecture. Therophytes and Hemicriptophytes exhibited higher median values than the other life forms, while the Geophyte group showed very high power density values despite a lower median value. In contrast, CWPMFCs do not appeared to be significantly affected by the botanical traits considered, likely due to the limited data collected on this experimental configuration. The plant species that performed the best in PMFCs include *Carex hirta*, *Alisma plantago-aquatica*, *Glyceria maxima* and *Canna indica*, all of which have an adventitious root system. *C. hirta*, *G. maxima* and *C. indica* are geophytes, while *A. plantago-aquatica* is a hydrophyte. Consequently, epiphytes, chamaephytes and nanophanerophytes, as well as plants with fibrous root systems, appeared to be not recommended for PMFCs. Nevertheless, the results of our study may have certain limitation due to nomenclature issues that prevented the accurate identification of species used in the PMFCs, the absence of a standardized benchmark for electrical measurement, and the lack of clear match between each species and its bioelectrical performance, reducing the data pool.

Keywords

Plant microbial fuel cells (PMFCs), Life forms, Root system, Bioelectricity, Plant nomenclature

Heliyon 10 (2024) e38733 - https://doi.org/10.1016/j.heliyon.2024.e38733

Introduction

Conventional non-renewable sources of energy have been extensively exploited to meet energy demands [1], significantly contributing to the current energy crisis. The diminishing availability of fossil fuels, along with their impact on climate and the environment, underscores the urgent need to seek alternative energy sources [2]. Plant microbial fuel cells (hereafter PMFCs) represent a promising biotechnology in the context of energy harvesting and are currently under study in many countries [3]. PMFCs are a derivative technology of microbial fuel cells (MFCs) and consist of a plant and two electrodes: one anode coupled to a cathode, with or without a membrane in between, as schematically represented in **Figure 1.1**.

They utilize plant rhizodeposition (organic compounds released from plant roots into the soil) as nourishment for the electrochemically active bacteria (EAB) growing on the anode surface, thereby enabling the generation of bioelectricity [4]. While plants absorb energy from the environment (e.g., light and CO^2) and convert it into nutrients, a portion of these nutrients is released into the soil, and serves as sustenance for the bacteria. EAB, through anaerobic degradation (an oxidative process) occurring on the surface of the anode, release electrical charges into the soil in the form of ions and electrons. These electrons are then transferred to the cathode, generating electricity. This technology can potentially provide unlimited energy since it is completely self-sufficient. However, many challenges must be addressed before it can be applied on a large-scale [5], such as the stability and power of electrical performance, the standardization of working conditions [5], the quantity of rhizodeposition and the selection of plant species [1].

Selecting the appropriate plant species can enhance bioelectrical performance. Ideal criteria for plant selection may include plant hardiness, growth rate, the microbial community at the rhizosphere, the extensiveness of the root system, adaptability, etc. [4,6]. For example, plant species with C4 photosynthetic pathways are generally preferred in PMFCs because they exhibit high rates of solar energy conversion and high photosynthetic efficiency, leading to increased rhizodeposition that serves as a substrate for microbial oxidation [4]. Initially, PMFCs were restricted to aquatic plants and indoor plants; the first proposed and tested PMFCs were developed by planting the graminoid *Glyceria maxima* Hartm. et Holmb. at the anode of a sediment microbial fuel cell [7]. However, over the last 15 years, this technology has gradually extended to terrestrial plants [3]. Recent reviews have primarily focused on technological and electrochemical issues [1,6], variability in configuration and applications [4,5,8,9,10], microbiological aspects [1,8,10] and a bibliometric analysis [3]. Botanical aspects were also considered, mainly focusing on photosynthetic pathways, the rhizosphere and soil type [1,5,6,8], with plant species selection primarily based on availability rather than an in-depth knowledge of their physiology [9]. One of the most overlooked aspects concerns the names reported in papers on PMFCs, which are often incorrect, making it difficult to trace the actual species tested.

In this study, we examined the nomenclature and characteristics (plant traits) of various plant species used in PMFCs, which have been little, or not at all, investigated in previous reviews. Specifically, we analyzed life forms and root types as plant traits.

Life forms, according to the Raunkiær system [11], categorize plants based on the location of their growth point during adverse season, which gives them the ability to survive hostile conditions. Depending on the region, the unfavorable period can be the cold winter or the dry summer. In Europe, the growth point during the unfavorable season usually corresponds to winter buds. Raunkiær life forms include: Epiphytes (which grow attached to other living plants), Phanerophytes (with the growth point in the unfavorable season at least 50 cm above ground level, often on stems), Nanophanerophytes (with the growth point in the unfavorable season from about 25 to 50 cm above ground level) Chamaephytes (with the growth point in the unfavorable seasons up to about 25 cm above ground level), Hemicryptophytes (with the growth point in unfavorable season at or just below the ground level), Therophytes (which survive adverse season as seeds), Cryptophytes or Geophytes (with the growth point in the unfavorable season below ground level), Helophytes (with the growth point - winter buds - below water, and flowering parts above water) and Hydrophytes (water plants). Life forms express the plant's life cycle and their biomass persistence over one or more years: Therophytes are annual species that persist for only few months each year; Hemicryptophytes are herbaceous perennial species that persist for several years, generally with vegetative parts throughout the year; Geophytes/Helophytes/Hydrophytes are herbaceous perennial species that persist for several years, generally with vegetative parts during only part of the year; Chamaephytes are perennial herbaceous/lignified species; Nanophanerophytes and Phanerophytes are woody perennial species, both persisting for several years and with green biomass during all or part of the year (depending on whether they are evergreen or not). These differences in biomass growth and persistence can influence bioelectrical performance in PMFCs experiments.

Root types reflect the extensiveness and complexity of the root system (around which microbial community develops) and, therefore, can contribute to the bioelectrical performance of plants.

With this work, we want to focus on the botanical issues crucial for ensuring a well-functioning system, which also serves as a mirror to the functionality of the technology. Specifically, we sought to answer the following questions: 1) How many and what recognizable species have been used in PMFCs? 2) Could life forms affect PMFCs electrical performance? 3) Could root system types affect PMFCs electrical performance? If the answer to questions 2 and 3 are affirmative, this work could help identify useful characteristics that make certain species eligible or recommended for PMFC technological applications.

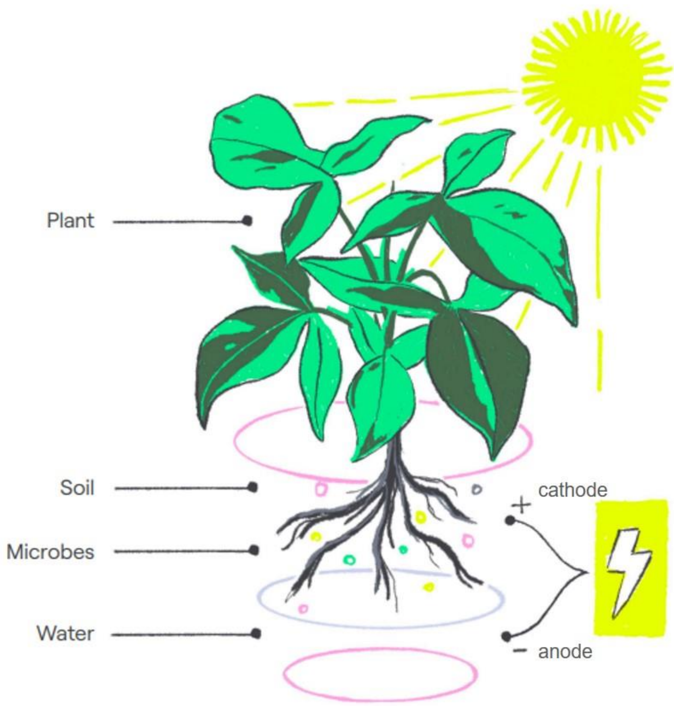

Figure 1.1. A schematic representation of a PMFC (Plant Microbial Fuel Cell).

Materials and methods

Paper collection

The Scopus database was queried on April 18, 2024, using the search term “plant microbial fuel cell”. The publication years were restricted to the decade 2012–2022, and the document type was limited to “Review” [search string: 〈TITLE-ABS-KEY ("plant microbial fuel cell") AND PUBYEAR >2011 AND PUBYEAR <2023 AND (LIMIT-TO (DOCTYPE, "re"))〉]. This search yielded a list of 13 documents. Since our focus was on the botanical aspect, we excluded reviews based on engineering, microbiochemical, and waste removal approaches. Relevant reviews were selected [1,3,4,6,8,10] to find original articles describing PMFC experiments, from which we selected papers containing pertinent information on plant species and bioelectrical performance. A list of 51 papers containing relevant information on plant species and bioelectrogenesis was compiled. Only documents written in English were considered. The present work focused on vascular species (Tracheophyta), excluding ferns and mosses (Pteridophyta and Bryophyta). We considered plant species used in Constructed Wetlands PMFCs (CW-PMFCs), and PMFCs, where plants serve as the fuel to power electrical performance.

Plant nomenclature

The names of all plants cited in the selected papers were verified on Plants of the World Online [12] and, when necessary, cross-referenced with the Flora of a Country within the native distribution range of the species considered [13,14,15,16,17].

Bioelectrical data collection

Due to the heterogeneity of the data concerning electrical performance, certain species were excluded from further analysis under the following conditions: a) multiple species were tested, but the electrical performance of each individual plant could not be clearly extrapolated; b) the study focused on other aspects, and the electrical performance was not calculated or published; c) only voltage or current values were provided; d) average power values and peak power value were too close; e) power density values were <0.001 or >950 mW/m^2. When multiple measurements were provided for a single species, the highest value was used for further data analysis.

Raunkiær life form

Most Raunkiær life form were verified on Plants of the World Online [12] or in the Flora of a country within the native distribution range of the species considered [13,14,15,16,17].

Root type

Root architecture types were grouped into the following three categories, representative of the structural complexity of the hypogeal apparatus: 1) Taproot (including tuberous and bulbous systems); 2) Adventitious (including stoloniferous and rhizomatous systems); 3) Fibrous (including fasciculate and branched systems). The assignment of categories was based on the "root type architecture" trait verified by a detailed study on TRY (Plant Trait Database) [18], when available for the species, and cross-referenced with the Flora of a country within the native distribution range of the species, or expert based.

Data analysis

For the life forms, Epiphytes, Chamaephytes and Nanophanerophytes, were grouped together as perennial non-herbaceous plants. For each life form, we considered the distribution of power density values of the plants included in that life form, and we compared the life forms to find significant differences in terms of power density. Similarly, for each root architecture type, we considered the distribution of power density values of plants within that type, and compared the root types to find significant difference in terms of power density. Analyses were performed separately for plants used in PMFCs and those used in CW-PMFCs experimental configurations. All analyses (Normality test, Mann-Whitney test for equal medians for two samples, Kruskal-Wallis test for equal medians for several samples and Dunn's post-hoc test with raw values) were performed using the software Past 4.09 [19].

Results and discussion

Data collection and nomenclature of plants

The literature analysis produced a list of 97 entities belonging to 37 Families [**Table 1**]. Some uncertain entities reported in the reviews, but not found in the cited original papers, were excluded *a priori* or replaced. *Anisogramma anomala*, an ascomycete plant pathogen reported in Deng et al. review [8], was replaced with *Arundinella anomala*, as used in the cited reference [20]. *Lythrum salicaria*, reported in Rusyn's review [10], without a cited reference, was excluded. *Schismus arabicus*, also reported in Rusyn's review [10], was replaced with "Sporobolusarabicus", as used in the cited reference [21].

The following 4 entities identified only at the genus level were excluded: *Carex* sp. [39], *Mentha* sp. [47], *Myriophyllum* sp. [37], *Sansevieria* sp [31].

The nomenclature of species was correct in most remaining cases. However, some nomenclatural issues led to the exclusion of certain species and ad hoc assumptions. The first case included species reported with their Latin name but without the author, making it impossible to identify the exact species used for PMFCs: *Lemna minuta* [25], which could be *Lemna minuta* Kunth or *Lemna valdiviana* Phil.; *Scirpus Validus* [43], which could be *Schoenoplectus tabernaemontani* (C.C.Gmel.) Palla, or *Eleocharis geniculata* (L.) Roem. & Schult., or *Schoenoplectus californicus* (C.A.Mey.) Soják; *Festuca arundinaceae* [52], which could be *Lolium arundinaceum* (Schreb.) Darbysh., or *Scolochloa festucacea* (Willd.) Link, or *Festuca rubra* L. Due to this uncertainty, these species were excluded from further analysis.

A second case involved cultivated species or varieties, not always clearly indicated: *Hyacinth* "pink" [30], for which we assumed the valid name *Hyacinthus orientalis* L.; *Canna indica* L. "Stuttgart" [32], for which we assumed the valid name *Canna indica* L.; *Papyrus diffuses* [28], for which we assumed the valid name *Cyperus diffusus* Vahl; *Oryza sativa* spp. *japonica* L. [59], for which we assumed the valid name *Oryza sativa* L.

A third case included reunited species: *Sedum reflexum* and *S. rupestre* were considered different species in the original paper [38], but the updated nomenclature considers them as a unique species, *Petrosedum rupestre* (L.) P.V.Heath (for further analysis, we considered the bioelectrical output *Sedum rupestre*); *Opuntia ficus-indica* and *O. joconostle* were considered different species in the original paper [33], but the updated nomenclature considers them as a single species, *Opuntia ficus-indica* (L.) Mill.

Updated species names, Family, native ranges of the species and geographical areas of experiments are summarized in **Table 1.1**.

Table 1.1. First list of 97 species: Family, updated name, name in the original paper, native range of species, and geographical area of the study.

Family	Updated Species name	Species name in the original paper	Species native range	Geographical area of study	Reference
Alismataceae	*Alisma plantago-aquatica* L.	*Alisma plantago-aquatica*	Temp. Eurasia, N. Africa to Tanzania	Ukraine	[22]
Amaryllidaceae	*Agapanthus africanus* (L.) Hoffmanns.	*Agapanthus africanus L. Hoffman*	SW. Cape Prov	Mexico	[23]
	Clivia miniata (Lindl.) Verschaff.	*Vallota miniata* Lindl.	S. Africa	Ukraine	[24]
	Clivia nobilis Lindl.	*Clivia nobilis* Lindl.	E. Cape Prov	Ukraine	[24]
Araceae	*Dieffenbachia seguine* (Jacq.) Schott	*Dieffenbachia seguine* (Jacq.) Schott	Somalia to S. Africa, W. Indian Ocean	Ukraine	[24]
	Epipremnum aureum (Linden & André) G.S.Bunting	*Epipremnum aureum*	Society Islands (Moorea)	India	
	-	*Lemna minuta*	-	Bulgaria	[25]
	Pistia stratiotes L.	*Pistia stratiotes*	Tropics & Subtropics	Philippines	[26]
	Spathiphyllum lanceifolium (Jacq.) Schott	*Spathiphyllum lanceifolium* (Jacq.) Schott	Colombia to Venezuela	Ukraine	[24]
Araliaceae	*Hedera helix* L.	*Hedera helix* L.	Europe to W. & N. Türkiye	Ukraine	[24]
	Hydrocotyle verticillata Thunb.	*Hydrocotyle verticillata*	New World, Somalia to S. Africa, Madagascar, Caucasus to N. Iran	Japan	[27]
Arecaceae	*Chamaedorea elegans* Mart.	*Chamaedorea elegans* Mart.	Mexico to Honduras	Ukraine	[24]
Asparagaceae	*Chlorophytum comosum* (Thunb.) Jacques	*Chlorophytum comosum*	W. Tropical Africa to Cameroon, Ethiopia to S. Africa	Algerie	[28]
	Dracaena braunii Engl.	*Dracaena braunii*	W. Central Tropical Africa (Cameroon, Congo, Equatorial Guinea, Gabon)	India	[29]

Family	Updated Species name	Species name in the original paper	Species native range	Geographical area of study	Reference
	Hyacinthus orientalis L.	*Hyacinth pink*	CULTIVAR	Ireland	[30]
	-	*Sansevieria* asparagaceae	-	Mexico	[31]
Asteraceae	*Artemisia fukudo* Makino	*Artemisia fukudo*	China (E. Zhejiang), Korea, Japan (Honshu, Kyushu), N. Taiwan	Japan	[27]
Betulaceae	*Alnus glutinosa* (L.) Gaertn.	*Alnus glutinosa* (L.) Gaerth.	Europe to W. Siberia and Iran	Ukraine	[24]
	Betula pendula Roth.	*Betula pendula* Roth.	Temp. Eurasia, NW. Africa, Alaska to Canada	Ukraine	[24]
	Betula pubescens Ehrh.	*Betula pubescens*	Newfoundland to Greenland, Europe to Russian Far East and N. Iran	Ukraine	[24]
	Carpinus betulus L.	*Carpinus betulus* L.	Europe to Iran	Ukraine	[24]
Brassicacee	*Brassica juncea* (L.) Czern.	*Brassica juncea*	Caucasus	India	[32]
Cactaceae	*Opuntia albicarpa* Scheinvar	*Opuntia albicarpa*	Mexico	Mexico	[33]
	Opuntia ficus-indica (L.) Mill.	*Opuntia ficus-indica* *Opuntia joconostle*	Mexico	Mexico	[33] [33]
	Opuntia robusta H.L. Wendl. ex Pfeiff.	*Opuntia robusta*	Mexico	Mexico	[33]
Cannaceae	*Canna indica* L.	*Canna indica*	Tropical & Subtropical America	USA / China	[34]
		Canna stuttgart	CULTIVAR	India	[32]
Commelinaceae	*Wachendorfia thyrsiflora* L.	*Wachendorfia thyrsiflora*	Cape Prov	South Africa	[35]
Convolvulaceae	*Ipomoea aquatica* Forssk.	*Ipomoea aquatica* Forssk.		China	[36]

Family	Updated Species name	Species name in the original paper	Species native range	Geographical area of study	Reference
			Tropical & Subtropical Old World (Africa, Asia, Oceania)	Philippines	[26]
Crassulaceae	*Crassula ovata* (Mill.) Druce	*Crassula ovata* (Miller) Druce (1917)	SE. Mozambique to SE. Cape Prov	Ukraine	[24]
	Kalanchoe pinnata (Lam.) Pers.	*Bryophyllum pinnatum*	Madagascar	India	[37]
	Petrosedum rupestre (L.) P.V.Heath	*Sedum rupestre* *Sedum reflexum*	Europe to Türkiye	Chile	[38]
	Phedimus hybridus (L.) 't Hart	*Sedum hybridum*	E. European Russia to Siberia and Mongolia	Chile	[38]
	Phedimus kamtschaticus (Fisch.) 't Hart	*Sedum kamtschaticum* Fisch. & Mey.	Russian Far East to N. China and N. Japan	Chile	[38]
	Phedimus spurius (M.Bieb.) 't Hart	*Sedum spurium* M. Bieb.	NE. Türkiye to N. Iran	Chile	[38]
	Sedum album L.	*Sedum album*	Europe to Medit. and NW. Iran	Chile	[38]
	Sedum sexangulare L.	*Sedum sexangulare*	Europe	Chile	[38]
Cyperaceae	-	*Carex sp.*	-	Italy	[39]
	Carex divisa Huds.	*Carex divisa* HUDSON	Europe to W. China	Turkey	[40]
	Carex hirta L.	*Carex hirta*	Europe to Iran, N. Africa	Ukraine	[41]
	Cyperus alternifolius subsp. *flabelliformis* Kük.	*Cyperus involucratus* Rottb.	Tropical Africa, KwaZulu-Natal, Madagascar, Arabian Peninsula	Thailand	[42]
	Cyperus diffusus Vahl	*Papyrus diffusus*	CULTIVAR	Algerie	[28]

Family	Updated Species name	Species name in the original paper	Species native range	Geographical area of study	Reference
	Cyperus prolifer Lam.	*Cyperus prolifer*	Somalia to S. Africa, W. Indian Ocean	South Africa	[35]
	Rhynchospora colorata (L.) H.Pfeiff.	*Rhynchospora colorata*	SE. U.S.A. to N. South America	Japan	[27]
	-	*Scirpus validus* Benth.	-	China	[43]
Fabaceae	*Trigonella foenum-graecum* L.	*Trigonella foenum-graecum*	Iraq to N. Pakistan	India	[32]
	Vigna radiata (L.) R.Wilczek	*Vigna radiata* Wilzeck	Arabian Peninsula, Taiwan to Tropical Asia and N. & E. Australia	Philippines	[44]
Fagaceae	*Fagus sylvatica* L.	*Fagus sylvatica* L.	Europe to Caucasus	Ukraine	[24]
	Quercus robur L.	*Quercus robur* L.	Europe to Iran	Ukraine	[24]
Grossulariaceae	*Ribes nigrum* L.	*Ribes nigrum* L.	Europe to Russian Far East and Central Asia	Ukraine	[24]
	Ribes rubrum L.	*Ribes rubrum* L.	W. Europe	Ukraine	[24]
	Ribes uva-crispa L.	*Ribes uva-crispa* L.	Europe, NW. Africa, NE. Türkiye to N. Iran	Ukraine	[24]
Haloragaceae	-	*Myriophyllum* sp.	-	India	[37]
Hydrocharitaceae	*Elodea nuttallii* (Planch.) H.St.John	*Elodea nuttalii*	S. Canada to U.S.A	Malaysia	[45]
	Hydrilla verticillata (L.f.) Royle	*Hydrilla verticillata*	Poland to Asia, Australia, Uganda to N. Zambia	India China	[37] [46]
Iridaceae	*Chasmanthe floribunda* (Salisb.) N.E.Br.	*Chasmanthe floribunda*	W. & SW. Cape Prov	Algerie	[28]
	Iris pseudacorus L.	*Iris pseudacorus*	Europe to Caucasus, Medit. to Iran	Ireland	[30]

Family	**Updated Species name**	**Species name in the original paper**	**Species native range**	**Geographical area of study**	**Reference**
Juglandaceae	*Juglans regia* L.	*Juglans regia* L.	NE. & E. Türkiye to Lebanon and W. Himalaya	Ukraine	[24]
Juncaceae	*Juncus effusus* L.	*Juncus effuses*	Temp. Northern Hemisphere to W. South America, Rwanda to S. Africa, W. Indian Ocean	China	[43]
	Juncus gerardi Loisel. subsp. *gerardi*	*Juncus gerardii* Loisel. subsp. gerardii	Europe, Medit. to Mongolia, Canada to N. U.S.A.	Turkey	[40]
Lamiaceae	*Clinopodium nepeta* (L.) Kuntze	*Calamintha nepeta* L.	Central Europe, Medit., N. Iran	Italy	[39]
	Lycopus europaeus L.	*Lycopus europaeus* L.	Azores, Europe to China	Italy	[39]
	-	*Mentha sp.* L.	-	Italy	[47]
	Mentha acquatica L.	*Mentha acquatica* L.	Africa, Europe to Central Siberia and W. Asia	Italy	[39]
Lythraceae	*Rotala rotundifolia* (Buch.-Ham. ex Roxb.) Koehne	*Rotala rotundifolia*	India to Temp. E. Asia	Taiwan	[48]
Marsileaceae	*Marsilea quadrifolia* L.	*Marsilea quadrifolia* L.	Canary Islands, Europe to Japan and Iran	Italy	[39]
Onagraceae	*Epilobium parviflorum* Schreb.	*Epilobium parviflorum* Schreb.	Temp. Eurasia	Italy	[39]
Pandanaceae	*Pandanus amaryllifolius* Roxb. ex Lindl.	*Pandanus amaryllifolius*	Maluku	Malaysia	[49]
Pinaceae	*Pinus sylvestris* L.	*Pinus silvestris* L.	Europe to Russian Far East and Caucasus	Ukraine	[24]
Poaceae	*Arundinella hirta* (Thunb.) Tanaka	*Arundinella anomala*	S. Siberia, Temp. E. Asia and N. Indo-China	Netherlands	[20]
	Arundo donax L.	*Arundo donax* L.	W. & Central Asia, Temp. E. Asia	Netherlands	[20]

Family	Updated Species name	Species name in the original paper	Species native range	Geographical area of study	Reference
	Cenchrus alopecuroides (L.) Thunb.	*Pennisetum alopecuroides*	China to Temp. E. Asia and W. & Central Malesia, NW. & E. Australia	Taiwan	[48]
	Cenchrus setaceus (Forssk.) Morrone	*Pennisetum setaceum*	N. Africa to Afghanistan and Tanzania	India	[50]
	Chrysopogon nemoralis (Balansa) Holttum	*Vetiveria nemoralis* A.	Indo-China to Philippines (Panay)	Thailand	[51]
	Chrysopogon zizanioides (L.) Roberty	*Vetiveria zizaniodes* Nash	Indo-China to Malesia	Ukraine	[51]
	Cynodon dactylon (L.) Pers.	*Cynodondactylon*	Temp. & Subtropical Old World to Australia	Pakistan	[21]
	-	*Festuca arundinacea*	-	Ukraine	[52]
	*Glyceria maxima (*Hartm.) Holmb.	*Glyceria maxima*	Europe to Xinjiang	Netherlands	[7]
				Netherlands	[53]
				Netherlands	[54]
				Netherlands	[55]
	Lolium perenne L.	*Lolium perenne*	Macaronesia, N. Africa, Europe to Siberia and Himalaya	China	[56]
	Oryza sativa L.	*Oryza sativa* L.	China	Japan	[57]
				Australia	[58]
				Italy	[39]
		Oryza sativa spp. *Japonica* cultivar Koshihirari	CULTIVAR	Japan	[59]
	Phragmites australis (Cav.) Trin. Ex Steud.	*Phragmites australis*		Japan	[27]

Family	Updated Species name	Species name in the original paper	Species native range	Geographical area of study	Reference
			Temp. & Subtropical to Tropical Mountains	South Africa	[35]
				Netherlands	[60]
				Netherlands	[61]
				Ireland	[30]
	Puccinellia distans (Jacq.) Parl.	*Puccinellia distans* (Jacq.) Parl.	Subarctic to Temp. Eurasia	Canada	[62]
	Sporobolus anglicus (C.E.Hubb.) P.M.Peterson & Saarela	*Spartina anglica*	NE. Türkiye to N. Iran	Netherlands	[20]
				Netherlands	[63]
				Netherlands	[64]
				Netherlands	[60]
				Netherlands	[65]
				Netherlands	[61]
	Sporobolus ioclados (Nees ex Trin.) Nees	*Sporobolasarabicus*	Africa to Indian Subcontinent	Pakistan	[21]
Pontederiaceae	*Pontederia crassipes* Mart.	*Eichhornia crassipes*	S. Tropical America	Philippines	[66]
Ranunculaceae	*Caltha palustris* L.	*Caltha palustris* L.	Temp. & Subarctic Northern Hemisphere	Ukraine	[67]
Rosaceae	*Malus domestica* (Suckow) Borkh.	*Malus domestica* Borkh.	Afghanistan to Central Asia and Xinjiang	Ukraine	[24]
	Prunus cerasus L.	*Prunus cerasus* L.	Caucasus	Ukraine	[24]
	Prunus domestica L.	*Prunus domestica* L.	Transcaucasus to N. Iran	Ukraine	[24]
	Pyrus communis L.	*Pyrus communis* L.	Europe to N. Iraq	Ukraine	[24]
	Rubus idaeus L.	*Rubus idaeus* L.	Temp. Northern Hemisphere to Mexico	Ukraine	[24]

Family	Updated Species name	Species name in the original paper	Species native range	Geographical area of study	Reference
Solanaceae	*Solanum lycopersicum* L.	*Solanum lycopersicum*	Peru	India	[37]
Typhaceae	*Typha angustifolia* L.	*Typha angustifolia*	Temp. Northern Hemisphere	Taiwan Turkey	[48] [40]
	Typha domingensis Pers.	*Typha domingensis* Pers.	Tropics & Subtropics	Mexico	[68]
	Typha latifolia L.	*Typha latifolia* L.	Temp. Northern Hemisphere to Colombia, W. Bolivia to S. South America, Nigeria to Kenya	Malaysia Turkey	[69] [40]
	Typha orientalis C.Presl	*Typha orientalis*	Mongolia to Japan and Philippines, Australasia	China	[43]
Viburnaceae	*Viburnum opulus* L.	*Viburnum opulus* L.	Europe to Siberia and Türkiye, N. Algeria	Ukraine	[24]
Vitaceae	*Vitis vinifera* L.	*Vitis vinifera* L.	S. Central & SE. Europe to Central Asia and N. Iran	Ukraine	[24]

Data collection about bioelectrical performance

The following 23 species of phanerophytes and lignified shrubs were excluded, as studies on these groups are at their early stages, and limited literature is available [24,33,49]. Moreover, many of them are reported without direct correspondence between the electrical performance and individual species [24]. These included: *Alnus glutinosa*, *Betula pendula*, *Betula pubescens*, *Carpinus betulus*, *Fagus sylvatica*, *Hedera helix*, *Juglans regia*, *Malus domestica* [24], *Opuntia albicarpa*, *Opuntia ficus-indica*, *Opuntia robusta* [33], *Pandanus amaryllifolius* [49], *Pinus sylvestris*, *Prunus cerasus*, *Prunus domestica*, *Pyrus communis*, *Quercus robur*, *Ribes nigrum*, *Ribes rubrum*, *Ribes uva-crispa*, *Rubus idaeus*, *Viburnum opulus*, and *Vitis vinifera* [24].

Another 27 species were excluded according to the criteria previously listed in "Materials and methods" and described as follows.

The absence of electrical performance clearly related to each single species caused the exclusion of: *Chamaedorea elegans* [24], *Clinopodium nepeta* = *Calamintha nepeta* [39], *Clivia miniata* = *Vallota miniata* [24], *Clivia nobilis* [24], *Crassula ovata* [24], *Dieffenbachia seguine* [24], *Epilobium parviflorum* [39], *Kalanchoe pinnata* = *Bryophyllum pinnatum* [37], *Lolium perenne* [56], *Lycopus europaeus* [39], *Marsilea quadrifolia* [39], *Mentha acquatica* [39], *Solanum lycopersicum* [37], *Spathiphyllum lanceifolium* [24].

The lack of calculated or published electrical performance caused the exclusion of *Cenchrus setaceus* = *Pennisetum setaceum* [50] and *Chrysopogon nemoralis* = *Vetiveria nemoralis* [51].

The provision of only voltage values or current values caused the exclusion of: *Artemisia fukudo* [27] *Arundo donax* [20], *Cyperus alternifolius* subsp. *flabelliformis* = *Cyperus involucratus* [42], *Hydrilla verticillata* [46] also reported in Chiranjeevi et al. [37], but without clearly related electrical perfomance, *Hydrocotyle verticillata* [27], *Juncus effusus* [43], *Puccinellia distans* [62].

The similarity between average power values and peak power values caused the exclusion of *Arundinella hirta* = *Arundinella anomala* [20].

Power density values <0.001 or >950 mW/m^2 led to the exclusion of the following species: *Phedimus kamtschaticus* = *Sedum kamtschaticum* [38], *Phedimus spurius* = *Sedum spurium* [38], *Rotala rotundifolia* [48].

The most reasonable value to consider would be the volumetric power density expressed as mW/m^3. However, since the produced energy does not increase indefinitely with volume for a given plant/soil system, the area can be considered the real parameter characterizing the interface between plant and soil. Moreover, most of the data reported in the considered literature were expressed as mW/m^2, so we used this unit for our elaboration.

When multiple measurements were provided for a single species, we considered the highest value for further data analysis. *Canna indica* was used by Lu et al. [34] in CW-PMFCs and Sophia and Sreeja [32] in PMFCs experiments, the latter obtaining the highest bioelectrical output. *Glyceria maxima* was used in several PMFCs experiments [7,53,54,55], with Timmers et al. [54] obtaining the highest bioelectrical output. *Ipomoea aquatica* was used by Liu et al. [36] in CW-PMFCs and by Pamintuan et al. [26] in PMFCs experiments, with the former achieving the highest bioelectrical output. *Oryza sativa* was used in several PMFC experiments [39,59,57,58], with Goto et al. [59] obtaining the highest bioelectrical output. *Phragmites australis* was used in several PMFC [27,60,61] and CW-PMFC [30,35] experiments, with Oodally et al. [35] obtaining the highest bioelectrical output. *Sporobolus anglicus =Spartina anglica* was used in several PMFC experiments [20,60,61,63,64,65], with Wetser et al. [65], obtaining the highest bioelectrical output. *Typha angustifolia* was used by Guan and Yu [48] in PMFCs and by Saz et al. [40] in CW-PMFC experiments, with the latter obtaining the highest bioelectrical output. *Typha latifolia* was used by Oon et al. [69] and Saz et al. [40] in CW-PMFC experiments, with the latter obtaining the highest bioelectrical output.

Finally, we were able to provide a power density value (mW/m^2) for 40 species, comprising 28 species used in PMFCs and 12 species used in CW-PMFCs.

Their scientific name, experimental configuration, electrical output, life form and root type are summarized in **Table S.1** (*Author's Note: "Supplementary material" in the paper*).

Table S.1 List of 40 species used for elaboration in this work: updated name, experimental configuration in the original paper, bioelectrical output, life form (Ch=Chamaephyte, Ep=Epiphyte, G=Geophyte, H=Hemicryptophyte, He=Helophyte, Hy=Hydrophyte, NP=Nanophanerophyte, T= Therophytes) and root type.

Note: "Electrical performance" column does not have a single unit of measurement as it collects the output data, collected differently in each work.

Updated Species name	Reference number	Experimental configuration	Electrical Performance	Maximum Power density mW/m²	Life Form	Root Type
Agapanthus africanus (L.) Hoffmanns.	[63]	PMFC	Maximum voltage generation 690 mV - Average voltage generation 420 mV - Highest power density 15,55 mW/m² - Highest current generation 6,24 mA	15,55	G	Adventitious
Alisma plantago-aquatica L.	[66]	PMFC	Maximum power density 702 mW/m²	702	Hy	Adventitious
Brassica juncea (L.) Czern.	[30]	PMFC	power density 69,32 mW/m²	69,32	T	Taproot
Caltha palustris L.	[62]	PMFC	Maximum power density 0.18 W/m² - Maximum current density 1.2 A/m²	0,18	H	Adventitious
Canna indica L.	[45]	Constructed Wetlands MFC	Maximum current density 105 mA/m² - Maximum power density 18 mW/m²	*higher value available*	G	Adventitious
	[30]	PMFC	Power density 222,54 mW/m²	222,54		
Carex divisa Huds.	[59]	Constructed Wetlands MFC	Mean power density 4.19 ± 4.49 mW/m² - Maximum power density 8,8 mW/m² - Max current density 29,5 mA/m² - Mean current density 22.9 ± 7.72 mA/m²	8,8	G	Adventitious
Carex hirta L.	[64]	PMFC	Maximum average weekly current 21.36 mA - Highest power density 950 mW/m²	950	G	Adventitious

Updated Species name	**Reference number**	**Experimental configuration**	**Electrical Performance**	**Maximum Power density mW/m²**	**Life Form**	**Root Type**
Cenchrus alopecuroides (L.) Thunb.	[44]	PMFC	Maximum power density 2.86 ± 1.03 - Monthly average power density 1.07 ± 0.66 mW/m^2	2,86	H	Fibrous
Chasmanthe floribunda (Salisb.) N.E.Br.	[31]	PMFC	Highest power density 0,21 mW/m^2	0,21	G	Taproot
Chlorophytum comosum (Thunb.) Jacques	[31]	PMFC	Highest power density 18 mW/m^2	18	G	Taproot
Chrysopogon zizanioides (L.) Roberty	[39]	PMFC	Maximum power density 68 mW/m^2	68	He	Fibrous
Cynodon dactylon (L.) Pers.	[21]	PMFC	Maximum power density 58 mW/m^2	58	G	Adventitious
Cyperus diffusus Vahl	[31]	PMFC	Highest power density 1,083 mW/m2	1,083	G	Adventitious
Cyperus prolifer Lam.	[55]	Constructed Wetlands MFC	Maximum power density 229 ± 52 mW/m^3 - Maximum CCV 510 mV - Average CCV 240 mV	229	G	Adventitious
Dracaena braunii Engl.	[68]	PMFC	max power density 12,78 mW/m^2	12,78	NP	Adventitious
Elodea nuttallii (Planch.) H.St.John	[69]	Constructed Wetlands MFC	Maximum voltage output 545.77 ± 25 mV - Power density 184.75 ± 7.50 mW/m^3	184,75	Hy	Adventitious
Epipremnum aureum (Linden & André) G.S.Bunting	[68]	PMFC	Max power density 15,38 mW/m^2	15,38	Ep	Adventitious
*Glyceria maxima (*Hartm.) Holmb.	[7]	PMFC	Maximum power production 67 mW/m^2	*higher value available*	G	Adventitious
	[46]	PMFC	Maximum power density 32 mW/m^2	*higher value available*		
	[47]	PMFC	Maximum power output 390 mW/m^2	390		

Updated Species name	Reference number	Experimental configuration	Electrical Performance	Maximum Power density mW/m²	Life Form	Root Type
	[48]	PMFC	Average power output 36,2 mW/m²	*higher value available*		
Hyacinthus orientalis L.	[29]	Constructed Wetlands MFC	Total maximum power density 8,74 mW/m² - Maximum power density 4,86 mW/m² - Maximum current density 71,20 mA/m²	4,86	G	Taproot
Ipomoea aquatica Forssk.	[49]	Constructed Wetlands MFC	Max power density 12,42 ,W/m²	12,42	He	Adventitious
	[50]	PMFC	Max power density 6,35 mW/m²	*higher value available*		
Iris pseudacorus L.	[29]	Constructed Wetlands MFC	Total maximum power density 25,14 mW/m² Maximum power density 13,27 mW/m² - Maximum current density 80,49 mA/m²	13,27	G	Adventitious
Juncus gerardi Loisel. subsp. *gerardi*	[59]	Constructed Wetlands MFC	Mean power density 1.91 ± 2.71 mW/m² - Maximum power density 8,1 mW/m² - Max current density 21,6 mA/m² - Mean current density 11.4 ± 8.6 mA/m²	8,1	G	Adventitious
Oryza sativa L.	[32]	PMFC	Maximum power density 49 mW/m²	49	T	Fibrous
	[51]	PMFC	Highest voltage value 700 mV - Maximum power density 23 mW/m²	*higher value available*		
	[52]	PMFC	Mean power outoput 9,9 ± 6,0 mW/m²	*higher value available*		
Petrosedum rupestre (L.) P.V.Heath	[33]	PMFC	Maximum power density 0,0155 mW/m²	0,0155	Ch	Fibrous
Phedimus hybridus (L.) 't Hart	[33]	PMFC	Maximum power density 0,092 mW/m²	0,092	Ch	Fibrous

Updated Species name	Reference number	Experimental configuration	Electrical Performance	Maximum Power density mW/m²	Life Form	Root Type
Phragmites australis (Cav.) Trin. Ex Steud.	[40]	PMFC	Maximum cell voltage 520 mV - Maximum power production 40 mW	*higher value available*	G	Adventitious
	[55]	Constructed Wetlands MFC	Maximum power density 109 ± 29 mW/m³ - Maximum CCV 400 mV - Average CCV 170	109		
	[54]	PMFC	Maximum average power generation 21mW/m² -	*higher value available*		
	[53]	PMFC	Average current density 14 mA/m² - Average cell voltage 93 mV - Maximum average powe density 3,1 mW/m²	*higher value available*		
	[29]	Constructed Wetlands MFC	Total maximum power density 21,7 mW/m² - Maximum power density 11,87 mW/m² - Maximum current density 86,68 mA/m²	*higher value available*		
Pistia stratiotes L.		PMFC	Max power density 3,54 mW/m²	3,54	He	Fibrous
Pontederia crassipes Mart.		PMFC	Maximum power density 0,86 mW/m²	0,86	Hy	Fibrous
Rhynchospora colorata (L.) H.Pfeiff.	[40]	PMFC	Peak voltage 200 mV - Maximum power production 20 mW/m²	20	G	Adventitious
Sedum album L.		PMFC	Maximum power density 0,0024 mW/m²	0,0024	Ch	Fibrous
Sedum sexangulare L.	[33]	PMFC	Maximum power density 0,0084 mW/m²	0,0084	Ch	Fibrous
Sporobolus anglicus (C.E.Hubb.) P.M.Peterson & Saarela	[20]	PMFC	Maximum power density 222 mW/m² - Average powe output 10 mW/m²	*higher value available*	H	Adventitious
	[56]	PMFC	Maximum current production 469 mA/m²	*incomplete/inconsistent data*		

Updated Species name	Reference number	Experimental configuration	Electrical Performance	Maximum Power density mW/m²	Life Form	Root Type
	[57]	PMFC	Maximum power density 88 mW/m²	*higher value available*		
	[53]	PMFC	Average current density 83 mA/m² - Average cell voltage 214 mV - Maximum average powe density 34 mW/m²	*higher value available*		
	[58]	PMFC	Maximum power output 679 mW/m² - Average power density 240 mW/m²	679		
	[54]	PMFC	Maximum daily average current density 541 mA/m² - Maximum daily average power generation 22 mW/m²	*higher value available*		
Sporobolus ioclados (Nees ex Trin.) Nees	[21]	PMFC	Maximum power density 120 mW/m²	120	H	Adventitious
Trigonella foenum-graecum L.	[30]	PMFC	power density 80,26 mw/m²	80,26	T	Taproot
Typha angustifolia L.	[44]	PMFC	Monthly average power density 0.21 ± 0.13 - Maximum power density 0.44 ± 0.19	*higher value available*	G	Adventitious
	[59]	Constructed Wetlands MFC	maximum average output voltage 1.01 ± 0.14 V - Mean power density 7.47 ± 13.7 mW/m² - Maximum power density 18,1 mW/m² - Max current density 33,8 mA/m² - Mean current density 25.2 ± 20.01 mA/m²	18,1		
Typha domingensis Pers.	[65]	PMFC	Electrical current production 47,9 ± 10,98 mA/m2 - Power density 6.12±2.53 mW/m²	6,12	G	Adventitious
Typha latifolia L.	[60]	Constructed Wetlands MFC	Maximum power density 6,12 mW/m²	*higher value available*	G	Adventitious

Updated Species name	Reference number	Experimental configuration	Electrical Performance	Maximum Power density mW/m²	Life Form	Root Type
	[59]	Constructed Wetlands MFC	Mean power density 4.12 ± 9.06 mW/m² - Maximum power density 13,4 mW/m² - Max current density 31,4 mA/m² - Mean current density 17.1 ± 16.2 mA/m²	13,4		
Typha orientalis C.Presl	[27]	Constructed Wetlands MFC	Average bioelectricity generation 0.235 ± 0.028 V - Maximum power density 21.53 mW/m² - Highest current density 50,96 mA/m²	21,53	He	Adventitious
Vigna radiata (L.) R.Wilczek	[61]	PMFC	Maximum power density 0,35 mW/m²	0,35	T	Fibrous
Wachendorfia thyrsiflora L.	[55]	Constructed Wetlands MFC	Maximum power density 106 ± 21 mW/m³ - Maximum CCV 310 mV - Average CCV 170 mV	106	G	Taproot

Raunkiær life forms in PMFCs

We compared the distribution of power density values among plant species used in PMFCs, according to their life forms. Therophytes (T) included *Brassica juncea* [32], *Oryza sativa* [59], *Trigonella foenum-graecum* [32], and *Vigna radiata* [44].

Hemicriptophytes (H) included *Caltha palustris* [67], *Cenchrus alopecuroides =Pennisetum alupecuroides* [48], *Sporobolus anglicus* [65], and *Sporobolus ioclados =Sporobolus arabicus* [21]. Geophytes (G) included *Agapanthus africanus* [23], *Canna indica* [32], *Carex hirta* [41], *Chasmanthe floribunda* [28], *Chlorophytum comosum* [28], *Cynodon dactylon* [21], *Cyperus diffusus* [28], *Glyceria maxima* [54], *Rhynchospora colorata* [27], and *Typha domingensis* [68]. Helophytes/Hydrophytes (He/Hy) included *Chrysopogon zizaniodes* = *Vetiveria zizaniodes* [51] and *Pistia stratiotes* [26] as helophytes; *Alisma plantago-acquatica* [22] and *Pontederia crassipes* = *Eichhornia crassipes* [66] as hydrophytes.

Epiphytes/Chamaephytes/Nanophanerophytes (Ep/Ch/NP) included *Epipremnum aureum* [29] as epiphyte; *Petrosedum rupestre*, *Phedimus hybridus* = *Sedum hybridum*, *Sedum album*, and *Sedum sexangulare* [38] as chamaephytes; *Dracaena braunii* [29] as Nanophanerophyte.

The distributions of power density values for each life form category were found to be non-normal, except for Therophytes. We therefore conducted the Kruskal-Wallis non-parametric test for equal medians and followed it with Dunn's Post-hoc test using raw values. The Kruskal-Wallis test indicated no significant differences among the groups [H (chi^2): 7.896; Hc (tie-corrected): 7.896; p (same): 0.09548]. However Dunn's Post-hoc test revealed significant differences between the Ep/Ch/NP and G groups (raw p value = 0.01006), and among Ep/Ch/NP and T groups (raw p value = 0,04133). Violin plots representing the distribution of power density values **[Figure 1.2a]** illustrate that Therophytes and Hemicriptophytes have comparable median values, which are higher than those of other life forms. Despite the low median value, the Geophyte group includes an outlier with a very high power density value (*Carex hirta* = 950 mW/m^2).

Raunkiær life forms in CW-PMFCs

We also compared the distribution of power density values among plant species used in CW-PMFCs according to their life forms. Geophytes (G) included *Carex divisa* Huds. [40], *Cyperus prolifer* Lam. [35], *Hyacinthus orientalis* L., *Iris pseudacorus* L. [30], *Juncus gerardi* Loisel. subsp. gerardi [40], *Phragmites australis* (Cav.) Trin. ex Steud. [35], *Typha angustifolia* L. [40], *Typha latifolia* L. [40], and *Wachendorfia thyrsiflora* L [35]. Helophytes/Hydrophytes (He/Hy) included *Ipomoea aquatica* Forssk [36]. and *Typha orientalis* C.Presl [43]as helophytes; *Elodea nuttalii* (Planch.) H.St.John [45] as hydrophyte.

The distribution of power density values of Geophytes was non-normal. Given that the samples were only two, we used the Mann-Whitney non-parametric test for equal medians, which returned no significant differences between the groups [*p (*same): 0.6]. Violin plots representing the distribution of power density values show that the medians of the two groups do not differ **[Figure 1.2b]**.

Plant species, categorized by life form for each experimental configuration (PMFCs an CW-PMFCs), and arranged in order of decreasing power density for each category, are summarized in **Table 1.2**.

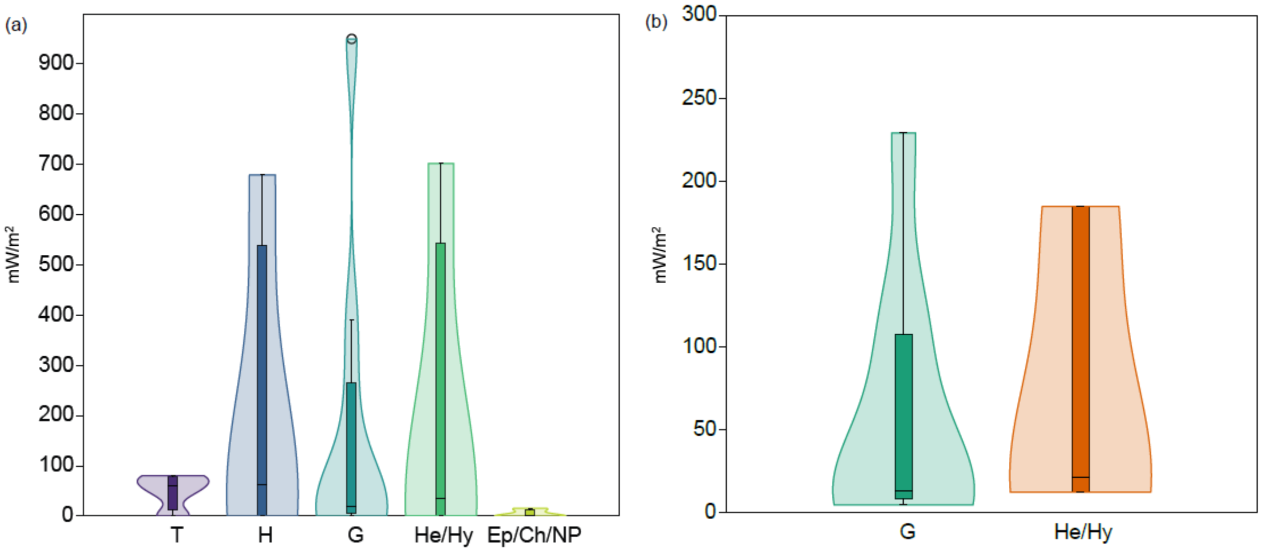

Figure 1.2. Violin plot representation of the power density distributions of life forms used in PMFCs (a) and CW-PMFCs (b). T = Therophytes; H = Hemycriptophytes, G = Geophytes, He/Hy = Helophytes/Hydrophytes, Ep/Ch/NP = Epiphytes/Chamaephytes/Nanophanerophytes.

Table 1.2. Plant species divided by Life form for each Experimental configuration (PMFCs an CW-PMFCs), arranged in order of decreasing power density for each category.

Experimental configuration	**Life Form**	**Updated Species name**	**Maximum Power density mW/m²**
PMFC	Geophytes	*Carex hirta* L.	950
		*Glyceria maxima (*Hartm.) Holmb.	390
		Canna indica L.	222,54
		Cynodon dactylon (L.) Pers.	58
		Rhynchospora colorata (L.) H.Pfeiff.	20
		Chlorophytum comosum (Thunb.) Jacques	18
		Agapanthus africanus (L.) Hoffmanns.	15,55
		Typha domingensis Pers.	6,12
		Cyperus diffusus Vahl	1,083
		Chasmanthe floribunda (Salisb.) N.E.Br.	0,21
	Hydrophytes	*Alisma plantago-aquatica* L.	702
		Pontederia crassipes Mart.	0,86
	Helophytes	*Chrysopogon zizanioides* (L.) Roberty	68
		Pistia stratiotes L.	3,54
	Hemycriptophytes	*Sporobolus anglicus* (C.E.Hubb.) P.M.Peterson & Saarela	679
		Sporobolus ioclados (Nees ex Trin.) Nees	120
		Cenchrus alopecuroides (L.) Thunb.	2,86
		Caltha palustris L.	0,18
	Terophytes	*Trigonella foenum-graecum* L.	80,26

Experimental configuration	Life Form	Updated Species name	Maximum Power density mW/m^2
		Brassica juncea (L.) Czern.	69,32
		Oryza sativa L.	49
		Vigna radiata (L.) R.Wilczek	0,35
	Epiphytes	*Epipremnum aureum* (Linden & André) G.S.Bunting	15,38
	Nano-Phanerophytes	*Dracaena braunii* Engl.	12,78
	Chamaephytes	*Phedimus hybridus* (L.) 't Hart	0,092
		Petrosedum rupestre (L.) P.V.Heath	0,0155
		Sedum sexangulare L.	0,0084
		Sedum album L.	0,0024
Constructed Wetlands MFC	Geophytes	*Cyperus prolifer* Lam.	229
		Phragmites australis (Cav.) Trin. Ex Steud.	109
		Wachendorfia thyrsiflora L.	106
		Typha angustifolia L.	18,1
		Typha latifolia L.	13,4
		Iris pseudacorus L.	13,27
		Carex divisa Huds.	8,8
		Juncus gerardi Loisel. subsp. *gerardi*	8,1
		Hyacinthus orientalis L.	4,86
	Hydrophytes	*Elodea nuttallii* (Planch.) H.St.John	184,75
	Helophytes	*Typha orientalis* C.Presl	21,53
		Ipomoea aquatica Forssk.	12,42

Root system type in PMFCs

We compared the distribution of power density values of plant species grouped by root system type used in PMFCs. Taproot group included *Chasmante floribunda*, *Cholorophytum comosum*, *Brassica juncea* and *Trigonella foenum-graecum*. Adventitous group included *Agapanthus africanus*, *Canna indica*, *Carex hirta*, *Cynodon dactylon*, *Cyperus diffusus*, *Glyceria maxima*, *Rhynchospora colorata*, *Typha domingensis*, *Caltha palustris*, *Sporobolus anglicus*, *Sporobolus ioclados*, *Alisma plantago-aquatica*, *Epipremnum aureum* and *Dracaena braunii*. Fibrous group included *Cenchrus alopecuroides*, *Oryza sativa*, *Vigna radiata*, *Chrysopogon zizanioides*, *Pistia stratiotes*, *Pontederia crassipes*, *Petrosedum rupestre*, *Phedimus hybridus*, *Sedum sexangulare*.

The distributions of power density values were non-normal, except for Taproot group. Therefore, we performed the Kruskal-Wallis non-parametric test for equal medians, followed by Dunn's Post-hoc test using raw values. Kruskal-Wallis test indicated a significant difference among groups [H (chi^2): 8.758; Hc (tie corrected): 8.758; *p* (same): 0.01254]. Dunn's Post-hoc test revealed significant differences between the Adventitious and Fibrous groups (raw *p* value = 0,003461). Violin plots representing the distributions of power density values **[Figure 1.3a]** show comparable median values for Taproot and Adventitious groups, with the Adventitious exhibiting the widest distribution, while the Taproot group presents more condensed values.

Root system type in CW-PMFCs

We compared the distribution of power density values of plant species grouped by root system type and used in CW-PMFCs. Taproot include *Hyacinthus orientalis* and *Wachendorfia thyrsiflora*. Adventitous included *Carex hirta*, *Cyperus prolifer*, *Iris pseudacorus*, *Juncus gerardi* subsp. *gerardi*, *Phragmites australis*, *Typha angustifolia*, *Typha latifolia*, *Ipomoea acquatica*, *Typha orientalis*, and *Elodea nuttalii*. The distribution of power density values for Adventitious plants was non-normal. Given that the samples are only two, we used Mann-Whitney non-parametric test for equal medians, which returned no significant differences between the groups [*p* (same): 0.59] Violin plots representing the distribution of power density values show a higher median value for Taproot than for Adventitious root system **[Figure 1.3b]**.

Plant species, categorized by root system type for each experimental configuration (PMFCs an CW-PMFCs), arranged in order of decreasing power density for each category, are summarized in **Table 1.3**.

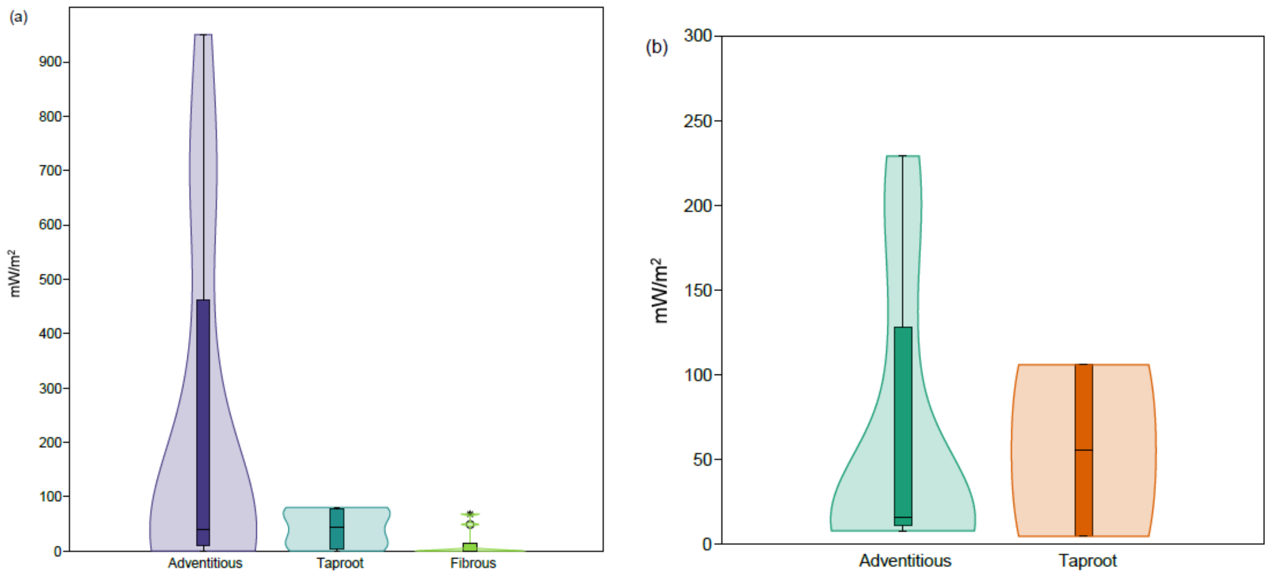

Figure 1.3. Violin plot representation of power density distributions of root types used in PMFCs (a) and CW-PMFCs (b).

Table 1.3. Plant species divided by Root type for each Experimental configuration (PMFC and CW-PMFC), arranged in order of decreasing power density for each category.

Experimental configuration	Root Type	Updated Species name	Maximum Power density mW/m²
PMFC	Adventitious	*Carex hirta* L.	950
		Alisma plantago-aquatica L.	702
		Sporobolus anglicus (C.E.Hubb.) P.M.Peterson & Saarela	679
		*Glyceria maxima (*Hartm.) Holmb.	390
		Canna indica L.	222,54
		Sporobolus ioclados (Nees ex Trin.) Nees	120
		Cynodon dactylon (L.) Pers.	58
		Rhynchospora colorata (L.) H.Pfeiff.	20
		Agapanthus africanus (L.) Hoffmanns.	15,55
		Epipremnum aureum (Linden & André) G.S.Bunting	15,38
		Dracaena braunii Engl.	12,78
		Typha domingensis Pers.	6,12
		Cyperus diffusus Vahl	1,083
		Caltha palustris L.	0,18
	Taproot	*Trigonella foenum-graecum* L.	80,26
		Brassica juncea (L.) Czern.	69,32
		Chlorophytum comosum (Thunb.) Jacques	18
		Chasmanthe floribunda (Salisb.) N.E.Br.	0,21
	Fibrous	*Chrysopogon zizanioides* (L.) Roberty	68

Experimental configuration	Root Type	Updated Species name	Maximum Power density mW/m²
		Oryza sativa L.	49
		Pistia stratiotes L.	3,54
		Cenchrus alopecuroides (L.) Thunb.	2,86
		Pontederia crassipes Mart.	0,86
		Vigna radiata (L.) R.Wilczek	0,35
		Phedimus hybridus (L.) 't Hart	0,092
		Petrosedum rupestre (L.) P.V.Heath	0,0155
		Sedum sexangulare L.	0,0084
		Sedum album L.	0,0024
Constructed Wetlands MFC	Adventitious	*Cyperus prolifer* Lam.	229
		Elodea nuttallii (Planch.) H.St.John	184,75
		Phragmites australis (Cav.) Trin. Ex Steud.	109
		Typha orientalis C.Presl	21,53
		Typha angustifolia L.	18,1
		Typha latifolia L.	13,4
		Iris pseudacorus L.	13,27
		Ipomoea aquatica Forssk.	12,42
		Carex divisa Huds.	8,8
		Juncus gerardi Loisel. subsp. *gerardi*	8,1
	Taproot	*Wachendorfia thyrsiflora* L.	106
		Hyacinthus orientalis L.	4,86

Conclusions

Our results allow us to address the questions posed in the introduction. The nomenclature analysis of taxa used in PMFCs resulted in a list of 90 identifiable species, including 23 Phanerophytes and lignified shrubs, and other 67 other vascular plants. However only 40 species were used for statistical analysis due to the limitations related to their electrical performance.

For 7 taxa reported in the literature, it was not possible to accurately identify the species and therefore the associated traits. Additionally, for 50 taxa, valid bioelectrical output values could not be obtained, reducing the dataset available for analysis by more than 63 %.

PMFCs performances appeared to be significantly influenced by both life forms and root architecture. Therophytes and Hemicriptophytes exhibited higher median values than other life forms, though the Geophyte group showed a very high power density value despite having a lower median. In contrast, CW-PMFCs do not seemed to be significantly affected by the botanical traits considered, likely due to the limited data collected for this type of experimental configuration.

The best performing plant species in PMFCs were found to include *Carex hirta*, *Alisma plantago-aquatica*, *Glyceria maxima* and *Canna indica*, all of which have adventitious (stoloniferous/rhizomatous) root type. *G. maxima* and *C. indica* are geophytes, while *A. plantago-aquatica* is a hydrophyte.

Consequently, epiphytes, chamaephytes and nanophanerophyte, and plants with fibrous, fasciculated or branched root types appeared to be less suitable for PMFCs, as they exhibited lower median values and are significantly different from other groups by each criterion. While Therophytes, as annual species, are not the most practical for technological applications in experimental context, Hemicryptophytes and Geophytes seemed to be recommended for PMFCs.

However, this study faced several constraints that reduced the dataset, and may have affected our results and final considerations. Nomenclature issues hindered the identification of the correct species used in PMFCs, making it difficult to replicate experiments, an essential requirement in scientific research. Additionally, the absence of a common benchmark for reporting electrical performance and the lack of unambiguous matches with each species, led to further reduction of the data pool.

Therefore, we strongly recommend to accurately indicating the scientific name (including the author of the name) of plants to ensure replicability of experimental designs, and defining a standard measure for reporting electrical performance.

The choice of species for use in PMFCs should be based not only on the traits considered in this study but also on the implications for biodiversity, especially when PMFC are used outdoors. Biodiversity is a crucial component of sustainability. If PMFCs produce clean energy but use invasive alien species in outdoor applications, their sustainability is compromised.

Our literature review identified several species of concern in this regard. For example, *Arundo donax, Ipomea aquatica, Cenchrus setaceus, Pistia stratiotes* and *Sporobolus anglicus* are considered invasive alien species in many countries outside their natural distribution range, where they negatively affect natural habitats.

Cenchrus setaceus, native to North Africa and the Middle East, is one of the most invasive species in Tenerife and other areas (e.g. California, Hawaii, South Africa), where it rapidly spreads along roads from urbanized to natural areas [70].

Pistia stratiotes, native to South America (Bolivia, Brazil, Paraguay), is considered invasive in Asia, Papua New Guinea, Canary Island, where its dense growth can impact native plant communities and aquatic organisms (macro- and micro-invertebrates, fishes) and reduce water flow in drainage and irrigation systems. This species can transform and alter trophic dynamics, resulting in long-term changes [71].

Ipomea aquatica, native to Southeast Asia, has been naturalized in Africa, Australia, the Pacific Islands, and North and South America. It is considered invasive in parts of its introduced range and is listed as a noxious weed in Florida and Texas in the U.S., where it spreads in human-made aquatic environments such as canals and ditches, as well as in natural lakes and along riverbanks [72].

Arundo donax and *Sporobolus anglicus* are among the 100 World's Worst Invasive Alien Species [73], posing a serious threat to biodiversity.

Given these considerations, we strongly recommend using native plants for PMFCs in outdoor applications. If non-native species must be considered, a risk assessment of their invasion potential, such as the method proposed by Weber and Gut [74], should be conducted.

In conclusion, the species used to construct PMFCs represent only one of the many variables that can influence their performance. However, the choice of species should consider not only their electrical performance but also their implications for biodiversity to enhance the sustainability of PMFCs.

References

[1] S. Maddalwar, K.K. Nayak, M. Kumar, L. Singh, Plant microbial fuel cell: opportunities, challenges, and prospects, *Bioresour. Technol.* 341 (2021) 125772, https://doi.org/10.1016/j.biortech.2021.125772.

[2] S. Mohyudin, R. Farooq, F. Jubeen, T. Rasheed, M. Fatima, F. Sher, Microbial fuel cells a state-of-the-art technology for wastewater treatment and bioelectricity generation, *Environ. Res.* 204 (2022) 112387, https://doi.org/10.1016/j.envres.2021.112387.

[3] P.N. Prasad, S. Kalla, Plant-microbial fuel cells - a bibliometric analysis, *Process Biochem* 111 (2021) 250–260, https://doi.org/10.1016/j.procbio.2021.10.001.

[4] F.T. Kabutey, Q. Zhao, L. Wei, J. Ding, P. Antwi, F.K. Quashie, W. Wang, An overview of plant microbial fuel cells (PMFCs): configurations and applications, *Renew. Sustain. Energy Rev.* 110 (2019) 402–414, https://doi.org/10.1016/j.rser.2019.05.016.

[5] R. Shaikh, A. Rizvi, M. Quraishi, S. Pandit, A.S. Mathuriya, P.K. Gupta, J. Singh, R. Prasad, Bioelectricity production using plant-microbial fuel cell: present state of art, *S. Afr. J. Bot*. 140 (2021) 393–408, https://doi.org/10.1016/j.sajb.2020.09.025.

[6] R. Nitisoravut, R. Regmi, Plant microbial fuel cells: a promising biosystems engineering, *Renew. Sustain. Energy Rev.* 76 (2017) 81–89, https://doi.org/ 10.1016/j.rser.2017.03.064.

[7] D.P.B.T.B. Strik, H.V.M. Hamelers Bert, J.F.H. Snel, C.J.N. Buisman, Green electricity production with living plants and bacteria in a fuel cell, *Int. J. Energy Res.* 32 (2008) 870–876, https://doi.org/10.1002/er.1397.

[8] H. Deng, Z. Chen, F. Zhao, Energy from plants and microorganisms: progress in plant-microbial fuel cells, *ChemSusChem* 5 (6) (2012) 1006–1011, https://doi.org/10.1002/cssc.201100257.

[9] R. Regmi, R. Nitisoravut, J. Ketchaimongkol, A decade of plant-assisted microbial fuel cells: looking back and moving forward, *Biofuels* 9 (2018) 605–612, https://doi.org/10.1080/17597269.2018.1432272.

[10] I.B. Rusyn, Role of microbial community and plant species in performance of plant microbial fuel cells, *Renew. Sustain. Energy Rev.* 152 (2021) 111697, https://doi.org/10.1016/j.rser.2021.111697.

[11] C. Raunkiær, The Life Forms of Plants and Statistical Plant Geography, Clarendon Press, Oxford, 1934.

[12] POWO – Plants of the World Online, Facilitated by the, Royal Botanic Gardens, Kew, 2023. http://www.plantsoftheworldonline.org/. (Accessed 28 March 2024).

[13] IPFI – index plantarum florae italicae. http://www.actaplantarum.org/, 2011. (Accessed 28 March 2024).

[14] M. Chytrý, J. Danihelka, Z. Kaplan, J. Wild, D. Holubová, P. Novotný, M. ˇRezníčková, M. Rohn P. Dřevojan, V. Grulich, J. Klimešová, J. Lepš, Z. Lososová, J. Pergl, J. Sádlo, P. Šmarda, P. Štěpánková, L. Tichý, I. Axmanová, A. Bartušková, P. Blazek, J. Jr. Chrtek, F.M. Fischer, W.-Y. Guo, T. Herben, Z. Janovský, M. Konečná, I. Kühn, L. Moravcová, P. Petřík, S. Pierce, K. Prach, H. Prokešová, M. ˇStech, J. Těšitel, T. Těšitelová, M. Večeřa, D. Zelený, P. Pyšek, Pladias database of the Czech Flora and vegetation, Preslia 93 (1) (2021) 1–87, https://doi.org/10.23855/preslia.2021.001.

[15] Flora of China @ ’eFloras, Missouri Botanical Garden, St. Louis, MO, Harvard University Herbaria, Cambridge, MA, 2008. http://flora.huh.harvard.edu/china/. (Accessed 28 March 2024).

[16] Native Plant Information Network, NPIN Lady Bird Johnson Wildflower Center at, The University of Texas, Austin, TX, 2013. http://www.wildflower.org/plants/. (Accessed 28 March 2024).

[17] R.D. Spencer, R.G. Cross, The international code of botanical nomenclature (ICBN), the international code of nomenclature for cultivated plants (ICNCP), and the cultigen, Taxon 56 (2007) 938–940, https://doi.org/10.2307/25065875.

[18] J. Kattge, G. Boenisch, S. Diaz, et al., TRY plant trait database – enhanced coverage and open access, Global Change Biol. 26 (2020) 119–188, https://doi.org/10.1111/gcb.14904.

[19] Ø. Hammer, D.A.T. Harper, P.D. Ryan, PAST: paleontological statistics software package for education and data analysis, *Palaeontol. Electron.* 4 (1) (2001) 9.

[20] M. Helder, D.P.B.T.B. Strik, H.V.M. Hamelers, A.J. Kuhn, C. Blok, C.J.N. Buisman, Concurrent bio-electricity and biomass production in three Plant-Microbial Fuel Cells using Spartina anglica, Arundinella anomala and Arundo donax, *Bioresour. Technol.* 101 (10) (2010) 3541–3547, https://doi.org/10.1016/j. biortech.2009.12.124.

[21] S.R. Gilani, A. Yaseen, S.R.A. Zaidi, M. Zahra, Z. Mahmood, Photocurrent generation through plant microbial fuel cell by varying electrode materials, *J. Chem. Soc. Pak.* 38 (1) (2016) 17–27.

[22] I.B. Rusyn, K.R. Hamkalo, Bioelectricity production in an indoor plant-microbial biotechnological system with Alisma plantago-aquatica, *Acta Biol. Szeged.* 62 (2) (2018) 170–179.

[23] J.C. Gómora-Hernández, J.H. Serment-Guerrero, M.C. Carreno-de-León, N. Flores-Alamo, Voltage Production in a plant microbial fuel cell using Agapanthus africanus, *Rev. Mex. Ing. Quim.* 19 (1) (2020) 227–237.

[24] I.B. Rusyn, O.V. Medvediev, B.T. Valko, Enhancement of bioelectric parameters of multi-electrode plant–microbial fuel cells by combining of serial and parallel connection, *Int. J. Environ. Sci. Technol.* 18 (6) (2021) 1323–1334. https://link.springer.com/article/10.1007/s13762-020-02934-3.

[25] Y. Hubenova, M. Mitov, Conversion of solar energy into electricity by using duckweed in direct photosynthetic plant fuel cell, *Bioelectrochemistry* 87 (2012) 185–191, https://doi.org/10.1016/j.bioelechem.2012.02.008.

[26] K.R.S. Pamintuan, J.A.A. Clomera, K.V. Garcia, G.R. Ravara, E.J.G. Salamat, Stacking of aquatic plant-microbial fuel cells growing water spinach (Ipomoea aquatica) and water lettuce (Pistia stratiotes), IOP *Conf. Ser. Earth Environ. Sci.* 191 (1) (2018) 012054.

[27] M.A. Moqsud, T.A. Gazali, K. Omine, Y. Nakata, Green electricity by water plants in organic soil and marine sediment through microbial fuel cell, Energy Sources, Part A Recovery, *Util. Environ. Eff.* 39 (2) (2017) 160–165.

[28] Y.M. Azri, I. Tou, M. Sadi, L. Benhabyles, Bioelectricity generation from three ornamental plants: Chlorophytum comosum, Chasmanthe floribunda and Papyrus diffuses, Int. J. *Green Energy* 15 (4) (2018) 254–263, https://doi.org/10.1080/15435075.2018.1432487.

[29] P.J. Sarma, K. Mohanty, Epipremnum aureum and Dracaena braunii as indoor plants for enhanced bio-electricity generation in a plant microbial fuel cell with electrochemically modified carbon fiber brush anode, *J. Biosci. Bioeng.* 126 (2018) 404–410, https://doi.org/10.1016/j.jbiosc.2018.03.009.

[30] Y. Yang, Y. Zhao, C. Tang, L. Xu, D. Morgan, R. Liu, Role of macrophyte species in constructed wetland-microbial fuel cell for simultaneous wastewater treatment and bioenergy generation, *Chem. Eng. J.* 392 (2020) 123708, https://doi.org/10.1016/j.cej.2019.123708.

[31] D. Ayala-Ruiz, A.C. Atoche, E. Ruiz-Ibarra, E.O. de la Rosa, J.V. Castillo, A self-powered PMFC-based wireless sensor node for smart city applications, *Wireless Communi. Mobile Comput.* 2019 (2019) 1–10, https://doi.org/10.1155/2019/8986302.

[32] A.C. Sophia, S. Sreeja, Green energy generation from plant microbial fuel cells (PMFC) using compost and a novel clay separator, *Sustain. Energy Technol. Ass.* 21 (2017) 59–66, https://doi.org/10.1016/j.seta.2017.05.001.

[33] W. Apollon, S.-K. Kamaraj, H. Silos-Espino, C. Perales-Segovia, L.L. Valera-Montero, V.A. Maldonado-Ruelas, M.A. V´azquez-Guti´errez, R.A. Ortiz-Medina, S. Flores-Benítezm, J.F. G´omez-Leyva, Impact of Opuntia species plant bio-battery in a semi-arid environment: demonstration of their applications, *Appl. Energy* 279 (2020) 115788, https://doi.org/10.1016/j.apenergy.2020.115788.

[34] L. Lu, D. Xing, Z.J. Ren, Microbial community structure accompanied with electricity production in a constructed wetland plant microbial fuel cell, *Bioresour. Technol.* 195 (2015) 115–121, https://doi.org/10.1016/j.biortech.2015.05.098.

[35] A. Oodally, M. Gulamhussein, D.G. Randall, Investigating the performance of constructed wetland microbial fuel cells using three indigenous South African wetland plants, *J. Water Process Engineering* 32 (2019) 100930, https://doi.org/10.1016/j.jwpe.2019.100930.

[36] S. Liu, H. Song, X. Li, F. Yang, Power generation enhancement by utilizing plant photosynthate in microbial fuel cell coupled constructed wetland system, *Int. J. Photoenergy* 2013 (2013) 172010, https://doi.org/10.1155/2013/172010.

[37] P. Chiranjeevi, R. Chandra, S.V. Mohan, Ecologically engineered submerged and emergent macrophyte based system: an integrated eco-electrogenic design for harnessing power with simultaneous wastewater treatment, *Ecol. Eng.* 51 (2013) 181–190, https://doi.org/10.1016/j.ecoleng.2012.12.014.

[38] N.F. Tapia, C. Rojas, C.A. Bonilla, I.T. Vargas, Evaluation of Sedum as driver for plant microbial fuel cells in a semi-arid green roof ecosystem, *Ecol. Eng.* 108 (2017) 203–210, https://doi.org/10.1016/j.ecoleng.2017.08.017.

[39] A. Schievano, A. Colombo, M. Grattieri, S.P. Trasatti, A. Liberale, P. Tremolada, P. Pino, P. Cristiani, Floating microbial fuel cells as energy harvesters for signal transmission from natural water bodies, *J. Power Sources* 340 (2017) 80–88, https://doi.org/10.1016/j.jpowsour.2016.11.037.

[40] Ç. Saz, C. Türe, O.C. Türker, A. Yakar, Effect of vegetation type on treatment performance and bioelectric production of constructed wetland modules combined with microbial fuel cell (CW-MFC) treating synthetic wastewater, *Environ. Sci. Pollut. Control Ser.* 25 (2018) 8777–8792. https://link.springer.com/article/10. 1007/s11356-018-1208-y.

[41] I.B. Rusyn, K.R. Hamkalo, Use of Carex hirta in electro-biotechnological systems on green roofs, *Regulatory Mechanisms in Biosystems* 10 (1) (2019) 39–44.

[42] N. Klaisongkram, K. Holasut, Electricity generation of plant microbial fuel cell (PMFC) using Cyperus involucratus R, *Eng. Appl. Sci. Res.* 42 (1) (2015) 117–124.

[43] J. Wang, X. Song, Y. Wang, J. Bai, M. Li, G. Dong, F. Lin, Y. Lv, D. Yan, Bioenergy generation and rhizodegradation as affected by microbial community distribution in a coupled constructed wetland-microbial fuel cell system associated with three macrophytes, *Sci. Total Environ.* 607 (2017) 53–62, https://doi. Org/10.1016/j.scitotenv.2017.06.243.

[44] K.R.S. Pamintuan, K.M. Sanchez, Power generation in a plant-microbial fuel cell assembly with graphite and stainless steel electrodes growing Vigna Radiata, *IOP Conf. Ser. Mater. Sci. Eng.* 703 (1) (2019) 012037.

[45] Y.-L. Oon, S.-A. Ong, L.-N. Ho, Y.-S. Wong, F.A. Dahalan, Y.-S. Oon, K.L. Harvinder, W.-E. Thung, N. Nordin, Role of macrophyte and effect of supplementary aeration in up-flow constructed wetland-microbial fuel cell for simultaneous wastewater treatment and energy recovery, *Bioresour. Technol.* 224 (2017) 265–275, https://doi.org/10.1016/j.biortech.2016.10.079.

[46] X. Shen, J. Zhang, D. Liu, Z. Hu, H. Liu, Enhance performance of microbial fuel cell coupled surface flow constructed wetland by using submerged plants and enclosed anodes, *Chem. Eng. J.* 351 (2018) 312–318, https://doi.org/10.1016/j.cej.2018.06.117.

[47] M. Rossi, P. Tosato, L. Gemma, L. Torquati, C. Catania, S. Camal`o, D. Brunelli, Long range wireless sensing powered by plant-microbial fuel cell, *Design. Automation & Test in Europe Conference & Exhibition*, IEEE press, 2017, pp. 1651–1654.

[48] C.Y. Guan, C.P. Yu, Evaluation of plant microbial fuel cells for urban green roofs in a subtropical metropolis, *Sci. Total Environ.* 765 (2021) 142786, https://doi. Org/10.1016/j.scitotenv.2020.142786.

[49] T.H. Cheng, K.B. Ching, C. Uttraphan, Y.M. Heong, Electrical energy production from plant biomass: an analysis model development for pandanus amaryllifolius plant microbial fuel cell, *Indonesian Journal of Electrical Engineering and Computer Science* 18 (3) (2020) 1163–1171.

[50] P. Chiranjeevi, G. Mohanakrishna, S.V. Mohan, Rhizosphere mediated electrogenesis with the function of anode placement for harnessing bioenergy through CO2 sequestration, *Bioresour. Technol.* 124 (2012) 364–370, https://doi.org/10.1016/j.biortech.2012.08.020.

[51] R. Regmi, R. Nitisoravut, S. Charoenroongtavee, W. Yimkhaophong, O. Phanthurat, Earthen pot–plant microbial fuel cell powered by Vetiver for bioelectricity production and wastewater treatment, *CLEAN – Soil, Air, Water* 46 (3) (2018) 1700193, https://doi.org/10.1002/clen.201700193.

[52] I.B. Rusyn, B.T. Valko, Container landscaping with Festuca arundinacea as bioelectrical minisystems in modern buildings, *Int. J. Ener. Clean Environ.* 20 (3) (2019), https://doi.org/10.1615/InterJEnerCleanEnv.2019026674.

[53] R.A. Timmers, M. Rothballer, D.P.B.T.B. Strik, M. Engel, S. Schulz, M. Schloter, A. Hartmann, B. Hamelers, C. Buisman, Microbial community structure elucidates performance of Glyceria maxima plant microbial fuel cell, *Appl. Microbiol. Biotechnol.* 94 (2012) 537–548. https://link.springer.com/article/10. 1007/s00253-012-3894-6.

[54] R.A. Timmers, D.P. Strik, H.V. Hamelers, C.J. Buisman, Characterization of the internal resistance of a plant microbial fuel cell, *Electrochim. Acta* 72 (2012) 165–171, https://doi.org/10.1016/j.electacta.2012.04.023.

[55] R.A. Timmers, D.P. Strik, H.V. Hamelers, C.J. Buisman, Electricity generation by a novel design tubular plant microbial fuel cell, *Biomass Bioenergy* 51 (2013) 60–67, https://doi.org/10.1016/j.biombioe.2013.01.002.

[56] N. Habibul, Y. Hu, Y.K. Wang, W. Chen, H.Q. Yu, G.P. Sheng, Bioelectrochemical chromium (VI) removal in plant-microbial fuel cells, *Environ. Sci. Technol.* 50 (7) (2016) 3882–3889, https://doi.org/10.1021/acs.est.5b06376.

[57] M.A. Moqsud, J. Yoshitake, Q.S. Bushra, M. Hyodo, K. Omine, D. Strik, Compost in plant microbial fuel cell for bioelectricity generation, *Waste Management* 36 (2015) 63–69, https://doi.org/10.1016/j.wasman.2014.11.004.

[58] L.D. Schamphelaire, L.V.D. Bossche, H.S. Dang, M. H¨ofte, N. Boon, K. Rabaey, W. Verstraete, Microbial Fuel Cells Generating Electricity from Rhizodeposits of Rice Plants (2008) 3053–3058.

[59] Y. Goto, N. Yoshida, Y. Umeyama, T. Yamada, R. Tero, A. Hiraishi, Enhancement of electricity production by graphene oxide in soil microbial fuel cells and plant microbial fuel cells, *Front. Bioeng. Biotechnol.* 3 (2015) 42, https://doi.org/10.3389/fbioe.2015.00042.

[60] K. Wetser, J. Liu, C. Buisman, D. Strik, Plant microbial fuel cell applied in wetlands: spatial, temporal and potential electricity generation of Spartina anglica salt marshes and Phragmites australis peat soils, *Biomass Bioenergy* 83 (2015) 543–550, https://doi.org/10.1016/j.biombioe.2015.11.006.

[61] K. Wetser, K. Dieleman, C. Buisman, D. Strik, Electricity from wetlands: tubular plant microbial fuels with silicone gas-diffusion biocathodes, *Appl. Energy* 185 (2017) 642–649, https://doi.org/10.1016/j.apenergy.2016.10.122.

[62] J.M. Khudzari, J. Kurian, Y. Gari´epy, B. Tartakovsky, G.V. Raghavan, Effects of salinity, growing media, and photoperiod on bioelectricity production in plant microbial fuel cells with weeping alkaligrass, *Biomass Bioenergy* 109 (2018) 1–9, https://doi.org/10.1016/j.biombioe.2017.12.013.

[63] M. Helder, D.P.B.T. Strik, H.V.M. Hamelers, R.C.P. Kuijken, C.J.N. Buisman, New plant-growth medium for increased power output of the Plant-Microbial Fuel Cel, *Bioresour. Technol.* 104 (2012) 417–423, https://doi.org/10.1016/j.biortech.2011.11.005.

[64] M. Helder, D.P. Strik, R.A. Timmers, S.M. Raes, H.V. Hamelers, C.J. Buisman, Resilience of roof-top plant-microbial fuel cells during Dutch winter, *Biomass Bioenergy* 51 (2013) 1–7, https://doi.org/10.1016/j.biombioe.2012.10.011.

[65] K. Wetser, E. Sudirjo, C.J.N. Buisman, D.P.B.T. Strik, Electricity generation by a plant microbial fuel cell with an integrated oxygen reducing biocathode, *Appl. Energy* 137 (2015) 151–157, https://doi.org/10.1016/j.apenergy.2014.10.006.

[66] K.R.S. Pamintuan, A.J.S. Gonzales, B.M.M. Estefanio, B.L.S. Bartolo, Simultaneous phytoremediation of Ni2+and bioelectricity generation in a plant-microbial fuel cell assembly using water hyacinth (Eichhornia crassipes), *IOP Conf. Ser. Earth Environ. Sci.* 191 (1) (2018) 012093.

[67] I.B. Rusyn, V.V. Vakuliuk, O.V. Burian, Prospects of use of Caltha palustris in soil plant-microbial eco-electrical biotechnology, *Regulatory Mechanisms in Biosystems* 10 (2) (2019) 233–238.

[68] R. Cervantes-Alcalá, A.A. Arrocha-Arcos, L.A. Peralta-Peláez, L.A. Ortega-Clemente, Electricity generation in sediment plant microbial fuel cells (SPMFC) in warm climates using Typha domingensis Pers, *Int. Res. J. Biotechnol.* 3 (9) (2012) 166–173.

[69] Y.-L. Oon, S.-A. Ong, L.-N. Ho, Y.-S. Wong, Y.-S. Oon, H.K. Lehl, W.E. Thung, Hybrid system up-flow constructed wetland integrated with microbial fuel cell for simultaneous wastewater treatment and electricity generation, *Bioresour. Technol.* 186 (2015) 270–275, https://doi.org/10.1016/j.biortech.2015.03.014.

[70] D. Da Re, E. Tordoni, F. De Pascalis, Z. Negrín-Pérez, J.M. Fernández-Palacios, Ramón J. Arévalo, D. Rocchini, F.M. Medina, R. Otto, E. Arlé, G. Bacaro, Invasive fountain grass (Pennisetum setaceum (Forssk.) Chiov.) increases its potential area of distribution in Tenerife island under future climatic scenarios, *Plant Ecol.* 221 (2020) 867–882. https://link.springer.com/article/10.1007/s11258-020-01046-9.

[71] EPPO (European and Mediterranean Plant Protection Organization), L. Pistia stratiotes, Datasheets on pests recommended for regulation, *OEPP/EPPO Bulletin* 47 (3) (2017) 537–543, https://doi.org/10.1111/epp.12429.

[72] H.F. Lin, P. Alpert, F.H. Yu, Effects of fragment size and water depth on performance of stem fragments of the invasive, amphibious, clonal plant Ipomoea aquatic, *Aquat. Bot.* 99 (2012) 34–40, https://doi.org/10.1016/j.aquabot.2012.01.004.

[73] S. Lowe, M. Browne, S. Boudjelas, M. De Poorter, 100 of the World's Worst invasive alien species. A selection from the global invasive species database, in: The Invasive Species Specialist Group (ISSG), a Specialist Group of the Species Survival Commission (SSC) of the World Conservation Union, (IUCN), 2020, p. 12.

[74] E. Weber, D. Gut, Assessing the risk of potentially invasive plant species in central Europe, *J. Nat. Conserv.* 12 (2004) 171–179, https://doi.org/10.1016/j. jnc.2004.04.002.

Chapter 2

Evaluating a New Prototype of Plant Microbial Fuel Cell: Is the Electrical Performance Affected by Carbon Pellet Layering and Urea Treatment?

Ilaria Brugellis, Marco Grassi, Piero Malcovati, Silvia Assini

Abstract

Plant Microbial Fuel Cells (PMFCs) represent a promising technology that uses electroactive bacteria to convert the chemical energy in organic matter into electrical energy. The addition of carbon pellet on electrodes may increase the specific surface area for colonization via bacteria. Use of nutrients such as urea could enhance plant growth. Our study aims to address the following questions: (1) Does carbon pellet layering affect the electrical performance of PMFCs? (2) Does urea treatment of the plants used to feed the PMFCs affect the electrical performance? A new prototype of PMFC has been tested: the plant pot is on the top, drainage water percolates to the tub below, containing the Microbial Fuel Cells (MFCs). To evaluate the best layering setup, two groups of MFCs were constructed: a “Double layer” group (with carbon pellet both on the cathode and on the anode), and a “Single layer” group (with graphite only on the cathode). All MFCs were plant-fed by *Spathiphyllum lanceifolium* L. leachate. After one year, each of the previous two sets has been divided into two subsets: one wetted with percolate from plants fertilized with urea, and the other with percolate from unfertilized plants. Open circuit voltage (mV), short circuit peak current, and short circuit current after 5 s (mA) produced values that were measured on a weekly basis. PMFCs characterized by a “Single layer” group performed better than the “Double layer” group most times, in terms of higher and steadier values for voltage and calculated power. Undesirable results regarding urea treatment suggest the use of less concentrated urea solution. The treatment may provide consistency but appears to limit voltage and peak values, particularly in the “Double layer” configuration.

Keywords

plant microbial fuel cells; bioelectricity; graphite granules; microbial fuel cell design; urea

Energies **2025**, 18, 5320 - https://doi.org/10.3390/en18195320

Introduction

The transition to clean energy is essential to address issues such as climate change, environmental pollution, and energy security. Reliance on fossil fuels has caused significant environmental harm, making the shift to sustainable sources – such as solar, wind, bioenergy, and bioelectricity – urgently necessary. Growing global energy demand requires innovative solutions that integrate economic development with environmental responsibility [1,2].

In this context, Plant Microbial Fuel Cells (PMFCs) represent a promising technology, supporting the United Nations Sustainable Development Goals, particularly SDG 7 (affordable and clean energy) and SDG 11 (sustainable cities and communities) [1]. The PMFC is an advanced form of the Microbial Fuel Cell (MFC), a bioenergy system that uses electroactive bacteria (e.g., *Shewanella*, *Geobacter*, *Rhodoferax*) [3,4] to convert the chemical energy in organic matter into electrical energy. These microorganisms generate electricity by oxidizing organic compounds and transferring electrons to external electron acceptors such as electrodes [5,6].

The MFC operates by creating a potential difference between an anode and a cathode, facilitated by microbial activity and the breakdown of organic waste in the substrate. PMFC technology incorporates living plants into the system. Plants continuously release organic compounds in the form of rhizodeposition through their roots. These include root exudates, which serve as an energy source for the electroactive microbes in the anode region [4,6,7].

The rhizosphere, the soil zone surrounding plant roots, plays a key role in this process as it is rich in microbial activity influenced by root secretions. PMFCs leverage this interaction by combining plant photosynthesis, rhizodeposition, and microbial metabolism to form a bioelectrochemical system that produces electricity. Since PMFCs rely on living plants to maintain continuous energy production, they create a mutually beneficial symbiotic relationship between plants and microbial communities [1,4].

Although the concept is promising, PMFC technology is still in an early developmental phase and faces multiple challenges. These include low power output, variability linked to plant species and plant functional traits [8], microbial diversity within the substrate, limitations in electron transfer mechanisms, and concerns related to long-term stability, scalability, and implementation costs on a large scale. Additionally, the performance of PMFCs is strongly influenced by microbial activity, electrochemical interactions at the electrodes, environmental conditions, irrigation regimes, the type of soil-bacteria interaction, and the quantity and rate of rhizodeposit release [1].

One of the major challenges is to improve electrode performance. Selecting appropriate electrode materials is crucial for ensuring efficient bioelectricity generation in the construction of Plant Microbial Fuel Cells. The electrode material should have high electrical conductivity, electrochemical stability, porosity, and biocompatibility. Metals and carbon materials are usually used as electrodes in bioelectrochemical systems [3]. On one hand, metals have higher electrical conductivity in comparison with carbon materials.

On the other, graphite electrodes (felt/fiber) have a surface that promotes the adhesion of microorganisms and the sorption of organic compounds, and is not subject to corrosion [3].

Moreover, the addition of granular graphite or activated carbon to the surface of the electrodes improves the adsorption of organic compounds and increases the specific surface area for colonization via bacteria [3].

Moreover, past studies have not addressed the sustainable, direct re-use of nutrients in conjunction with PMFC systems. Integrating such an approach could not only enhance plant growth but also support smart, integrated farming practices through the simultaneous generation of green electricity [9].

Any compost that is cheap and abundant is a viable candidate for the MFC [10]. Urea is a suitable fuel for MFCs. It is an advantage for the soil-based system to go through the natural processes by following nitrification and denitrification in the nitrogen cycle by ammonification to nitrogen (N^2) formation in soil [10,11].

Urea has been relatively underexplored in PMFC applications despite offering a promising route to produce low-cost fertilizers while simultaneously reducing environmental impacts. Moreover, PMFC technology can be implemented in any crop-production field without competing with or harming the plants [9]. The soil itself is a source of many bacteria and microorganisms in aerobic and anaerobic forms. Urea and ammonium are sources of nitrogen, and the density of urea is higher compared to other nitrogen sources [10,12].

When urea comes into contact with the soil, hydrolysis releases urease enzymes which work as a catalyst with bacteria. Therefore, soil systems can be a neutral medium to transport electrons and protons easily in an eco-friendly medium for power generation and maintain the pH level for the proper working of the MFC [10,13].

Based on these premises, our study aims to address the following questions:

· Does carbon pellet layering affect the electrical performance of PMFCs?

· Does urea treatment of the plants used to feed the PMFCs affect the electrical performance?

The work focuses solely on electrical parameters (OCV, current, power). However, essential characteristics of the drainage electrolyte solutions entering the PMFC – such as electrical conductivity, pH, COD, ORP, and nitrogen compound speciation – were not considered.

Materials and Methods

Design of the PMFC

A new prototype of PMFC has been developed: the pot containing the plants is on the top, drainage water percolates to the container below, which contains the cells (**Figure 2.1**).

This is highly advantageous for the maintenance of the prototype and allows the MFCs to retain their potential thanks to the nourishment provided by the plant.

The plant pot is on the top, drainage water percolates to the tub below, containing the MFCs. The leachate fills the tub, submerging the MFCs. A key characteristic of this prototype is the separation between the rhizosphere zone and the Microbial Fuel Cell, allowing a more accurate control of bioelectrochemical processes.

Figure 2.1. Novel prototype of PMFC.

Carbon Pellet Stratification

To evaluate the best layering setup, 48 MFCs were constructed, using 8 cm × 8 cm × 4 cm derivation boxes (**Figure 2.2a**) with the following stratification (from the bottom to the top of the cell): aluminum foil anode (**Figure 2.2b**), carbon pellets (when needed for the experimental setup) (**Figure 2.2e**), soil, polyethylene nonwoven fabric (**Figure 2.2c**), carbon felt cathode (**Figure 2.2d**), carbon pellets. The carbon felt cathodes measured 8 cm × 8 cm (surface area 64 cm^2) and were approximately half a centimeter thick. The aluminum foil anodes measured 8 cm × 8 cm (surface area 64 cm^2) and were approximately 2 mm thick. Carbon pellet layers were approximately 5 mm thick. Main technical data of carbon pellets are reported in **Table 2.1**. Nonwoven polyethylene fabric was used as a membrane due to its low cost and easy availability. Twenty-four MFCs were built with a double layer of C pellets, one layer on the cathode and one layer on the anode compartment (hereafter "Double layer" group), while the other 24 MFCs were built with C pellets only on the cathode compartment (hereafter "Single layer" group). All 48 MFCs were plant-fed by *Spathiphyllum lanceifolium* L.

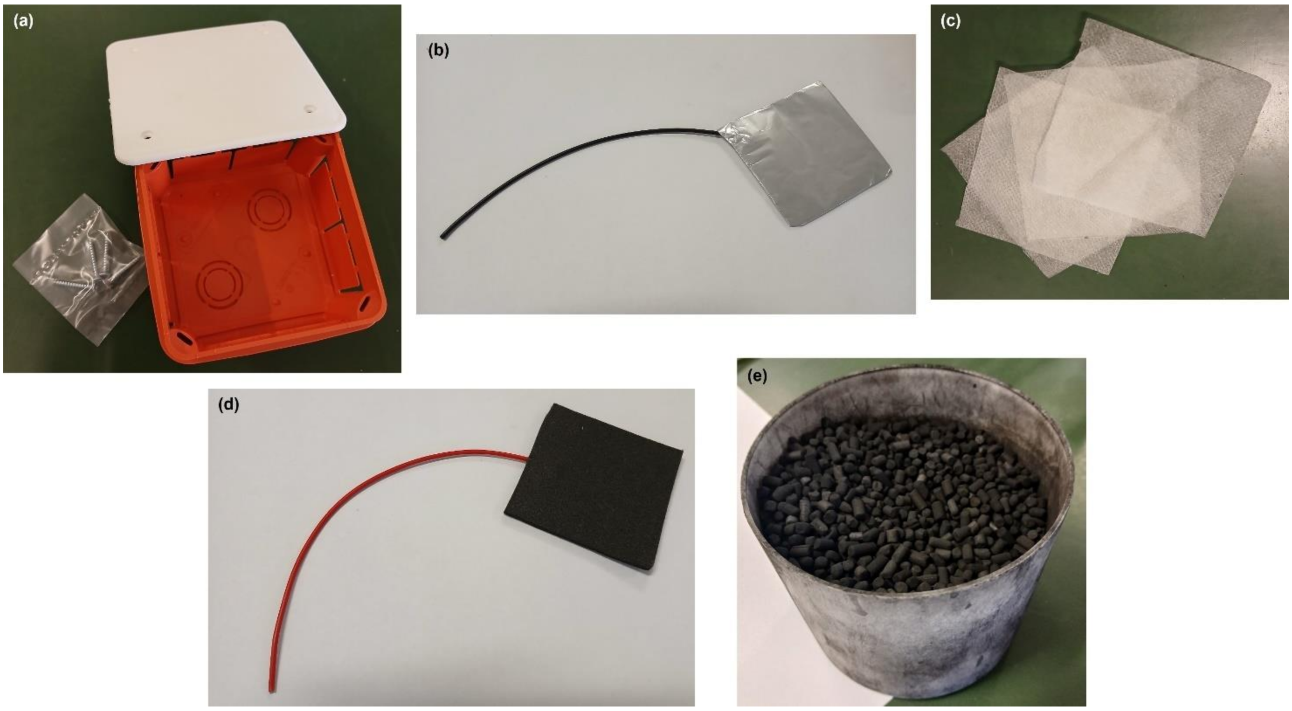

Figure 2.2. MFC's construction material: (**a**) derivation box; (**b**) aluminum anode; (**c**) membrane; (**d**) carbon felt cathode; (**e**) carbon pellet.

Table 2.1. Main technical data of carbon pellets.

Main Technical Data of Carbon Pellets	
Pellet diameter	4 mm
Abrasion resistance	98%
Bulk density	490 Kg/m^3
Ash content	0%
Moisture at bagging	2%
Internal surface area	900 m^2/m^3
Combustion temperature	480 °C
Vapor pressure (mm Hg at 20 °C)	0
Solubility	not soluble

Urea Treatment

From February 2024, each of the previous two sets has been divided into two subsets: one wetted with percolate from plants fertilized with urea, and the other with percolate from unfertilized plants. This resulted in 12 “Treated Double layer” cells, 11 “Control Double layer” cells (a cell broke), 12 “Treated Single layer” cells and 12 “Control Single layer” cells.

Urea, a nitrogen fertilizer containing 46% urea nitrogen, is easily absorbed and quickly transforms into ammoniacal nitrogen and then nitric nitrogen within a few days. It simultaneously provides immediate (nitrates) and reserve (ammonium salts) nutrition to plants. Its high water solubility ensures immediate availability for soil and plants. Usage recommendations, reported on the package of urea, suggest applying 40 g per m^2 of soil in cultivated fields. The pots used for plants had the following sizes: upper diameter 20 cm, height 15 cm, lower diameter 12 cm, giving a calculated volume of approximately 2333 cm^3 (0.002333 m^3). Consequently, 0.09333 g of urea per pot was recommended (40 g $\times$ 0.002333 m^3), which was rounded to 0.1 g of urea per pot. We considered the volume instead of the surface because in the pot the urea dispersion is less than in a cultivated field and we wanted to avoid a surplus of nutrients that could inhibit bacterial activity [1,14]. A stock solution with 0.1 gr/ml of water was prepared and 1 ml of this solution was used to water the “Treated” plants every 4/5 weeks (on February 26, March 25, April 22, May 28, July 5, and August 19).

A schematic diagram of the complete laboratory setup is shown in **Figure 2.3**.

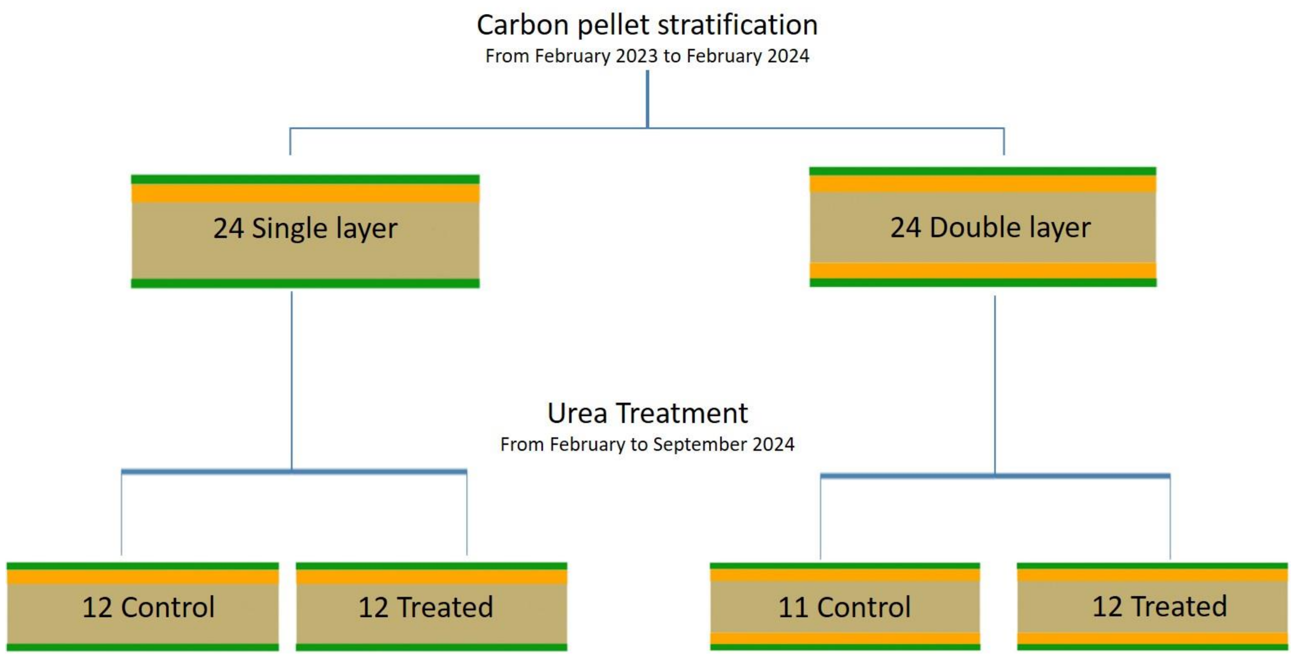

Figure 2.3. Schematic diagram of the laboratory setup.

Data Collection

Open circuit voltage (mV), short circuit peak current, and short circuit current after 5 s (mA) values produced by every single MFC were measured on a weekly basis using a digital multimeter (KEITHLEY 2000 MULTIMETER). Power figure of merit (mW) was calculated by multiplying open circuit voltage per short circuit current and per an arbitrary coefficient. According to theoretical maximum power point transfer (matched load), the coefficient could be set to ¼ [15].

Measures were collected from February 2023 to February 2024 to assess the influence of C pellet layering.

Measures were collected from February 2024 to September 2024 to assess the influence of urea treatment and to assess the effect of C pellet layering on “Control” groups.

Data Elaboration

Value distribution for each measured variable was examined across all cells. The means of the value distributions for open circuit voltage, short circuit peak current, and short circuit current after 5 s, and the corresponding power figure of merit values, were calculated for each MFC of each experimental setup.

To compare two groups, the t-test was performed when the distributions were normal, and the Mann‑Whitney non-parametric test for equal medians was used when the distributions were non-normal. To compare multiple groups, the ANOVA one-way for equal means followed by Tuckey pairwise test was performed when the distributions were normal, and Kruskal‑Wallis non-parametric test for equal medians followed by Dunn's post hoc test with raw values was performed when the distributions were non-normal. All analyses were performed using Past 4.09 software. This method allowed the calculation of the *p*-value as a test of statistical significance. For all cases, a confidence of 95% was established with configurations with *p*-value less than 0.05 being significant. To verify and compare the trends of the different groups, the PMFC mean of each group under consideration was calculated for each day over the course of the experiment.

Results and Discussion

Carbon Pellet Stratification of PMFCs from Feb 2023 to Feb 2024

Distributions of the voltage mean values showed significant differences; the current values did not show significant differences between the groups, whereas the power values showed evidence of equality of the medians (**Table 2.2**). Violin plots (**Figure 2.4**) show "Single layer" group having higher median value in the distribution of voltage mean values (**Figure 2.4a**), and having a more compact distribution around the median value in peak current (**Figure 2.4c**), current after s5 s (**Figure 2.4d**), and power (**Figure 2.4b**) mean values distributions than "Double layer" group.

Table 2.3 provides the minimum, maximum, and median values of the average distributions for all four parameters analysed. Interestingly, the "Single layer" group consistently shows higher minimum values compared to the "Double layer" group.

The time series of data for voltage, current, and power across the two configurations – "Double layer" and "Single layer" - (**Figure 2.5**) revealed distinct trends and differences.

As shown in **Figure 2.5a**, the mean voltage values were consistently higher for the "Single layer" group compared to the "Double layer" group throughout most of the observation period. This supports the significant difference in voltage between the two groups.

However, the values gradually converged toward the end of the observation time span, suggesting a possible stabilization or degradation effect affecting both groups equally in the long term. This trend does not deviate from that of previous work [16‑19].

On the contrary, the current values—both peak current (**Figure 2.5c**) and current after 5 s (**Figure 2.5d**)—did not show clear or systematic differences between the groups. While some fluctuations exist, especially during the first high-activity period (February‑April 2023), the overall patterns were similar and suggest no significant differences in current were observed between the "Double" and "Single layer" groups.

Regarding power (**Figure 2.5b**), both groups exhibited a pronounced peak early in the timeline, followed by a steep decline and stabilization, probably due to anode state and bacteria limitations at catalysis [16,18,20,21,22]. The distribution of power values over time suggests no substantial or consistent separation between the groups. The statistical analysis confirmed that the medians of power values were equal between the groups, supporting the interpretation that both groups performed similarly in terms of power output over time.

Table 2.2. Summary of the results of carbon pellet stratification from Feb 2023 to Feb 2024 [*p* (same mean) when normal distributions were tested, *p* (same median) when non-normal distributions were tested, calculated using Montecarlo permutation]. Significantly different results are highlighted.

	24 Double Layer vs. 24 Single Layer PMFCs
Open circuit voltage	*p* (same): 0.0001
Peak current	*p* (same): 0.3274
Current 5 s	*p* (same): 0.0797
Power	*p* (same): 0.6131

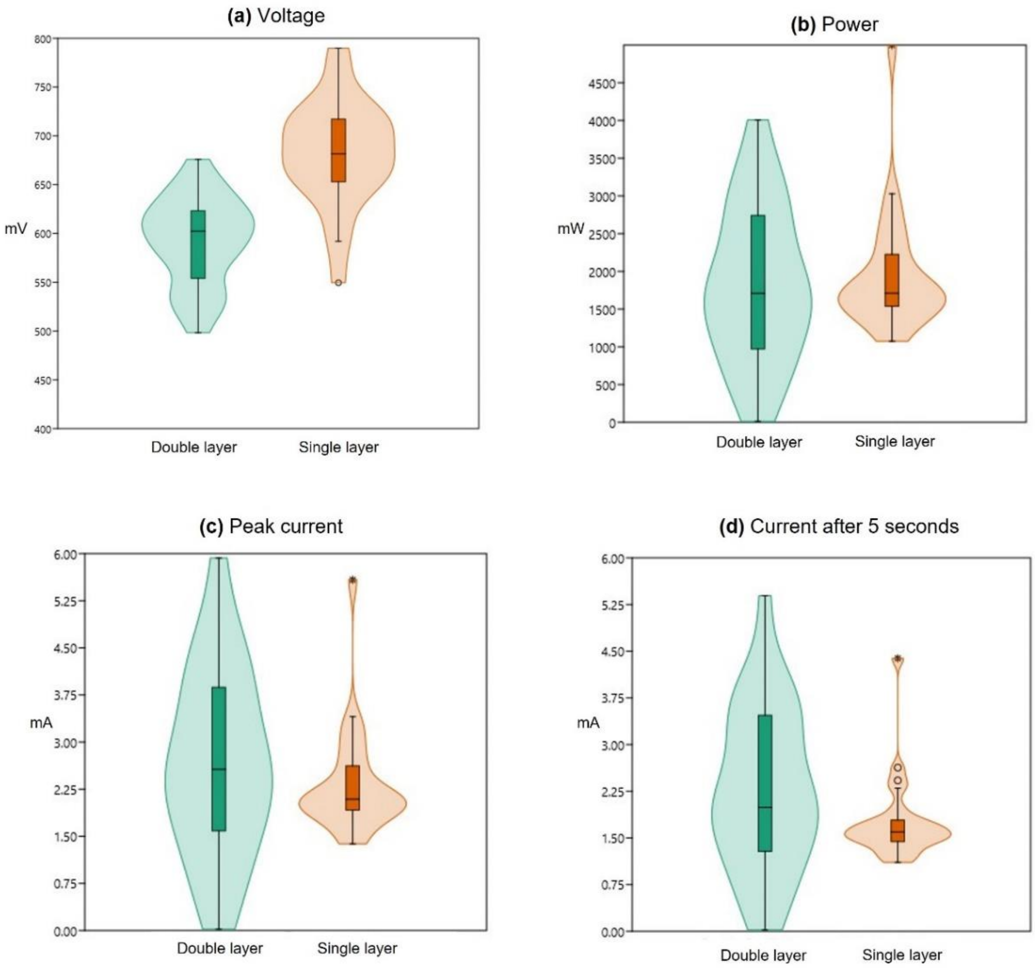

Figure 2.4. Violin and box plots comparing "Single layer" and "Double layer" groups in terms of distribution of PMFCs mean values for each variable: (**a**) open circuit voltage, (**b**) power, (**c**) peak current, (**d**) current after 5 s.

Table 2.3. Minimum, maximum, and median values of the average distributions of open circuit voltage, peak current, current after 5 s, and power in "Single layer" and "Double layer" groups.

	Voltage (mV)		**Peak Current (mA)**		**Current at 5 s (mA)**		**Power (mW)**	
	Double Layer	**Single Layer**	**Double Layer**	**Single Layer**	**Double Layer**	**Single Layer**	**Double Layer**	**Single Layer**
Max	676	790	5.929	5.582	5.391	4.385	4006.571	4998.021
Min	498	550	0.020	1.379	0.019	1.106	11.110	1074.454
Median	602	682	2.567	2.090	1.991	1.594	1708.636	1709.784

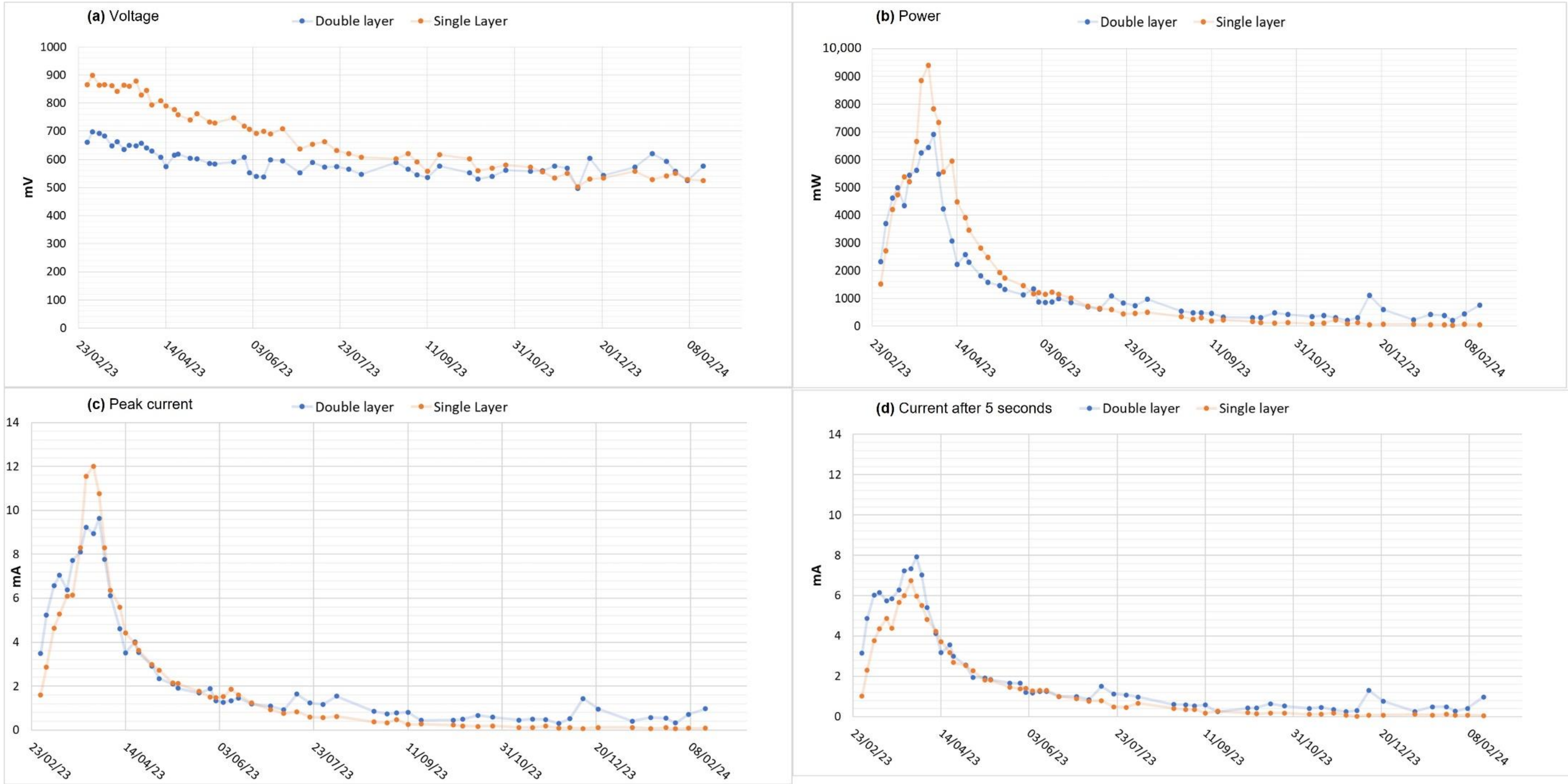

Figure 2.5. Comparison of group mean between "Double layer" and "Single layer" of carbon pellets from 28 February 2023 to 16 February 2024 (24 "Double layer" PMFCs vs. 24 "Single layer" PMFCs in one year) for each variable: (**a**) open circuit voltage, (**b**) power, (**c**) peak current, (**d**) current after 5 s.

Carbon Pellet Stratification of "Control" PMFCs from Feb 2023 to Sep 2024

Distributions of the voltage mean values indicate strong evidence for unequal means; current after 5 s also shows a significant difference among groups; peak current values and the power values indicate no evidence for either equal or unequal medians (**Table 2.4**).

Table 2.4. Summary of the results of carbon pellet stratification of "Control" PMFCs from Feb 2023 to Sep 2024 [*p* (same mean) when normal distribution was tested, *p* (same median) when non-normal distribution was tested, calculated using Montecarlo permutation] of the conducted statistical analysis. Significantly different results are highlighted.

	11 Double Layer vs. 12 Single Layer "Control" PMFCs
Open circuit voltage	*p* (same): 0.0034
Peak current	*p* (same): 0.0903
Current 5 s	*p* (same): 0.0314
Power	*p* (same): 0.2555

Violin plots (**Figure 2.6**) show "Single layer" "Control" group having higher median value in the distribution of voltage mean values (**Figure 2.6a**) and having a more compact distribution around the median value in peak current (**Figure 2.6c**), current after 5 s (**Figure 2.6d**), and power (**Figure 2.6b**) mean values than the "Double layer" "Control" group. **Table 2.5** provides the minimum, maximum, and median values of the average distributions for the analyzed parameters.

In this case as well, the "Single layer" group consistently shows higher minimum values compared to the "Double layer" group, along with narrower value ranges around the median, indicating greater stability.

As seen in **Figure 2.7a**, the "Single layer" group consistently exhibited higher voltage values than the "Double layer" group for a large portion of the experimental period. Over time, both groups showed a gradual decline, but the "Single layer" maintained a higher voltage than "Double layer" in most cases. This supports the significant difference in voltage performance between the two groups.

In **Figure 2.7b**, the power output peaked early in the observation period (around March 2023) for both groups, with the "Double layer" showing slightly higher (peak) values. After the peak, power dropped substantially and remained low for the rest of the time. Overall, the distributions appeared to converge, suggesting no substantial difference in power medians over the long term.

Figure 2.7c and **2.7d** show similar trends. The "Double layer" group demonstrated higher current values, both at peak and after 5 s, particularly during the first months of the study. These differences persisted throughout most of the timeline, though the current values of both groups eventually flattened at low levels.

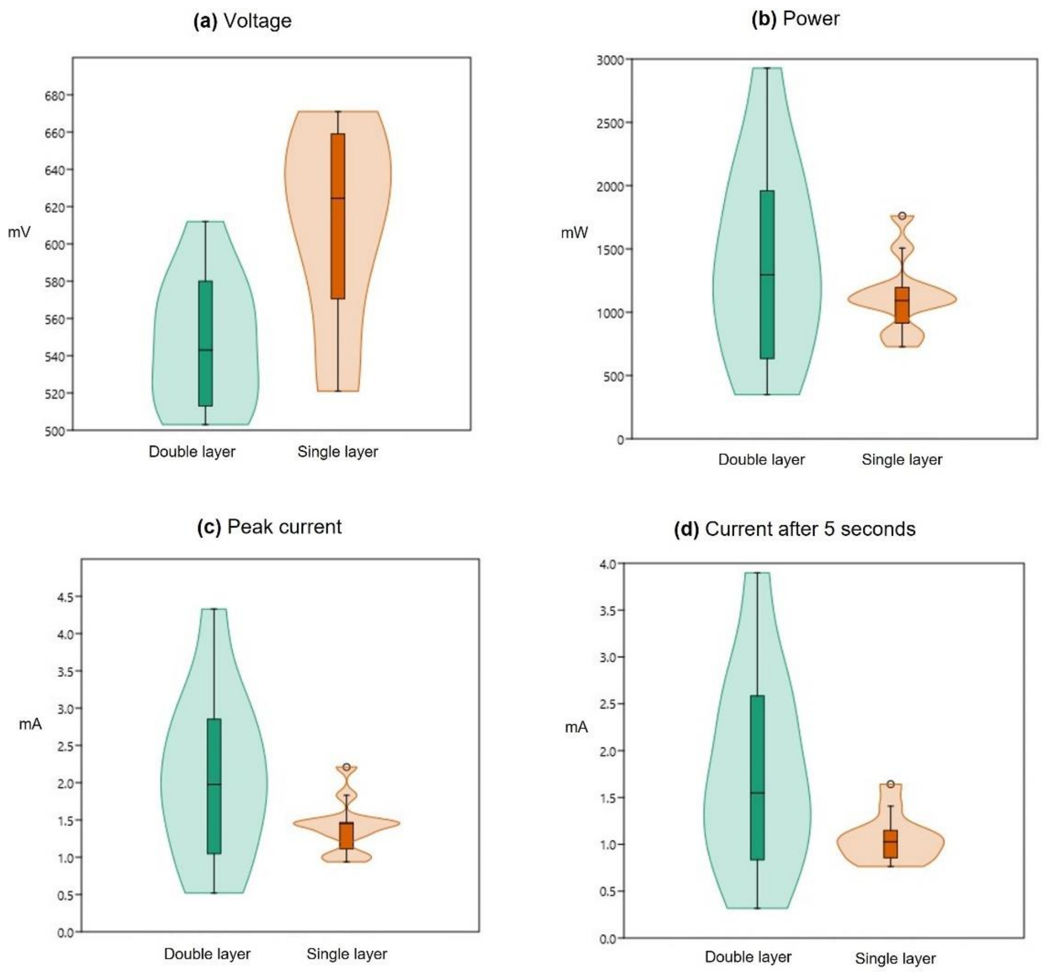

Figure 2.6. Violin and box plots comparing "Single layer" and "Double layer" "Control" groups in terms of distribution of PMFCs mean values for each variable: (**a**) voltage, (**b**) power, (**c**) peak current, (**d**) current after 5s.

Table 2.5. Minimum, maximum, and median values of the average distributions of open circuit voltage, peak current, current after 5 s, and power for carbon pellet stratification of "Control" PMFCs.

	Voltage (mV)		**Peak Current (mA)**		**Current After 5 s (mA)**		**Power (mW)**	
	Double Layer	**Single Layer**	**Double Layer**	**Single Layer**	**Double Layer**	**Single Layer**	**Double Layer**	**Single Layer**
Max	612	671	4.329	2.210	3.899	1.642	2928.805	1761.741
Min	503	521	0.518	0.938	0.316	0.764	348.722	806.163
Median	543	624	1.977	1.453	1.548	1.026	1295.568	1092.269

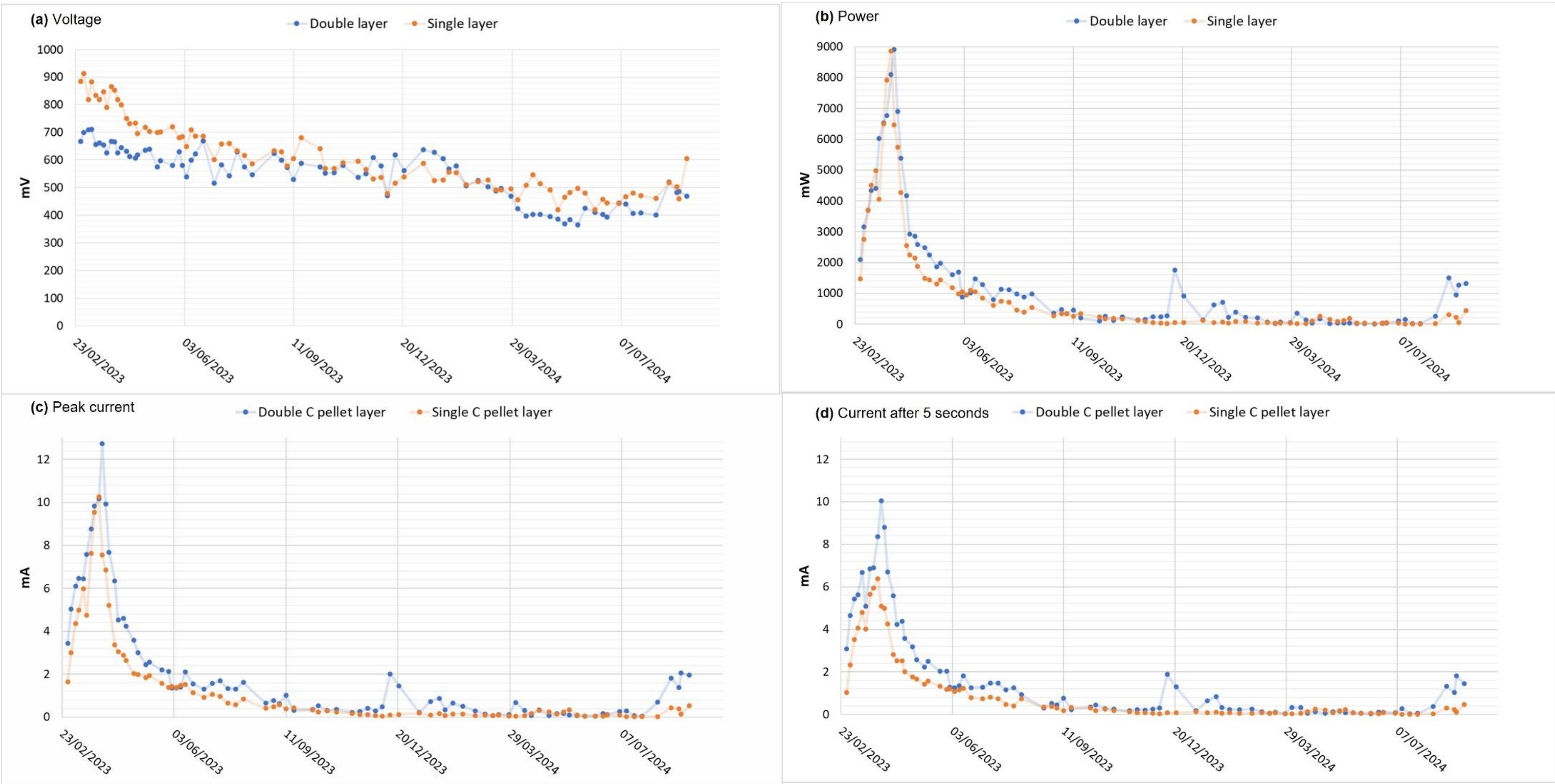

Figure 2.7. Comparison of sample averages between "Control Double layer" and "Control Single layer" groups from 28 March 2023 to 5 September 2024 (12 "Double layer" PMFCs vs. 12 "Single layer" PMFCs in one year and a half) for each variable: (**a**) open circuit voltage, (**b**) power, (**c**) peak current, (**d**) current after 5 s.

PMFCs Under Urea Treatment

Kruskal-Wallis test on the values of the voltage mean distributions indicates no significant difference between group medians; Dunn's post hoc test with raw values highlighted both "Treated" and "Control" "Single layer" groups being significantly different from the "Treated Double layer" group for voltage values.

Peak current, current after 5 s, and power resulted significantly different; Dunn's post hoc highlighted the "Treated Single layer" group being different from the other groups for all three parameters (**Table 2.6**).

Table 2.7 provides the minimum, maximum, and median values of the average distributions for the analyzed parameters.

Table 2.6. Summary of the results of urea treatment [*p* (same mean) when normal distribution was tested, *p* (same median) when non-normal distribution was tested, calculated using Montecarlo permutation] of the conducted statistical analysis. Significantly different results are highlighted.

	Multiple Samples Tested: 11 "Control Double Layer", 12 "Control Single Layer", 12 "Treated Double Layer", 12 "Treated Single Layer"
Open circuit voltage	*p* (same): 0.0503
Peak current	*p* (same): 0.0008
Current 5 s	*p* (same): 0.0014
Power	*p* (same): 0.0009

Table 2.7. Minimum, maximum, and median values of the average distributions of open circuit voltage, peak current, current after 5 s, and power for "Treated" and "Control" groups.

		Maximum	Minimum	Median
Voltage (Mv)	**Treated Double layer**	516	127	439
	Control Double layer	510	276	461
	Treated Single layer	632	130	521
	Control Single layer	610	226	515
Peak current (Ma)	**Treated Double layer**	2,.386	0.003	0.183
	Control Double layer	1.068	0.010	0.313
	Treated Single layer	0.077	0.006	0.028
	Control Single layer	0.406	0.025	0.103
Current after 5 s (Ma)	**Treated Double layer**	2.224	0.002	0.154
	Control Double layer	0.983	0.008	0.233
	Treated Single layer	0.059	0.003	0.021
	Control Single layer	0.309	0.018	0.079
Power (Mw)	**Treated Double layer**	1867.956	1.320	67.961
	Control Double layer	733.357	3.947	128.440
	Treated Single layer	42.868	2.694	12.857
	Control Single layer	277.253	12.500	44.909

Violin plots (**Figure 2.8**) show comparable median values between the distributions of voltage (**Figure 2.8a**). "Treated Single layer" group shows the lowest distribution values for power (**Figure 2.8b**), while "Control Single layer" group distribution appears to be more compact. Distribution of values for the variable peak current and current after 5 s have very similar trends than power and are shown in **Figures S1** and **S2** (*Author's Note: "Supplementary material" in the paper*).

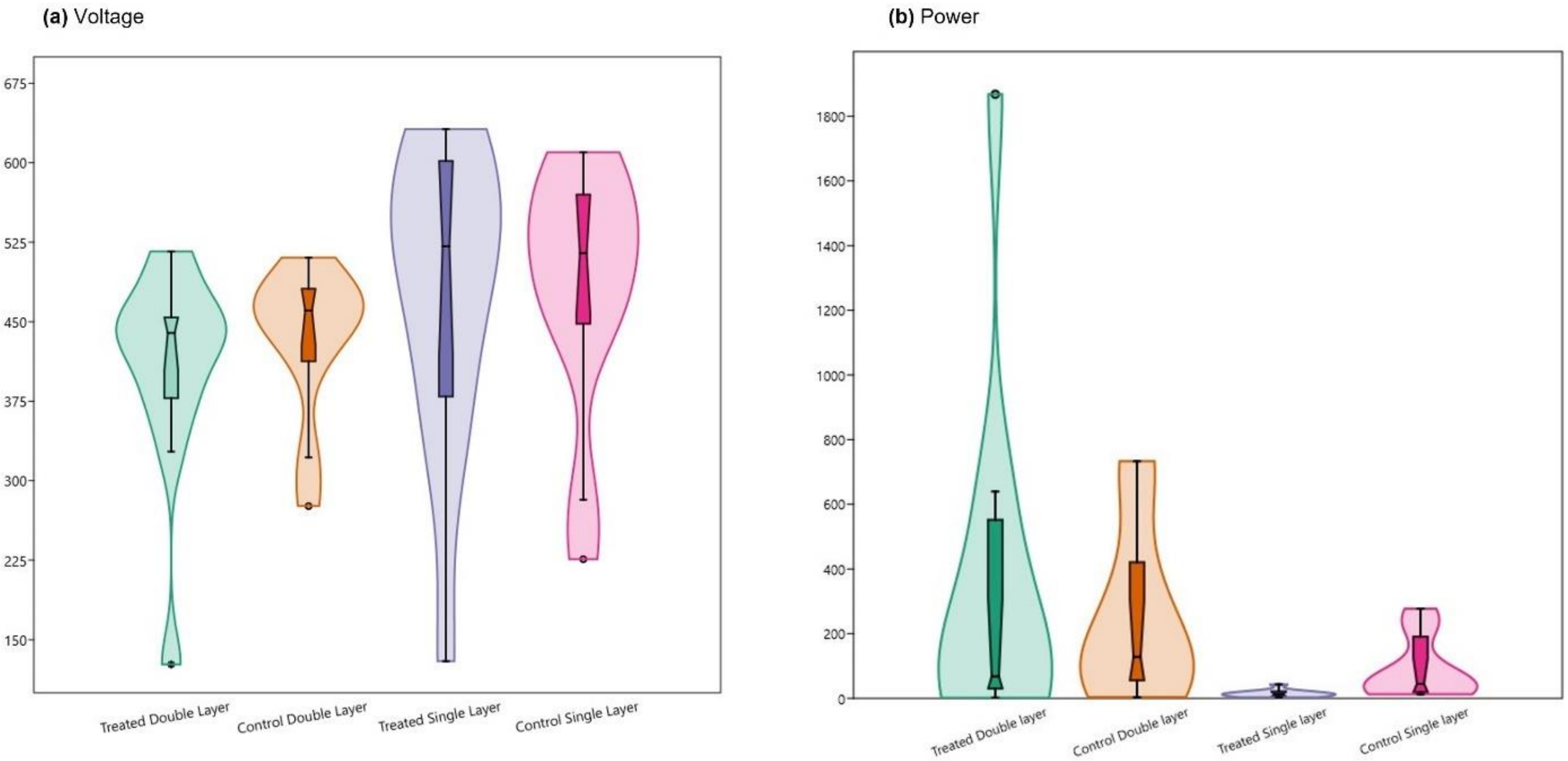

Figure 2.8. Violin and box plots comparing "Treatment Double layer", "Control Double layer", "Treatment Single layer", and "Control Single layer" groups of PMFCs in terms of distribution of mean values for the variable: (**a**) voltage, (**b**) power.

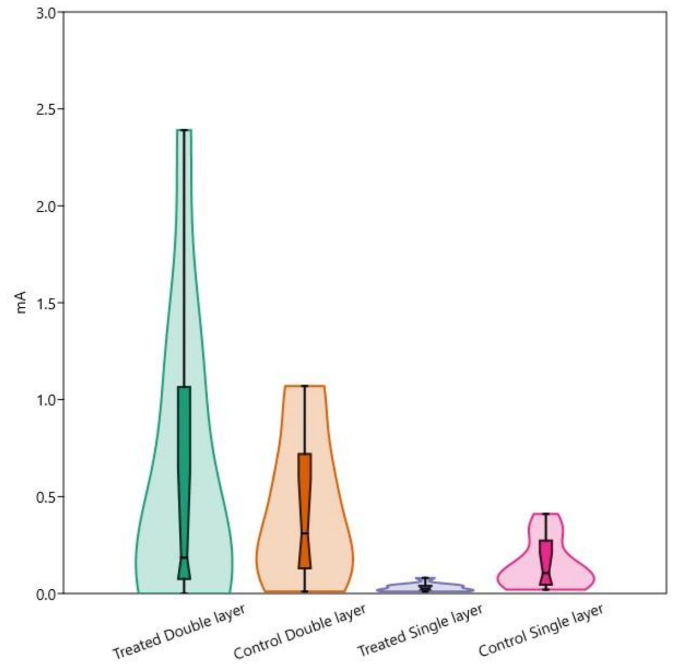

Figure S1. Violin and box plots comparing "Treatment Double layer", "Control Double layer", "Treatment Single layer", "Control Single layer" groups of PMFCs in terms of distribution of mean values for the variable peak current.

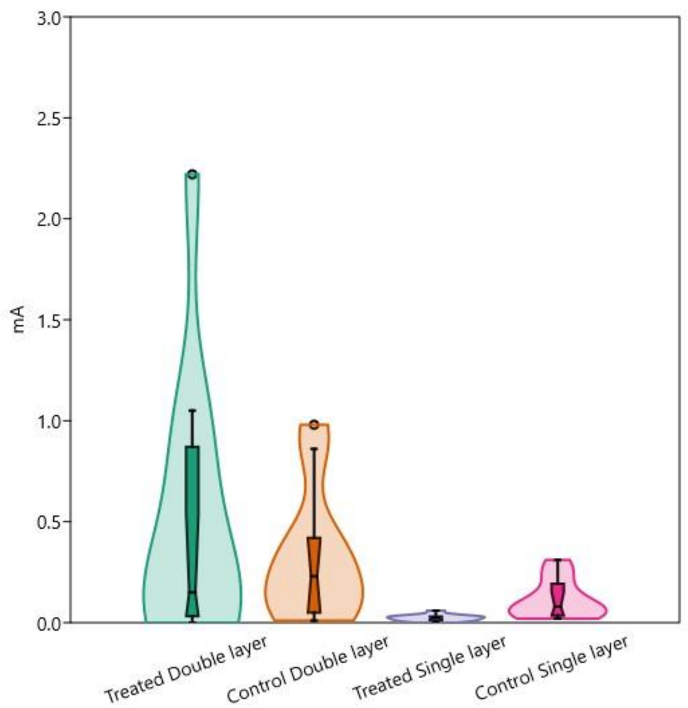

Figure S2. Violin and box plots comparing "Treatment Double layer", "Control Double layer", "Treatment Single layer", "Control Single layer" groups of PMFCs in terms of distribution of mean values for the variable current after 5 seconds.

Data presented in **Figure 2.9** show electrical performance over time, comparing “Treated” and “Control” samples for both “Single layer” and “Double layer” groups. Looking at voltage trends (**Figure 2.9a**), we observe that the “Treated Double layer” group consistently shows the lowest voltage values throughout the entire observation period. This suggests that the treatment may have negatively affected voltage output, at least in the “Double layer” group. On the contrary, both “Treated Single layer” and “Control Single layer” groups maintain higher and more stable voltage values. Interestingly, the “Control Double layer” group falls somewhere in between, showing a slight decline over time but still performing better than the “Treated Double layer” group. Overall, this pattern suggests that the urea treatment seems to reduce voltage, particularly in more complex configurations like the ”Double layer”. Peak current reveals some contrasts among groups (**Figure 2.9c**). Once again, the “Control Double layer” group shows a clear increase toward the end of the timeline, while the “Treated Double layer” maintains intermediate current values for most of the time. Both “Treated” and “Control” “Single layer” groups show very low peak current.

The current measured after five seconds closely mirrors the peak current trends (**Figure 2.9d**). The “Control Double layer” group achieves the highest values toward the end, followed by the “Treated Double layer”, which again shows more stable but lower values. In contrast, the “Single layer” groups remain low and flat across the entire observation period.

Power output follows a similar pattern to current (**Figure 2.9b**). Toward the end of the measurement period, the “Control Double layer” group shows a sharp increase in power, far exceeding all other groups. Meanwhile, the “Treated Double layer” group displays more moderate but stable power values throughout. Both “Treated” and “Control” “Single layer” groups remain consistently low, suggesting a limited capacity for power output regardless of treatment. These data suggest that the urea treatment seems to stabilize the power output, but, at the same time, limit the peak performance, especially when compared to the “Control Double-layer” group.

Anyway, the obtained results in cells treated with urea did not produce the expected results, in contrast with the literature data [10,23] and our previous experiments realized in the contest of degree thesis.

This could be due to the high concentration of urea in the solution used to water the plants feeding the cells, with consequent decline in the bacterial activity. Anyway, our study did not consider other parameters (e.g., soil chemistry, microbial load, urea concentration), which could be implied in the found results, limiting a comprehensive understanding of the processes.

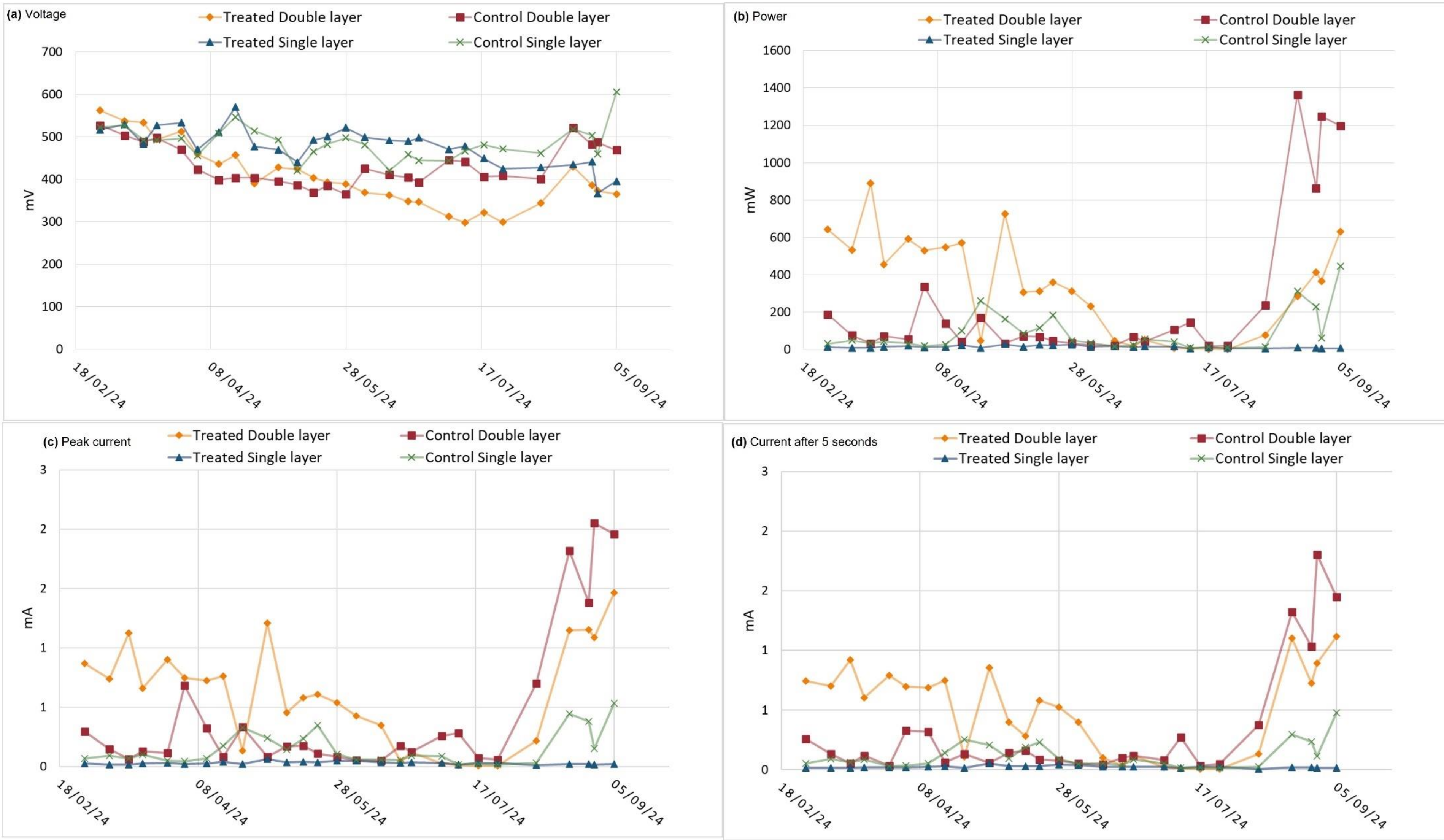

Figure 2.9. Comparison of sample averages of "Treated Double layer", "Control Double layer", "Treated Single layer", and "Control Single layer" groups from 27 February 2024 to 5 September 2024 for each variable: (**a**) voltage, (**b**) power, (**c**) peak current, (**d**) current after 5 s.

Conclusions

In this study, we found C pellet stratification influencing electrical performances of PMFCs, while urea treatment is not as expected.

PMFCs characterized by a "Single layer" of C pellet performed better than "Double layer" of C pellet ones most of times, in terms of higher values for voltage and power and more stable values. This can be considered a positive outcome, with practical implications for future experiments. In fact, this is also cost-effective for the construction of cells, which will result a little more economic and easier to build.

Undesirable results regarding urea treatment suggest repeating the experiment using less concentrated urea solution. Anyway, some interesting points emerge from our study.

The treatment may provide consistency but appears to limit voltage and peak values, particularly in the "Double layer" configuration.

Although this study has certain limitations, as it analyses few parameters related to the MFCs, the results refer to a novel prototype and an original setup. Our primary objective was to evaluate the functionality of the new prototype under different conditions (Single layer, Double layer, urea provision) and in terms of electrical performances, establishing a first baseline dataset. Future research on similar configurations will address other chemical and/or microbiological parameters useful to understand their implications in the processes related to electricity production.

References

[1] P.L. Chong, J.H. Chuah, C.O. Chow, P.K. Ng, Plant microbial fuel cells: A comprehensive review of influential factors, innovative configurations, diverse applications, persistent challenges, and promising prospects, *Int. J. Green Energy* 22 (2025) 599–648.

[2] A.T. Hoang, P.S. Varbanov, S. Nižetić, R. Sirohi, A. Pandey, R. Luque, K.H. Ng, V.V. Pham, Perspective review on municipal solid waste-to-energy route: Characteristics, management strategy, and role in circular economy, *J. Clean. Prod.* 359 (2022) 131897.

[3] R. Lepikash, D. Lavrova, D. Stom, V. Meshalkin, O. Ponamoreva, S. Alferov, State of the art and environmental aspects of plant microbial fuel cells' application, *Energies* 17 (2024) 752.

[4] S. Maddalwar, K.K. Nayak, M. Kumar, L. Singh, Plant microbial fuel cell: Opportunities, challenges, and prospects, *Bioresour. Technol.* 341 (2021) 125772, https://doi.org/10.1016/j.biortech.2021.125772.

[5] R. Shaikh, A. Rizvi, M. Quraishi, S. Pandit, A.S. Mathuriya, P.K. Gupta, J. Singh, R. Prasad, Bioelectricity production using plant-microbial fuel cell: Present state of art, *S. Afr. J. Bot.* 140 (2021) 393–408.

[6] D.P. Strik, H.V.M. Hamelers, J.F. Snel, C.J.N. Buisman, Green electricity production with living plants and bacteria in a fuel cell, *Int. J. Energy Res.* 32 (2008) 870–876.

[7] F.T. Kabutey, Q. Zhao, L. Wei, J. Ding, P. Antwi, F.K. Quashie, W. Wang, An overview of plant microbial fuel cells (PMFCs): Configurations and applications, *Renew. Sustain. Energy Rev.* 110 (2019) 402–414.

[8] I. Brugellis, M. Grassi, P. Malcovati, S. Assini, Plant microbial fuel cells in a botanical perspective: Nomenclatural constraints and new insights on plant traits potentially affecting bioelectrical performance, *Heliyon* 10 (2024) e38733.

[9] W. Apollon, A.I. Luna-Maldonado, S.K. Kamaraj, J.A. Vidales-Contreras, H. Rodriguez-Fuentes, J.F. Gomez-Leyva, V.A. Maldonado-Ruelas, R.A. Ortiz-Medina, Self-sustainable nutrient recovery associated to power generation from livestock's urine using plant-based bio-batteries, *Fuel* 332 (2023) 126252.

[10] V.K. Magotra, S. Kumar, T.W. Kang, A.I. Inamdar, A.T. Aqueel, H. Im, G. Ghodake, S. Shinde, D.P. Waghmode, H.C. Jeon, Compost soil microbial fuel cell to generate power using urea as fuel, *Sci. Rep.* 10 (2020) 4154.

[11] W. Xu, Z. Wu, S. Tao, Urea-based fuel cells and electrocatalysts for urea oxidation, *Energy Technol.* 4 (2016) 1329–1337.

[12] R. Lan, S. Tao, J.T.S. Irvine, A direct urea fuel cell—Power from fertilizer and waste, *Energy Environ. Sci.* 3 (2010) 438–441.

[13] A. Wolinska, Z. Stępniewska, A. Bielecka, J. Ciepielski, Bioelectricity production from soil using microbial fuel cells, *Appl. Biochem. Biotechnol.* 173 (2014) 2287–2296.

[14] A. Parkash, S. Aziz, M. Abro, S.A. Soomro, A. Kousar, Design and fabrication of microbial fuel cell using cow manure for power generation, *Sci. Int.* 27 (2015) 4235–4238.

[15] M. Turhan, B. Dai, D. Yildirim, Analytical MPPT solution using Thevenin approach for solar panels, in: *Proc. Eurocon 2013*, Zagreb, Croatia, 1–4 July 2013, 803–808.

[16] O. Guadarrama-Perez, K.Y. Bahena-Rabadan, U. Dehesa-Carrasco, V.H. Guadarrama Perez, E.B. Estrada-Arriaga, Bioelectricity production using shade macrophytes in constructed wetlands–microbial fuel cells, *Environ. Technol.* 43 (2022) 1532–1543.

[17] X. Long, X. Cao, H. Song, O. Nishimura, X. Li, Characterization of electricity generation and microbial community structure over long-term operation of a microbial fuel cell, *Bioresour. Technol.* 285 (2019) 121395.

[18] Y.M. Azri, I. Tou, M. Sadi, L. Benhabyles, Bioelectricity generation from three ornamental plants: *Chlorophytum comosum*, *Chasmanthe floribunda* and *Papyrus diffusus*, *Int. J. Green Energy* 15 (2018) 254–263.

[19] P. Chiranjeevi, S. Aziz, M. Abro, S.A. Soomro, A. Kousar, Ecologically engineered submerged and emergent macrophyte-based system: An integrated eco-electrogenic design for harnessing power with simultaneous wastewater treatment, *Ecol. Eng.* 51 (2013) 181–190.

[20] R. Regmi, R. Nitisoravut, S. Charoenroongtavee, W. Yimkhaophong, O. Phanthurat, Earthen pot–plant microbial fuel cell powered by *Vetiver* for bioelectricity production and wastewater treatment, *Clean Soil Air Water* 46 (2018) 1700193.

[21] K. Kumar, K. Manmohan, P.M. Sreelakshmi, S. Gajalakshmi, Terracotta separator-based plant microbial fuel cells for bioelectricity and catholyte production, *Int. J. Appl. Eng. Res.* 13 (2018) 14948–14955.

[22] M.A. Moqsud, J. Yoshitake, Q.S. Bushra, M. Hyodo, K. Omine, D. Strik, Compost in plant microbial fuel cell for bioelectricity generation, *Waste Manag.* 36 (2015) 63–69.

[23] N.S. Khoirunnisa, Y.R. Alfiansah, F. Hazra, S. Anwar, U. Sudadi, D.A. Santosa, Impact of fertilizer, salinity and exo-electrogen bacteria on the performance of plant microbial fuel cell (PMFC) using *Oryza sativa*, *Biomass Convers. Biorefinery* 15 (2025) 25417–25431.

Chapter 3

Influence of *Trichoderma* Inoculation and Membrane Layering on PMFC Electrical Performance

Ilaria Brugellis, Mariam Mahmoud, Solveig Tosi

Abstract

This study investigates Plant Microbial Fuel Cells (PMFCs) as emerging technologies for the sustainable production of electricity from renewable sources, with a focus on evaluating how different system configurations can enhance electrical efficiency.

Microbial Fuel Cells (MFCs) exploit the ability of bacteria to degrade organic compounds under anaerobic conditions, releasing electrons that generate electricity through redox reactions between an anode and a cathode, typically separated by a proton exchange membrane. PMFCs extend this concept by integrating living plants, whose root exudates continuously supply organic substrates to soil microorganisms in the rhizosphere, thereby sustaining bioelectricity generation.

The proposed PMFC prototype introduces a novel configuration in which the plant is physically separated from the electrochemical cell. Plants are placed in an upper pot and irrigated regularly, while the nutrient-rich leachate derived from rhizodeposition percolates into the container below, feeding the bacterial communities within the cells.

Seventy-two cells were constructed and divided into six experimental sets to evaluate the effects of *Trichoderma asperellum* inoculation and membrane presence. *Trichoderma* was applied either to the plant soil or directly to the cell soil, and each condition was tested with and without a membrane.

Overall, PMFCs inoculated with *Trichoderma* exhibited improved electrical performance compared to control sets, highlighting its potential as a performance-enhancing additive. Additionally, systems incorporating a membrane generally achieved higher and more stable electrical outputs, suggesting that membrane inclusion may further positively influence PMFC activity. Anyway, degradation of the copper cathode wiring may have affected system performance and biased the interpretation of the measured bioelectrical outputs.

Keywords

plant microbial fuel cells; bioelectricity; *Trichoderma*; microbial fuel cell design; proton exchange membrane

Introduction

Microbial fuel cells (MFCs) are bioelectrochemical systems that exploit microorganisms as biocatalysts to oxidize organic or inorganic substrates and generate electricity. During this process, bacteria release electrons that are transferred to the anode and flow through an external circuit to the cathode, producing an electric current. Protons generated during substrate oxidation migrate internally toward the cathode, where they react with electrons and oxygen and form water. MFCs can be constructed using a wide variety of materials and configurations and can operate under different environmental and operational conditions, including variations in temperature, pH, electrode surface area, reactor size, and operating time [1]. Their performance can be enhanced through optimization of electrode materials, surface modifications, improved bacterial adhesion, and more efficient electron transport mechanisms [2].

Typically, MFCs consist of two compartments: an anaerobic anode chamber and a cathode chamber, separated by an ion exchange membrane. In the anode compartment, electrogenic microorganisms oxidize organic substrates, forming a biofilm on the electrode surface that catalyzes electron transfer. The cathode acts as an electron sink, where oxygen is commonly reduced to water. Maintaining oxygen-free conditions in the anode chamber is essential to ensure efficient electricity generation [3].

The membrane plays a crucial role by separating the anodic and cathodic reactions, preventing short-circuiting, and allowing selective proton transport. Membrane performance depends on properties such as proton conductivity, selectivity, ion exchange capacity, oxygen permeability, thickness, and resistance. Commercial membranes commonly used in MFCs include Nafion, Zirfon, and Ultrex [2].

Despite their potential, MFCs require a continuous supply of organic substrates to sustain electricity generation, which limits their long-term applicability. Plant microbial fuel cells (PMFCs) have been developed to overcome this limitation by integrating living plants into the system. In PMFCs, plants continuously release organic compounds into the rhizosphere through rhizodeposition, providing a renewable substrate for electroactive microorganisms [4].

An innovative aspect of this study is the evaluation of *Trichoderma* spp. application in PMFCs. *Trichoderma* is a genus of filamentous fungi widely distributed in soil ecosystems and known for its adaptability, competitiveness, and strong cellulolytic activity [5,6]. Optimal growth conditions include mildly acidic pH values and moderate temperatures. Due to its ability to degrade organic matter and suppress competing microorganisms, *Trichoderma* has attracted increasing interest for applications beyond biocontrol, including bioenergy production.

Trichoderma spp. are widely recognized as plant growth-promoting fungi capable of enhancing root development and increasing root biomass through rhizosphere colonization, phytohormone modulation, and improved nutrient uptake [7,8,9].

Recent studies have demonstrated the potential of *Trichoderma* species to contribute to electricity generation in PMFCs, as well as to the biodegradation of complex waste materials [10]. The integration of *Trichoderma* into PMFC systems therefore represents a promising strategy for enhancing bioelectricity production while supporting sustainable waste management.

The objective of this study is to evaluate the effect of different PMFC configurations on electrical performance, specifically focusing on:

- the presence or absence of a membrane;
- the influence of *Trichoderma asperellum* Samuels, Lieckf. & Nirenberg inoculation in plant soil or MFC substrate.

Materials and methods

PMFC prototype design

In this experiment, a novel PMFC prototype was tested, characterized by the physical separation between the plant compartment and the microbial fuel cell (**Figure 3.1**). The plant pots were positioned above the MFC units, allowing drainage water to percolate downward into a container housing the cells. In this configuration, plants indirectly supplied nutrients to the soil microbial communities through nutrient-rich leachate derived from rhizodeposition processes. A key feature of this prototype is the spatial separation between the rhizosphere and the MFC, which enables more precise control of bioelectrochemical processes. This design greatly facilitates system maintenance while allowing the MFCs to retain their bioelectrochemical potential through continuous plant-derived nourishment.

Cell construction and materials

Each MFC consisted of three main components: an anode compartment, a separation element between the electrodes, and a cathode compartment.

The anode was composed of a stripped 1.5 mm electrical copper cable wrapped in two layers of aluminum foil. Despite its susceptibility to corrosion, aluminium can be considered a viable anode material in MFCs due to its high electrical conductivity, low cost and wide availability, particularly attractive for real-world applications [11,12,13]. The cathode consisted of a stripped electrical copper cable stapled to carbon felt. The separation element varied depending on the experimental configuration and consisted of soil alone or soil combined with carbon pellets and/or a nonwoven polyethylene fabric.

Cells were constructed on November 18 and 19, 2024, using plastic derivation boxes measuring 8 × 8 × 4 cm. Aluminum foil anodes and carbon felt cathodes both measured 8 × 8 cm, corresponding to a surface area of 64 cm^2. The anode thickness was approximately 2 mm, while the cathode thickness was approximately 5 mm. Carbon pellet layers, when present, were approximately 5 mm thick.

The soil consisted of a basic growing substrate named "COMPO SANA COMPACT – high-quality universal potting compost" the composition of which comprises: neutral sphagnum peat, green compost soil amendment, expanded perlite (<5%), compound mineral fertilizer and trace elements. Additional characteristics are summarized in **Table 3.1**. As this is an industrial product, the described properties are mostly standardized; however, being organic in nature, some characteristics may vary depending on the production batch.

The nonwoven polyethylene fabric was used as a membrane due to its low cost, easy availability, water resistance, air permeability, and recyclability. Activated carbon pellets (4 mm granules) were used to increase surface area and enhance microbial activity. **Figure 3.2** illustrates the components used for cell construction.

Table 3.1. Main physical characteristics of the growing substrate.

Main physical characteristics of the growing substrate	
pH (H_2O)	6.5
Electrical conductivity	0.50 dS/m
Dry bulk density	150 kg/m^3
Total porosity	90% v/v

Figure 3.1. Novel Plant microbial fuel cell prototype.

Figure 3.2. Cells components: derivation box, anode, non-woven fabric, carbon pellet, cathode and soil.

Experimental design and cell configurations

A total of 72 cells were constructed and divided into six experimental sets, each comprising 12 cells, based on different layering configurations and *Trichoderma* treatments.

Twelve Soil Control (SC) cells were assembled as follows:

- 30 g carbon pellets
- carbon felt cathode
- 100 g universal potting soil
- aluminum foil anode

Twelve Membrane Control (MC) cells included:

- 30 g carbon pellets
- carbon felt cathode
- nonwoven polyethylene fabric
- 100 g universal potting soil
- aluminum foil anode

SC and MC cells were irrigated using leachate from *Spathiphyllum lanceifolium* (Jacq.) Schott plants, arranged in trays of four cells per plant. The only difference between these two sets was the presence of the nonwoven membrane in MC cells.

Twelve *Trichoderma* Plant–Membrane (TPM) cells were assembled with:

- 30 g carbon pellets
- carbon felt cathode
- nonwoven polyethylene fabric
- 100 g universal potting soil
- aluminum foil anode

Twelve *Trichoderma* Plant–Soil (TPS) cells were assembled identically, except without the membrane.

TPM and TPS cells were irrigated with leachate from *S. lanceifolium* plants whose soil had been inoculated with *Trichoderma asperellum* Samuels, Lieckf. & Nirenberg on November 14, 2024, at a rate of 200 ml per kg of soil (approximately 170 ml per 850 g pot). The difference between the two sets was the presence of the nonwoven membrane in TPM cells.

Twelve *Trichoderma* Cell–Soil (TCS) cells consisted of:

- 30 g carbon pellets
- carbon felt cathode
- 150 g soil inoculated with *Trichoderma* suspension
- aluminum foil anode

Twelve *Trichoderma* Cell–Membrane (TCM) cells were identical, with the addition of a nonwoven polyethylene fabric between cathode and soil.

For TCS and TCM cells, the universal potting soil within the cells was inoculated with *T. asperellum* on November 11, 2024, at a rate of 200 ml per kg of soil. These cells were irrigated with leachate from non-inoculated *S. lanceifolium* plants. **Figure 3.3** shows a schematic diagram of the laboratory setup.

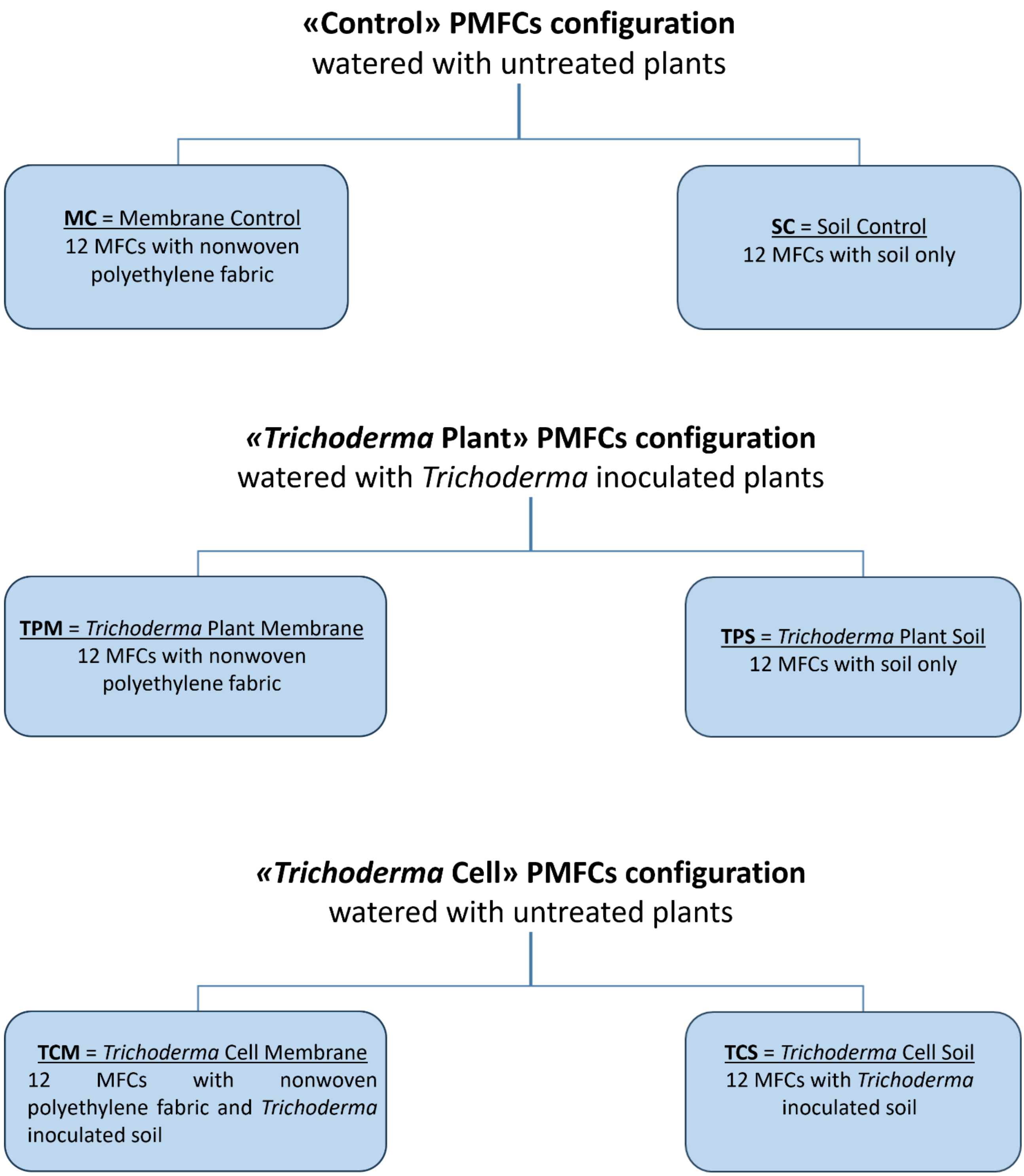

Figure 3.3. Schematic diagram of the laboratory setup.

Plant growth conditions

Spathiphyllum lanceifolium was selected due to its dense and extensive root system (**Figure 3.4**), which ensures a large rhizosphere surface area and promotes interactions between plant roots and electrogenic microorganisms. The species is well adapted to high soil moisture and partial submersion, conditions commonly encountered in PMFC systems.

Plants were grown under controlled environmental conditions with indirect natural or artificial light to avoid leaf damage. Irrigation was performed regularly, maintaining constant substrate moisture without prolonged waterlogging, at an average frequency of once per week. Ambient temperature was maintained between 20 and 27 °C.

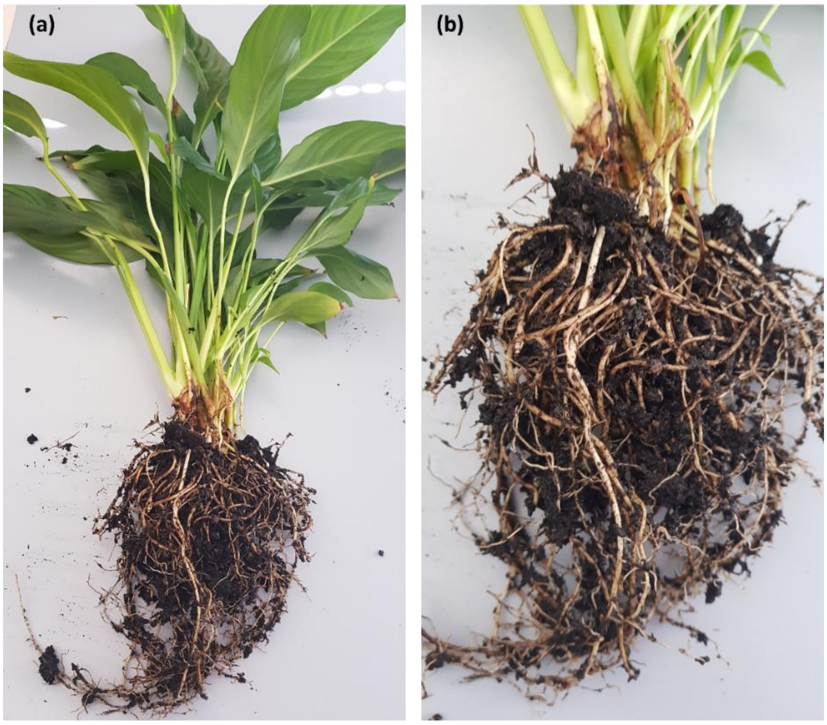

Figure 3.4. Root system of *Spathiphyllum lanceifolium* after removal from soil: (a) Whole plant with intact leaves and root system exposed; (b) Close-up view of the root apparatus showing the fine, fibrous structure and distribution of lateral roots still partially embedded in residual soil.

Electrical measurements and data analysis

Electrical performance was monitored using a Keithley 2000 digital multimeter. The following parameters were measured: open-circuit voltage (mV), short-circuit peak current (mA), and short-circuit current after 5 s (mA). Measurements were collected weekly from November 20, 2024, to April 24, 2025. Power figure of merit (mW) was calculated by multiplying open circuit voltage per short circuit peak current and per an arbitrary coefficient. According to theoretical maximum power point transfer (matched load), the coefficient could be set to ¼ [14].

All data were initially recorded manually and subsequently digitized in Microsoft Excel. Mean values for each parameter were calculated for each cell over the experimental period. Statistical analyses were performed using Past software (version 4.09) [15]. Normality was assessed prior to analysis. For normally distributed data, one-way ANOVA followed by Tukey's post-hoc test was applied. For non-normal distributions, the Kruskal–Wallis test followed by Dunn's post-hoc test was used. For all cases, a confidence of 95% was established, with configurations with *p*-values less than 0.05 being significant. Graphical representations generated in Past were used to facilitate interpretation of statistically significant differences among experimental groups. To compare temporal trends among the different configurations, the daily mean value for each electrical parameter was calculated for each PMFC group across the monitoring period.

To ensure that performance evaluation was not unduly influenced by electrode condition – particularly issues related to conductivity and material resistance – the state of the aluminium anode and the copper cathode cable embedded in the carbon felt was assessed upon disassembly of the cells at the end of the experimental period. Electrode condition was classified according to the following scale: Intact; Oxidised (still reasonably conductive though not optimal); Missing (fully degraded and non-conductive).

Results and discussion

For the voltage parameter the sets have a non-normal distribution. The non-parametric Kruskal-Wallis test is therefore performed, which does not return significance (**Table 3.2**). The subsequent Dunn's post hoc test with raw *p*-values returns a significant difference between the SC set and the TPS and TPM sets (**Table 3.3**). The violin and box plots show the distributions of the mean voltage values (mV) for each group (**Figure 3.5**).

For the peak current parameter all sets have normal value distributions. ANOVA is performed, which returns no significant difference (**Table 3.2**), confirmed by subsequent Tuckey's pairwise test (**Table 3.3**). The violin and box plots show the distributions of the mean peak current values (mA) for each group (**Figure 3.6**).

For the current after five seconds parameter the TCS set (*Trichoderma* inoculated in the cell) has a non-normal distribution. The non-parametric Kruskal-Wallis test is performed, which returns a significant difference between the samples (**Table 3.2**). Dunn's post hoc test with raw *p*-values shows a significant difference between the SC set and the TCS and TPM sets (**Table 3.3**). The violin and box plots show the distributions of the mean current after 5 second values (mA) for each group (**Figure 3.7**).

For the power parameter all sets have normal value distributions. ANOVA is performed, which returns no significant difference (**Table 3.2**) confirmed by subsequent Tuckey's pairwise test (**Table 3.3**). The violin and box plots show the distributions of the mean power values (mW) for each group (**Figure 3.8**).

Table 3.4 shows data of maximum, minimum and median values of distributions of mean values for each set for every measured parameter.

Table 3.2. Summary of the results of comparison between sets with different *Trichoderma* inoculation and membrane layering [*p* (same mean) when normal distributions were tested, *p* (same median) when non-normal distributions were tested, calculated using Montecarlo permutation]. Significantly different results are highlighted.

	Multiple Samples Tested: 12 "Soil Control", 12 "*Trichoderma* Plant Soil", 12 "*Trichoderma* Cell Soil", 12 "Membrane Control", 12 *Trichoderma* Plant Membrane, 12 "*Trichoderma* Cell Membrane"
Open circuit voltage	*p* (same): 0.2045
Peak current	*p* (same): 0.08196
Current 5 s	*p* (same): 0.0475
Power	*p* (same): 0.07131

Table 3.3. Summary of the results of post-hoc comparison between different configurations (SC = Soil Control; TPS = *Trichoderma* Plant Soil; TCS = *Trichoderma* Cell Soil; MC = Membrane Control; TPM = *Trichoderma* Plant Membrane; TCM = *Trichoderma* Cell Membrane) [*p* (same mean) when normal distributions were tested with Tuckey's, *p* (same median) when non-normal distributions were tested with Dunn's]. Significantly different results are highlighted.

		SC	TPS	TCS	MC	TPM	TCM
Voltage	SC		0.03958	0.2119	0.2989	0.01825	0.07506
	TPS	0.03958		0.4182	0.3081	0.7624	0.781
	TCS	0.2119	0.4182		0.8339	0.2662	0.595
	MC	0.2989	0.3081	0.8339		0.1863	0.4585
	TPM	0.01825	0.7624	0.2662	0.1863		0.5617
	TCM	0.07506	0.781	0.595	0.4585	0.5617	
Peak current	SC		0.6506	0.107	0.8978	0.4021	1
	TPS	2.155		0.8814	0.997	0.9988	0.7565
	TCS	3.704	1.549		0.6234	0.9809	0.1562
	MC	1.489	0.6652	2.215			0.9503
	TPM	2.709	0.5543	0.9952	1.219		0.5102
	TCM	0.2465	1.908	3.458	1.243	2.462	
Current after 5 seconds	SC		0.262	0.00753	0.06527	0.009475	0.4352
	TPS	0.262		0.121	0.4704	0.1408	0.7328
	TCS	0.00753	0.121		0.4071	0.9378	0.05847
	MC	0.06527	0.4704	0.4071		0.4526	0.2877
	TPM	0.009475	0.1408	0.9378	0.4526		0.06966
	TCM	0.4352	0.7328	0.05847	0.2877	0.06966	
Power	SC		0.2627	0.1319	0.9607	0.3384	0.9964
	TPS	3.078		0.9993	0.7586	1	0.5453
	TCS	3.57	0.4924		0.5408	0.9961	0.3343
	MC	1.175	1.903	2.395		0.837	0.9994
	TPM	2.867	0.2108	0.7032	1.692		0.6416
	TCM	0.6926	2.385	2.878	0.4824	2.174	

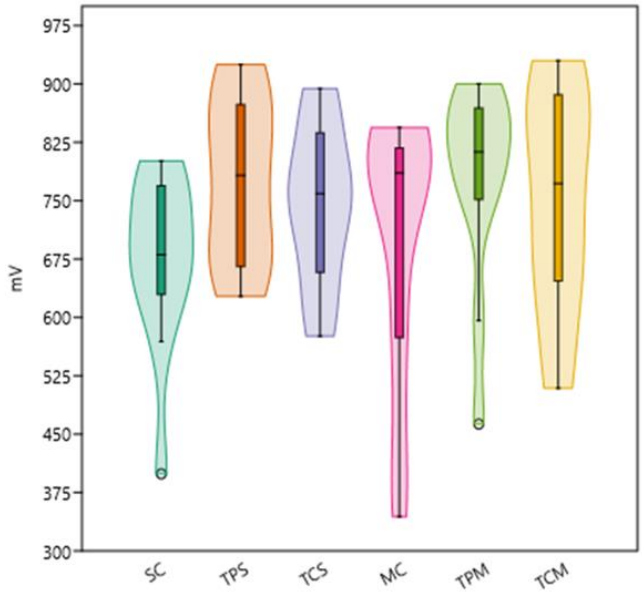

Figure 3.5. Violin and box plots comparing Soil Control (SC), *Trichoderma* Plant Soil (TPS), *Trichoderma* Cell Soil (TCS), Membrane Control (MC) *Trichoderma* Plant Membrane (TPM), *Trichoderma* Cell Membrane (TCM) groups of PMFCs in terms of distribution of mean values for the variable voltage.

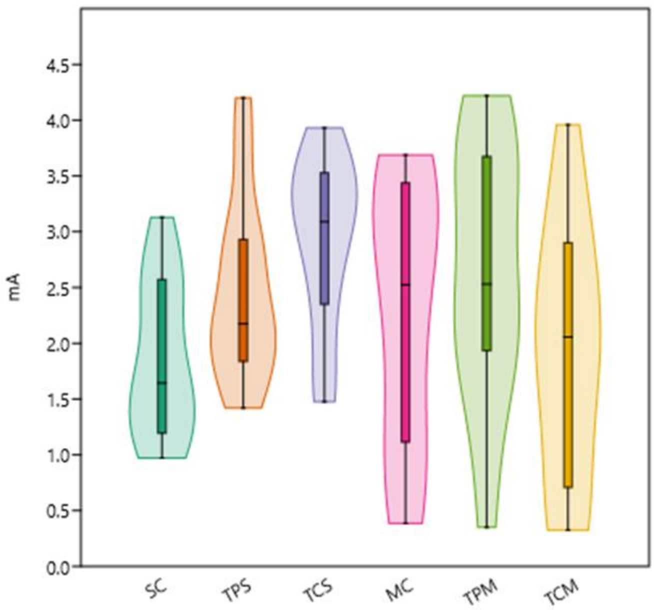

Figure 3.6. Violin and box plots comparing Soil Control (SC), *Trichoderma* Plant Soil (TPS), *Trichoderma* Cell Soil (TCS), Membrane Control (MC) *Trichoderma* Plant Membrane (TPM), *Trichoderma* Cell Membrane (TCM) groups of PMFCs in terms of distribution of mean values for the variable peak current.

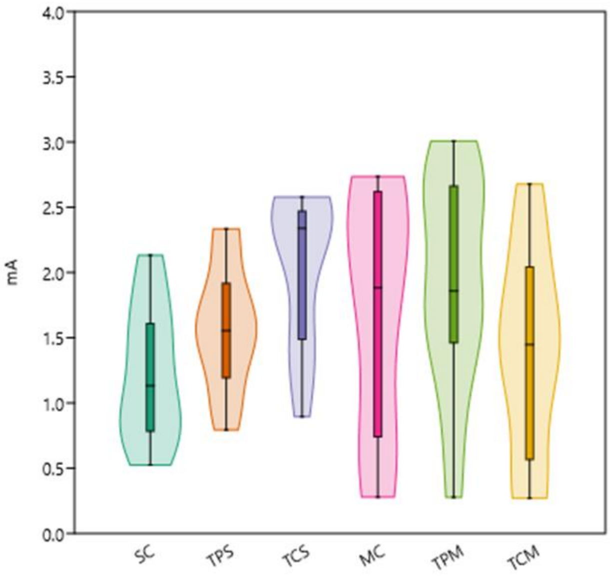

Figure 3.7. Violin and box plots comparing Soil Control (SC), *Trichoderma* Plant Soil (TPS), *Trichoderma* Cell Soil (TCS), Membrane Control (MC) *Trichoderma* Plant Membrane (TPM), *Trichoderma* Cell Membrane (TCM) groups of PMFCs in terms of distribution of mean values for the variable current after 5 seconds.

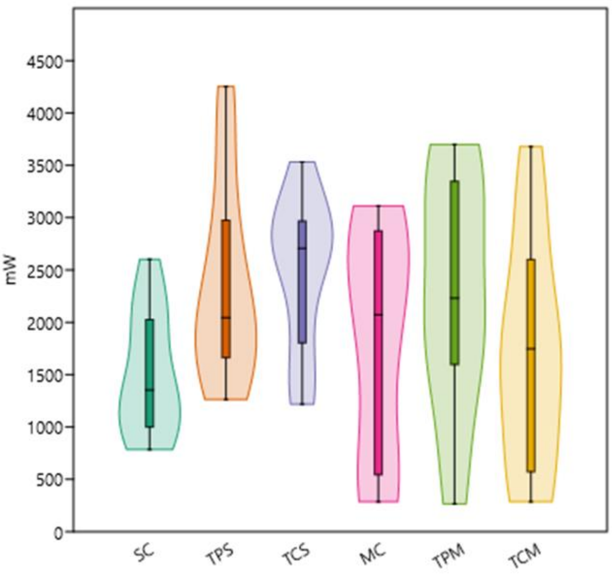

Figure 3.8. Violin and box plots comparing Soil Control (SC), *Trichoderma* Plant Soil (TPS), *Trichoderma* Cell Soil (TCS), Membrane Control (MC) *Trichoderma* Plant Membrane (TPM), *Trichoderma* Cell Membrane (TCM) groups of PMFCs in terms of distribution of mean values for the variable power.

Table 3.4. Maximum, minimum and median values of the average distributions of open circuit voltage, peak current, current after 5 s and power in PMFC groups: SC = Soil Control; TPS = *Trichoderma* Plant Soil; TCS = *Trichoderma* Cell Soil; MC = Membrane Control; TPM = *Trichoderma* Plant Membrane; TCM= *Trichoderma* Cell Membrane.

		Maximum	**Minimum**	**Median**
Voltage	SC	801	399	681
	TPS	925	627	783
	TCS	894	576	759
	MC	844	344	786
	TPM	900	463	812
	TCM	930	509	772
Peak current	SC	3.129	0.972	1.643
	TPS	4.199	1.419	2.175
	TCS	3.931	1.476	3.088
	MC	3.688	0.385	2.524
	TPM	4.219	0.351	2.531
	TCM	3.959	0.325	2.056
Current after 5 seconds	SC	2.132	0.524	1.133
	TPS	2.334	0.794	1.554
	TCS	2.579	0.894	2.339
	MC	2.735	0.278	1.883
	TPM	3.007	0.277	1.859
	TCM	2.677	0.269	1.447
Power	SC	2600.751	784.505	1352.958
	TPS	4252.145	1263.257	2044.605
	TCS	3531.297	1217.391	2706.130
	MC	3112.342	286.920	2073.269
	TPM	3698.499	265.267	2230.489
	TCM	3678.138	285.427	1746.116

For the voltage parameter, PMFCs treated with *Trichoderma* produced higher voltages than the control groups. In particular, *Trichoderma* treatment in the cell combined with the presence of a membrane (TCM) resulted in the highest absolute voltage value. Overall, the lowest voltages were consistently observed in the two control sets (SC and MC), with the membrane control (MC) showing slightly higher values than the soil control (SC). The highest voltage values were achieved by the sets in which *Trichoderma* was applied to the plant (TPM and TPS), compared to those in which *Trichoderma* was inoculated directly into the cell.

Regarding peak current, PMFCs treated with *Trichoderma* in the cell exhibited the highest median values, whereas PMFCs with *Trichoderma* treatment in the plant reached the highest maximum values. In all cases, *Trichoderma*-treated systems outperformed the control sets. The two plant-treated sets (TPS and TPM) achieved the highest maximum peak current values, with the membrane-containing set (TPM) showing superior performance.

For the current measured after 5 seconds, higher values were observed in PMFCs treated with *Trichoderma*, particularly when the treatment was applied directly to the cell. In this case, the median value was nearly twice that of the control. The highest maximum value was recorded in the membrane-equipped plant-treated set (TPM), while the highest median value was observed in the cell-treated, membrane-free set (TCS). The membrane control set (MC) also exhibited higher values compared to the control set without a membrane.

The power output followed trends consistent with those observed for voltage and current. Both *Trichoderma* treatments resulted in higher power generation than the control sets. Specifically, *Trichoderma* treatment applied to the plant yielded the highest maximum power values, whereas treatment in the cell resulted in the highest median power output.

Overall, these experimental results demonstrate that the electrical performance of PMFCs is influenced by different system configurations. Significant differences in voltage among the Soil Control (SC), *Trichoderma* Plant Soil (TPS), and *Trichoderma* Plant Membrane (TPM) sets suggest that the interaction between *Trichoderma* and the plant may promote enhanced electricity generation, compared to configurations in which *Trichoderma* is applied directly to the cell. Furthermore, the *Trichoderma* Plant Membrane (TPM) set appears to exhibit greater performance stability, as indicated by its higher median values relative to the other configurations.

Significant differences in the current after 5 seconds among the Soil Control (SC), *Trichoderma* Cell Soil (TCS), and *Trichoderma* Plant Membrane (TPM) sets further support this interpretation. These findings confirm that *Trichoderma* positively influences PMFC performance when inoculated either in the plant or directly in the cell.

Given the consistently low values recorded for the Soil Control set across all parameters, the experimental results clearly indicate that both the presence of *Trichoderma* and the inclusion of a membrane positively affect the electrical activity of PMFCs. However, when comparing the control sets with and without membranes, no statistically significant differences were observed, although slightly higher values were consistently measured in the membrane-equipped control. This suggests that the presence of a membrane may still contribute to improving the electrical performance of the cells.

The time series of data (**Figure 3.9**) confirms the trends and differences observed so far.

Voltage remained relatively high and stable for most groups until mid–late winter, but clear divergences emerged from late February onwards **(Figure 3.9a)**. The *Trichoderma* Plant Soil (TPS) group reached the highest early voltages (peaking close to 1.0 V in December) and then progressively declined, showing a marked drop in April. In contrast, *Trichoderma* Plant Membrane (TPM) maintained comparatively high and sustained voltages throughout the experiment, including the final weeks. The Soil Control (SC) displayed the most evident late decline, dropping sharply from late February and reaching the lowest end values, while the Membrane Control (MC) remained consistently higher than SC over time.

Power trends reflected current dynamics and highlighted stronger treatment effects **(Figure 3.9b)**. TPS showed the highest early power peak (≈4550 mW in December), whereas *Trichoderma* Cell Soil (TCS) achieved the maximum later (≈4444 mW around late January), followed by a progressive decrease. TPM exhibited the most persistent power output, remaining around ≈2.0–2.4 mW during the final phase, while SC and TPS decreased to the lowest values by the end of the monitoring period.

Figure 3.9c shows TCS produced the highest peak currents overall (maximum >5 mA in late January), while TPS showed high early peaks (≈4–4.5 mA) followed by a pronounced decline after February. Membrane-containing groups (MC, TPM, TCM) generally showed more sustained currents than their non-membrane counterparts, with TPM remaining relatively stable through late March–April. Current measured after 5 s showed similar behaviour **(Figure 3.9d)**. TCS group again reached the highest maximum (≈4 mA), TPS peaked around late January but then dropped to near-zero values by April, whereas TPM maintained the highest end-period values (≈2 mA), indicating better sustained delivery.

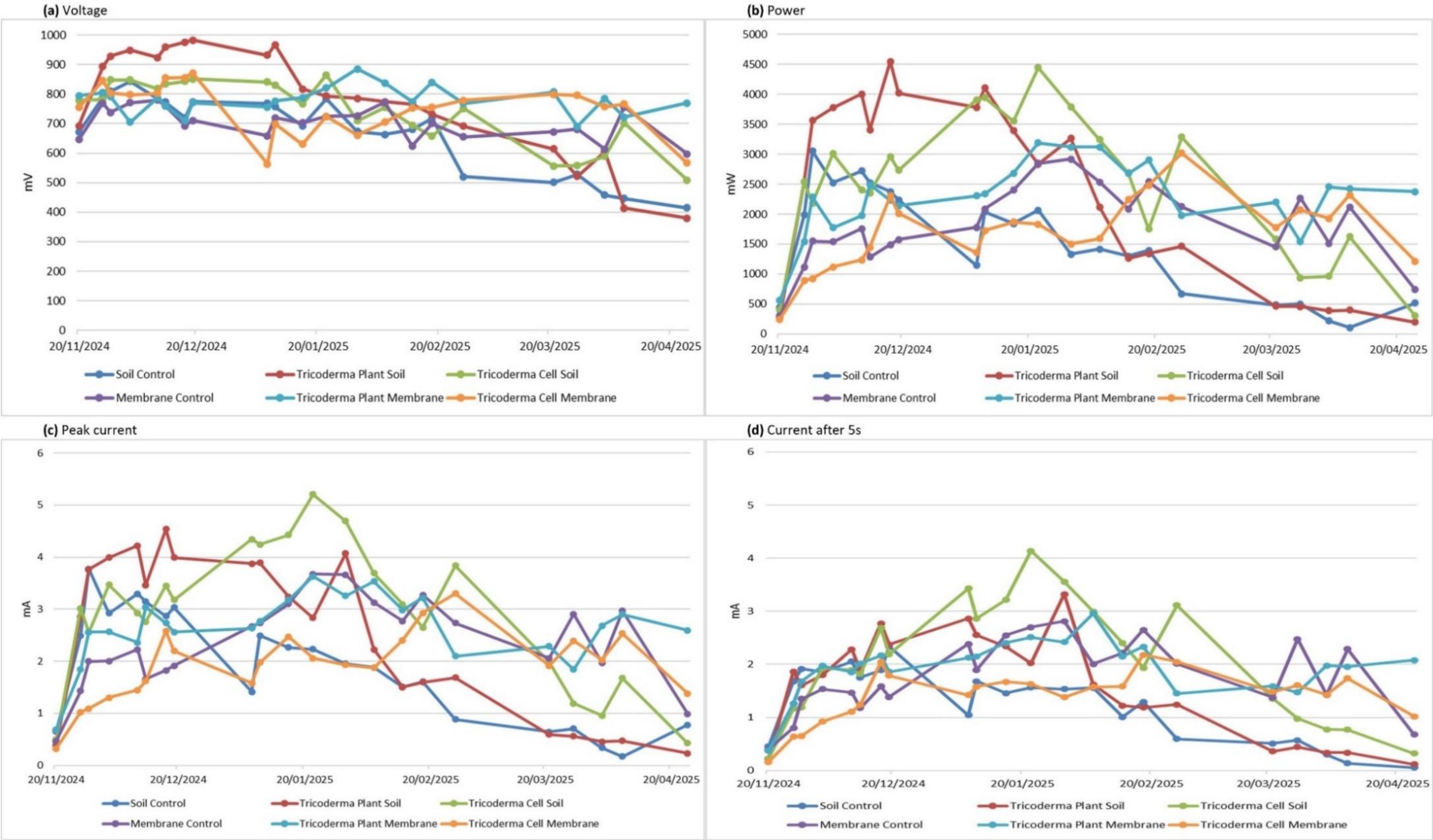

Figure 3.9. Comparison of group mean between different PMFCs configurations ("Soil Control", "*Trichoderma* Plant Soil", "*Trichoderma* Cell Soil", "Membrane Control", "*Trichoderma* Plant Membrane", "*Trichoderma* Cell Membrane") from 20 November 2024 to 24 April 2025 for each variable: (a) open circuit voltage, (b) power, (c) peak current, (d) current after 5 s.

Overall, *Trichoderma* inoculation enhanced electrical output compared with controls, while membrane inclusion was associated with improved persistence over time, particularly in the plant-inoculated configuration.
Concerning the physical state of the electrodes at dismantling, a summary is provided in **Table 3.5**. The aluminium anode was found to be in excellent condition across nearly all MFCs and experimental setups. Only two MFCs exhibited signs of oxidation (total percentage < 3%), and the anode was never found to be missing. In contrast, the copper cathode cable showed oxidation in the majority of cases across setups (percentage > 73%), was missing in one instance, and remained intact in approximately 25% of the observations.

Table 3.5. Physical state of the Aluminum Foil Anode and of the Copper Cathode Cable at dismantling in each experimental setup: SC = Soil Control; TPS = *Trichoderma* Plant Soil; TCS = *Trichoderma* Cell Soil; MC = Membrane Control; TPM = *Trichoderma* Plant Membrane; TCM= *Trichoderma* Cell Membrane.

		SC	TPS	TCS	MC	TPM	TCM
Aluminum Foil Anode	**Intact**	11	12	11	12	12	12
	Oxidised	1	.	1	.	.	.
	Missing	.	.	.	.	.	.
Copper Cathode Cable	**Intact**	.	.	4	4	3	7
	Oxidised	11	12	8	8	9	5
	Missing	1	.	.	.	.	.

Conclusions

This study demonstrates that PMFC electrical performance can be influenced by both biological enhancement and system configuration. Across all measured parameters, PMFCs treated with *Trichoderma asperellum* consistently outperformed the control systems, indicating that fungal inoculation represents a significant advantage for enhancing electrical activity and may be effectively exploited as a biological additive to improve PMFC performance.
Among the tested configurations, *Trichoderma* application to the plant proved particularly effective, yielding the highest maximum values of voltage, peak current, and power. This suggests that plant–fungus interactions can enhance rhizosphere processes and electron transfer more efficiently than direct inoculation into the cell. In contrast, *Trichoderma*

treatment applied straight to the cell primarily increased median values, indicating a beneficial but less stable effect over time. This may be due to the beneficial effect that *Trichoderma* has been shown to have directly on the roots, increasing the biomass and improving nutrient uptake [7,8,9] thereby likely promoting microbial activity and improving ion exchange processes as well.

The combined plant inoculation and membrane configuration (TPM) resulted in both high electrical output and improved performance stability, highlighting the importance of synergistic system design.

Another noteworthy outcome concerns the role of the membrane. Conventional PMFCs typically operate without artificial membranes, as the soil itself acts as a proton exchange medium [16,17]. In contrast, the prototype developed in this study physically separated the plant compartment from the electrochemical cell, allowing the specific evaluation of membrane inclusion within the cell stratification. Although the presence of a membrane did not produce statistically significant differences, membrane-equipped systems consistently exhibited higher values across all electrical parameters. This suggests that membrane inclusion may contribute to improving PMFC performance, particularly when combined with biological stimulation, but warrants further investigation.

Considering the possible effects of the electrodes on the obtained results, no specific quantitative analysis was conducted in the present work, but two main aspects can be highlighted. On the one hand, the integrity of the aluminium anode was preserved, suggesting that the PMFCs were adequately maintained and regularly irrigated; consequently, the anodic compartment likely remained under anoxic conditions throughout the experimental period. On the other hand, the cathode operates under fully oxic conditions and is directly exposed to water production associated with the bioelectrochemical reactions, which may accelerate material degradation over time. In this context, the conductivity and possible degradation of the copper cathode wiring may have influenced system performance, potentially introducing a bias in the interpretation of the measured bioelectrical outputs. From a practical standpoint, this represents a manageable limitation, as maintenance and replacement of the cathodic components in this type of prototype are relatively straightforward. Nevertheless, the adoption of non-oxidisable, highly conductive materials (e.g., stainless steel or graphite-based conductors) for cathode wiring should be considered in future design iterations to improve long-term stability and measurement reliability.

From an applied perspective, these findings indicate that optimizing PMFCs requires an integrated approach that combines biological additives, plant-mediated interactions, and appropriate physical configurations. Plant-associated *Trichoderma* inoculation emerges as a promising strategy to enhance both efficiency and stability, with good perspectives for outdoor or long-term applications.

Future research should focus on clarifying the mechanisms underlying plant–fungus–microbe interactions, systematically assessing the functional role of membranes in alternative PMFC designs, and evaluating long-term performance under varying environmental conditions. Expanding the range of plant species, microbial consortia, and system configurations will be essential to develop robust, scalable, and sustainable PMFC technologies for real-world deployment.

References

[1] B. E. Logan, B. Hamelers, R. Rozendal, U. Schröder, J. Keller, S. Freguia, P. Aelterman, W. Verstraete, K. Rabaey, Microbial Fuel Cells: Methodology and Technology, *Environmental Science & Technology* 40(17) (2006) 5181–5192, https://doi.org/10.1021/es0605016.

[2] R. Chakma, M. K. Hossain, P. Paramasivam, R. Bousbih, M. Amami, G. F. I. Toki, R. Haldhar, A.K. Karmaker, Recent Applications, Challenges, and Future Prospects of Microbial Fuel Cells: A Review. *Global Challenges* 9(5) (2025) 2500004, https://doi.org/10.1002/gch2.202500004.

[3] Y. Sharma, B. Li, The variation of power generation with organic substrates in single-chamber microbial fuel cells (SCMFCs), *Bioresource Technology* 101(6) (2010) 1844–1850, https://doi.org/10.1016/j.biortech.2009.10.040.

[4] R. Lepikash, D. Lavrova, D. Stom, V. Meshalkin, O. Ponamoreva, S. Alferov, State of the Art and Environmental Aspects of Plant Microbial Fuel Cells' Application, *Energies* 17(3) (2024) 752, https://doi.org/10.3390/en17030752.

[5] J. Poveda, P. Abril-Urias, C. Escobar, Biological Control of Plant-Parasitic Nematodes by Filamentous Fungi Inducers of Resistance: Trichoderma, Mycorrhizal and Endophytic Fungi, *Frontiers in Microbiology*, 11 (2020), https://doi.org/10.3389/fmicb.2020.00992.

[6] R. Tyśkiewicz, A. Nowak, E. Ozimek, J. Jaroszuk-Ściseł, Trichoderma: The Current Status of Its Application in Agriculture for the Biocontrol of Fungal Phytopathogens and Stimulation

of Plant Growth, *International Journal of Molecular Sciences*, 23(4) (2022) 2329, https://doi.org/10.3390/ijms23042329.

[7] S. L. Woo, R. Hermosa, M. Lorito, E. Monte, Trichoderma: a multipurpose, plant-beneficial microorganism for eco-sustainable agriculture. *Nature Reviews Microbiology*, *21*(5) (2023) 312-326, https://doi.org/10.1038/s41579-022-00819-5.

[8] L. B. P. R. dos Santos, N. Oliveira-Santos, D. P. S. D. Novais, V. Cruz-Magalhães, L. L. Loguercio, Beneficial plants-Trichoderma interactions on host tolerance to abiotic stresses: a meta-analysis. *Frontiers in Plant Physiology 3* (2025) 1569221, https://doi.org/10.3389/fphgy.2025.1569221.

[9] J. López-Bucio, R. Pelagio-Flores, A. Herrera-Estrella, Trichoderma as biostimulant: exploiting the multilevel properties of a plant beneficial fungus. *Scientia horticulturae 196* (2015) 109-123, https://doi.org/10.1016/j.scienta.2015.08.043.

[10] S. Rojas-Flores, R. Pimentel-Castillo, L. Cabanillas-Chirinos, L. M. Angelats Silva, Potential use of the fungus Trichoderma sp. as a plastic-reducing agent and electricity generator in microbial fuel cells, *Processes* 12(12) (2024) 2904, https://doi.org/10.3390/pr12122904.

[11] R. Dewangan, R. Ghosh, M. Behera, A. Mandal, From waste to watts: performance assessment of upcycled aluminium electrodes in microbial fuel cells for treatment of domestic wastewater, *Sustainable Energy Technologies and Assessments* 83 (2025) 104676, https://doi.org/10.1016/j.seta.2025.104676.

[12] A. Andola, R. R. Pandey, H. Pandey, A. Prakash, R. K. Pandey, Waste-to-Energy Conversion via a Dual-Chamber Microbial Fuel Cell Using Recycled Aluminum Beverage Cans. *ACS Sustainable Resource Management* 179-188 (2025), https://doi.org/10.1021/acssusresmgt.5c00473?urlappend=%3Fref%3DPDF&jav=VoR&rel=cite-as.

[13] S. S. Mirza, M. M. Al-Ansari, M. Ali, S. Aslam, M. Akmal, L. Al-Humaid, A. Hussain, Towards sustainable wastewater treatment: Influence of iron, zinc and aluminum as anode in combination with salt bridge on microbial fuel cell performance, *Environmental research*, *209* (2022) 112781, https://doi.org/10.1016/j.envres.2022.112781.

[14] M. Turhan, B. Dai, D. Yildirim, Analytical MPPT solution using Thevenin approach for solar panels, in: Proc. Eurocon 2013, Zagreb, Croatia, 1–4 July 2013, 803–808.

[15] Ø. Hammer, D.A.T. Harper, P.D. Ryan, PAST: paleontological statistics software package for education and data analysis, *Palaeontol. Electron*. 4 (1) (2001) 9.

[16] J. Greenman, R. Thorn, N. Willey, I. Ieropoulos, Energy harvesting from plants using hybrid microbial fuel cells; potential applications and future exploitation, *Frontiers in Bioengineering and Biotechnology* 12 (2024), https://doi.org/10.3389/fbioe.2024.1276176.

[17] R. Regmi, R. Nitisoravut, J. Ketchaimongkol, A decade of plant-assisted microbial fuel cells: Looking back and moving forward, *Biofuels* 9 (2018) 605–612. https://doi.org/10.1080/17597269.2018.1432272.

Chapter 4

Outdoor performance of Plant Microbial Fuel Cells: effects of plant life form and root architecture

Ilaria Brugellis, Silvia Assini

Abstract

Plant Microbial Fuel Cells (PMFCs) represent a promising bioelectrochemical technology for sustainable electricity generation, yet their practical applicability depends also on performance under outdoor conditions. This study investigates the influence of plant functional traits on PMFC electrical output through an outdoor experimental setup, focusing on the role of plant life form and root system architecture. A novel PMFC prototype featuring physical separation between the plant compartment and the microbial fuel cell was deployed outdoors in northern Italy. Thirty-six cells were realised and supplied with percolate derived from three native plant species characterized by distinct functional traits: *Allium angulosum* (geophyte, bulbous roots), *Lythrum salicaria* (hemicryptophyte, fasciculated roots), and *Carex remota* (hemicryptophyte, adventitious roots). Electrical performance was monitored weekly over one year by measuring voltage, peak current, current after five seconds, and calculated power output. Statistical analyses were conducted to assess differences among experimental groups.

Results demonstrated that plant species significantly affected PMFC electrical performance. Among the tested species, *Allium angulosum* consistently exhibited the highest values for measured parameters, indicating superior suitability for outdoor PMFC applications. While *Lythrum salicaria* reached comparable maximum power values, *Carex remota* showed consistently lower performance across all parameters. Electrode inspection suggests that maintaining electrode integrity under outdoor conditions is challenging, particularly for oxidation-prone cathodes, which may bias bioelectrochemical performance interpretation.

Overall, this study confirms that PMFC efficiency can be influenced by plant functional traits, particularly root system architecture and life form. The findings highlight the importance of trait-based plant selection for optimizing outdoor PMFC performance while supporting sustainable and biodiversity-conscious energy harvesting strategies.

Keywords

Plant Microbial Fuel Cell; Bioelectricity generation; Outdoor experimentation; Plant functional traits; Root system architecture; Life form; Native plant species; Sustainable energy

Introduction

Plant Microbial Fuel Cells (PMFCs) are an emerging bioelectrochemical technology that enables the conversion of solar energy into electricity through plant–microbe interactions in the rhizosphere [1]. While many studies have investigated PMFC performance under controlled laboratory conditions [2], their practical applicability depends on their behaviour in outdoor environments, where climatic variability, seasonal dynamics, and biotic interactions can strongly influence system efficiency. Field-based experimentation is therefore essential to assess the robustness, stability, and scalability of PMFCs under realistic operating conditions.

Within PMFCs, plants represent a key functional component. Through rhizodeposition, plants continuously supply organic compounds to the rhizosphere, sustaining electroactive microbial communities responsible for electron transfer at the anode. Consequently, plant functional traits play a central role in regulating substrate availability, microbial activity, and bioelectrochemical processes [3]. However, despite their importance, the influence of plant traits on PMFC performance remains insufficiently explored, particularly in outdoor settings.

Plant selection is a critical factor in optimizing PMFC efficiency. Relevant selection criteria include plant hardiness, growth rate, adaptability to environmental conditions, rhizosphere microbial communities, and the extensiveness and persistence of the root system [4,5,6]. Previous studies have shown that plant species with high photosynthetic efficiency, such as those employing C4 photosynthetic pathways, often enhance PMFC performance due to increased rhizodeposition, which provides substrates for microbial oxidation [7].

This outdoor experimental study investigates the influence of plant functional traits on the electrical performance of PMFCs by comparing different plant species characterized by distinct life forms and root system architectures. Traits such as root morphology, belowground biomass allocation, and life cycle strategies are expected to influence the extent and complexity of the rhizosphere, the structure of microbial communities, and electron transfer dynamics, ultimately affecting bioelectricity generation.

Root system architecture is especially relevant to PMFC performance, as it determines the spatial extent of the rhizosphere where plant–microbe interactions and electrochemical processes occur [8,9].

Plant life forms, as defined by the Raunkiær classification system, categorize species according to the position of their growth points during unfavourable seasons and reflect their survival strategies and biomass persistence. In Europe, this classification primarily refers to the position of winter buds and includes life forms such as therophytes, hemicryptophytes, geophytes, chamaephytes, and phanerophytes [10]. These groups differ in lifespan, seasonal biomass dynamics, and belowground persistence, factors that may significantly influence long-term PMFC performance in outdoor conditions.

The use of native plant species is particularly important for sustainable outdoor PMFC applications. Although non-native species may exhibit favorable electrical performance, their potential ecological impacts must be carefully assessed. Plant selection should therefore balance bioelectrochemical efficiency with biodiversity conservation and ecosystem sustainability.

The experiment was conducted using three native plant species selected for their botanical characteristics, as well as for their suitability to local environmental conditions. This study tests the hypothesis that PMFC electrical performance is significantly influenced by plant functional traits, particularly root system architecture and life form.

Materials and methods

PMFC prototype design

A novel PMFC prototype featuring physical separation between the plant compartment and the microbial fuel cell was tested (**Figure 4.1**). Plants were placed above the MFC units, allowing nutrient-rich leachate from rhizodeposition to percolate into the cell container and sustain soil microbial communities. This configuration enables improved control of bioelectrochemical processes, simplifies system maintenance, and preserves MFC performance through continuous plant-derived nutrient supply. The PMFCs were installed at Cascina Cassinino, located at Sommo (Province of Pavia, Lombardy), in the western Po Plain of North Italy (**Figure 4.2**). The PMFCs were installed on a veranda protected by a canopy, allowing exposure to natural environmental conditions while simultaneously enabling measurement and maintenance procedures to be carried out under adverse weather conditions.

Cell construction and materials

Cells were constructed on May 7 and 8, 2024, using plastic derivation boxes measuring 8 × 8 × 4 cm. Aluminum foil anodes and carbon felt cathodes both measured 8 × 8 cm, corresponding to a surface area of 64 cm^2.

Figure 4.1. Outdoor configuration of the PMFC prototype.

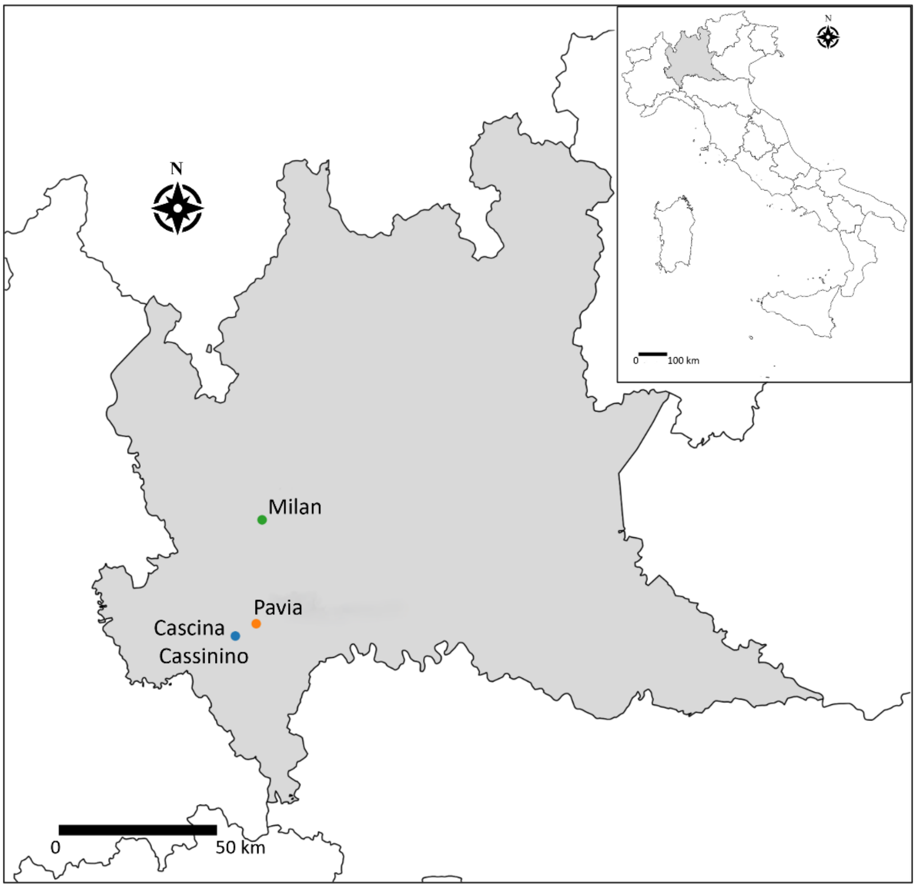

Figure 4.2. Geographical location of the site where the outdoor PMFCs testing took place (Cascina Cassinino = blue dot). The province of the location (Pavia = orange dot) and the regional capital (Milan = green dot) are also indicated.

Cells were assembled as follows:

- 35 g carbon pellets
- carbon felt cathode
- 100 g universal potting soil
- aluminum foil anode

The anode thickness was approximately 2 mm, while the cathode thickness was approximately 5 mm. The anode was composed of a stripped 1.5 mm electrical cable wrapped in two layers of aluminum foil. Although prone to corrosion, aluminium remains a viable anode material for MFCs owing to its high electrical conductivity, low cost, and widespread availability, making it especially appealing for practical, real-world applications [11,12,13]. The cathode consisted of a stripped electrical copper cable stapled to carbon felt. Carbon pellet layer were approximately 5 mm thick.

The universal potting soil was a commercial growing substrate named "COMPO SANA COMPACT" composed by: neutral sphagnum peat, green compost soil amendment, expanded perlite (<5%), compound mineral fertilizer and trace elements. Additional physical characteristics reported on the packaging were: pH (H_2O) = 6.5; Electrical conductivity = 0.50 dS/m; Dry bulk density = 150 kg/m^3; Total porosity = 90% v/v. Although most proterties are standardized (as an industrial product) the substrate was obviously organic, thus some characteristics were unpredictable and related on the production batch.

Experimental design

To assess the suitability of different plant species for outdoor PMFC applications, 36 microbial fuel cells were realised and organized into three sets of 12 cells, each supplied with percolate derived from plants characterized by distinct functional traits. Plant species selection was based on previous literature analyses [14], and only native species were chosen following a biodiversity-oriented approach.

The plant species selected for the experiment were *Carex remota* L., *Lythrum salicaria* L., and *Allium angulosum* L.. Their main botanical and ecological characteristics [15,16] are summarised in **Tables 4.1**, **4.2** and **4.3** respectively.

The experimental design and the evaluated functional traits of each species are summarized in **Table 4.4**.

Table 4.1. Main botanical and ecological characteristics of *Carex remota* L. (see **Annex I** for photo credits).

***Carex remota* L.**	
Family	Cyperaceae
Life form	Hemicryptophyte
General morphological characteristics	Perennial herbaceous plant, 30-60 cm, with dense bushes and short rhizomes
Habitat	Wet woods, mainly ash forests but also thickets of *Alnus glutinosa* (L.) Gaertn., stream banks, generally in shaded environments on waterlogged soil
Distribution in Italy	Present throughout the territory
Altitudinal distribution	From 0 to 1000 meters above sea level
Flowering season	From April to July

Table 4.2. Main botanical and ecological characteristics of *Lythrum salicaria* L. (see **Annex I** for photo credits).

***Lythrum salicaria* L.**	
Family	Lythraceae
Life form	Hemicryptophyte
General morphological characteristics	Perennial herbaceous plant, rhizomatous, with simple or branched erect stems, reddish, slightly woody at the base, tetragonal, pubescent. Height 4 to 20 dm. The leaves are elliptical, sessile, lanceolate, heart-shaped at the base, with entire margins; those at the base are opposite, while those above are alternate. Pink-purple flowers bloom from axillary bracts, forming long, showy terminal spikes
Habitat	Wetlands, marshes, lake and river banks, roadsides, brackish environments
Distribution in Italy	Present throughout the territory
Altitudinal distribution	From 0 to 2000 meters above sea level
Flowering season	From May to September

Table 4.3. Main botanical and ecological characteristics of *Allium angulosum* L. (see **Annex I** for photo credits).

***Allium angulosum* L.**		
Family	Amaryllidaceae	
Life form	Geophyte	
General morphological characteristics	Erect, rigid stems with a triangular cross-section, ranging from 30 to 70 cm in height. Linear basal leaves, narrow and deep green in colour. Spherical (or hemispherical) umbel inflorescences, pink in colour.	
Habitat	Wetlands, meadows, stream banks and ditches	
Distribution in Italy	Piedmont, Lombardy, Trentino Alto Adige, Veneto, Friuli Venezia Giulia, Emilia Romagna, Umbria	
Altitudinal distribution	From 0 to 500 meters above sea level	
Flowering season	From May to September	

Table 4.4. Experimental design and plant functional traits associated with each species.

N° of MFCs	**Plant species**	**Life form**	**Root type**
12	*Allium angulosum L.*	Geophyte	Bulbous
12	*Lythrum salicaria L*.	Hemicryptophyte	Fasciculated
12	*Carex remota L.*	Hemicryptophyte	Adventitious

Climatic data sources

For the period during which PMFC electrical measurements were collected, climatic data were retrieved from validated databases associated with the weather stations closest to the experimental site.

Monthly maximum, mean, and minimum temperatures (°C), as well as monthly precipitation (mm), were obtained from the Meteonetwork dataset of the Zinasco Vecchio (PV) weather station [17], located 4.4 km from the experimental site. Monthly average relative humidity (%) was retrieved from the ARPA Lombardia dataset of the Pavia via Folperti weather station [18,19], located 13.5 km from the experimental site. The extrapolated data are summarized in

Table 4.5 and provide contextual information useful for interpreting seasonal variations in PMFC electrical performance throughout the experimental period.

Table 4.5. Summary of climatic data extrapolated from the Zinasco Vecchio weather station (Maximum temperature, Average temperature, Minimum temperature, Rain) and the Pavia via Folperti weather station (Average relative humidity) for each month from May 2024, to May 2025.

	Maximum temperature (°C)	Average temperature (°C)	Minimum temperature (°C)	Rain (mm)	Average Relative Humidity (%)
May 2024	27.4	17.79	9.4	245.0	77.8
Jun 2024	33.9	21.99	12.6	56.2	71.8
Jul 2024	36.4	26.42	15.7	29.0	66
Aug 2024	35.3	26.35	17.8	24.0	68.2
Sep 2024	33.8	19.52	9.8	90.6	75.7
Oct 2024	22.9	15.70	8.4	217.2	93.6
Nov 2024	21.9	7.69	-1.4	15.2	90.1
Dec 2024	14.4	3.92	-2.6	48.8	85.6
Jan 2025	12.7	4.28	-3.3	75.6	93.9
Feb 2025	15.1	6.25	-0.4	57.2	90.8
Mar 2025	22.5	10.71	0.9	59.0	76.5
Apr 2025	27.4	15.02	4.7	109.6	72.2
May 2025	30.9	18.79	10.3	83.6	68

Electrical measurements and data analysis

Electrical performance measurements were carried out using an AMPROBE 37XR-A multimeter. Open-circuit voltage (mV), short-circuit peak current (mA), and short-circuit current after 5 s (mA) were measured weekly from 14 May 2024 to 12 May 2025. Power figure of merit (mW) was calculated by multiplying open circuit voltage per short circuit peak current and per an arbitrary coefficient. According to theoretical maximum power point transfer (matched load), the coefficient could be set to ¼ [20].

All data were initially recorded manually and subsequently digitized in Microsoft Excel. Mean values for each parameter were calculated for each cell over the experimental period. Statistical analyses were performed to compare electrical performance among the experimental groups. One-way ANOVA followed by Tukey's post-hoc was applied when data distributions met normality assumptions, whereas the Kruskal–Wallis non-parametric test for equal medians, followed by Dunn's post hoc test using raw values, was employed for non-normal distributions. All statistical analyses were performed using Past 4.09 software [21]. For all analyses, a 95%

confidence level was applied, and *p*-values below 0.05 were considered statistically significant. Graphical outputs generated in Past or Excel were used to facilitate the interpretation of differences among experimental groups. To assess temporal trends across configurations, the daily mean of each electrical parameter was calculated for each PMFC group throughout the monitoring period.

To assess potential correlations between the measured parameters and the climatic variables, Spearman's rank correlation analysis (r_s) was performed. For this purpose, the overall monthly mean of all PMFC units was calculated for the considered parameter.

To assess and reduce bias in performance evaluation due to electrode condition (e.g. conductivity or resistance issues), the aluminium anode and the copper cathode cable embedded in the carbon felt were inspected after cell disassembly at the end of the experiment. Electrode condition was classified as: Intact; Oxidised (still conductive, though suboptimal); or Missing (fully degraded and non-conductive).

Results and discussion

For the voltage parameter the distributions of mean values were normal. ANOVA indicates no significant difference between sample means (**Table 4.5**), confirmed by subsequent Tuckey's pairwise test (**Table 4.6**). The violin and box plots show the distributions of the mean voltage values (mV) for each group (**Figure 4.3**).

For the peak current parameter the distributions of mean values were normal. ANOVA indicates significant differences between sample means (**Table 4.5**). Tuckey's pairwise test shows *Allium angulosum* set being significantly different from the other two species sets (**Table 4.6**). The violin and box plots show the distributions of the mean peak current values (mA) for each group (**Figure 4.4**).

For the current after five seconds parameter the distribution of mean values of MFCs wetted with percolate of *Allium angulosum* were not normal. Kruskal-Wallis test indicates significant differences between sample medians (**Table 4.5**). Dunn's post hoc shows *Allium angulosum* set being significantly different from *Carex remota* set (**Table 4.6**). The violin and box plots show the distributions of the mean current after 5 second values (mA) for each group (**Figure 4.5**).

For the power parameter the distribution of mean values was normal. ANOVA indicates significant differences between sample means (**Table 4.5**). Tuckey's pairwise test shows *Allium angulosum* set being significantly different from the *Carex remota* set (**Table 4.6**). The violin and box plots show the distributions of the mean power values (mW) for each group (**Figure 4.6**). In **Table 4.7** there are the data of maximum, minimum and median values of the average distributions for the analysed parameters.

Table 4.5. Summary of the results of comparison between sets with different plants [*p* (same mean) when normal distributions were tested with ANOVA, *p* (same median) when non-normal distributions were tested with Kruskal-Wallis, calculated using Montecarlo permutation]. Significantly different results are highlighted.

	Multiple Samples Tested: 12 "*Carex remota* PMFCS", 12 "*Lythrum salicaria* PMFCs", 12 "*Allium angulosum* PMFCs"
Open circuit voltage	*p* (same): 0.4663
Peak current	*p* (same): 0.00096
Current 5 s	*p* (same): 0.001099
Power	*p* (same): 0.00832

Table 4.6. Summary of the results of post-hoc comparison between sets with different plants [*p* (same mean) when normal distributions were tested with Tuckey's, *p* (same median) when non-normal distributions were tested with Dunn's]. Significantly different results are highlighted.

		Carex remota	*Lythrum salicarica*	*Allium angulosum*
Voltage	*Carex remota*		0.8255	0.7899
	Lythrum salicarica	0.8368		0.4338
	Allium angulosum	0.9288	1.766	
Peak current	*Carex remota*		0.2105	0.0004355
	Lythrum salicarica	2.442		0.04015
	Allium angulosum	6.05	3.609	
Current after 5 seconds	*Carex remota*		0.06708	0.0002231
	Lythrum salicarica	0.06708		0.06286
	Allium angulosum	0.0002231	0.06286	
Power	*Carex remota*		0.4137	0.005186
	Lythrum salicarica	1.817		0.1061
	Allium angulosum	4.781	2.964	

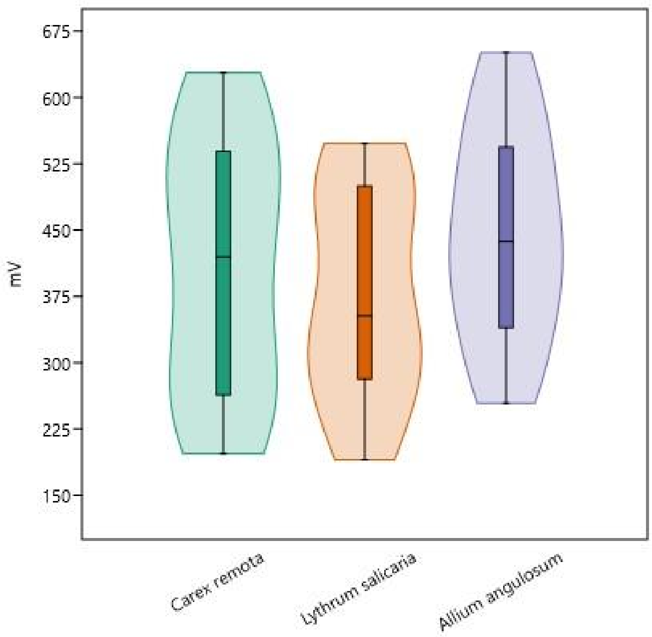

Figure 4.3. Violin and box plots comparing PMFC sets watered respectively with *Carex remota*, *Lythrum salicaria* and *Allium angulosum* leachate in terms of distribution of mean values for the variable voltage.

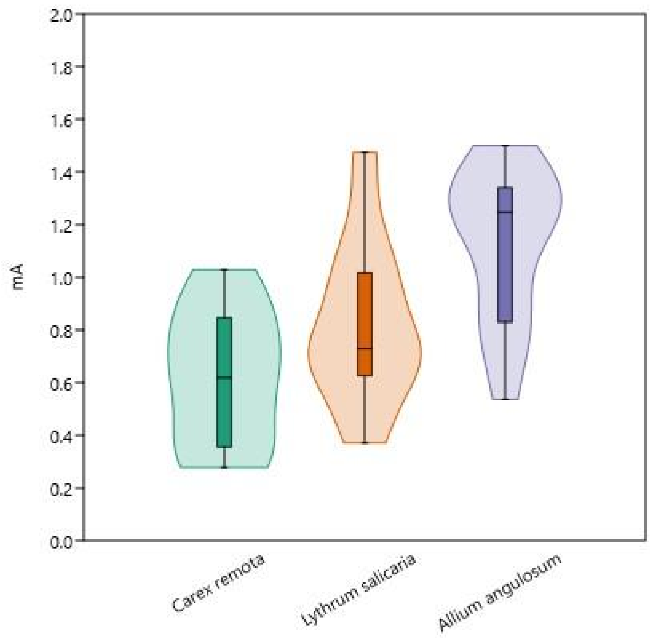

Figure 4.4. Violin and box plots comparing PMFC sets watered respectively with *Carex remota*, *Lythrum salicaria* and *Allium angulosum* leachate in terms of distribution of mean values for the variable peak current.

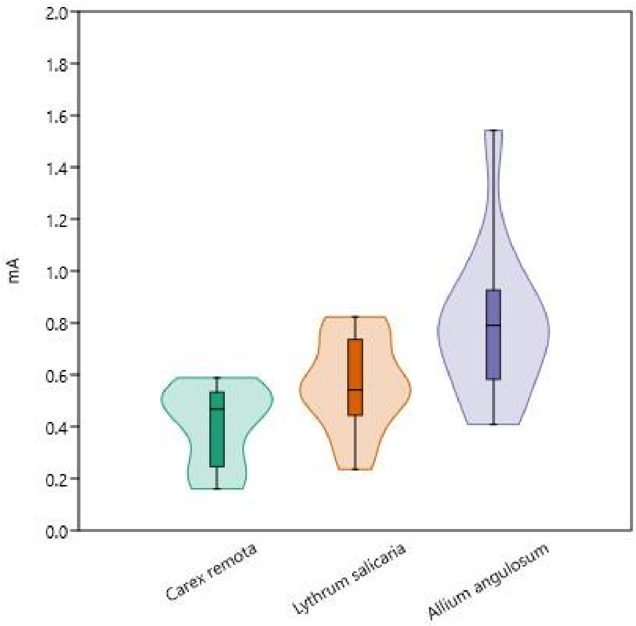

Figure 4.5. Violin and box plots comparing PMFC sets watered respectively with *Carex remota*, *Lythrum salicaria* and *Allium angulosum* leachate in terms of distribution of mean values for the variable current after 5 seconds.

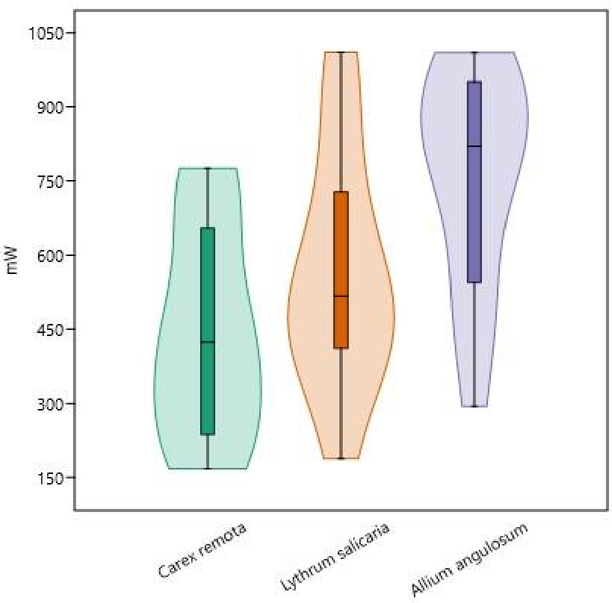

Figure 4.6. Violin and box plots comparing PMFC sets watered respectively with *Carex remota*, *Lythrum salicaria* and *Allium angulosum* leachate in terms of distribution of mean values for the variable power.

Table 4.7. Maximum, minimum, and median values of mean open-circuit voltage, peak current, current after 5 seconds, and power for PMFC groups irrigated with percolate from *Carex remota*, *Lythrum salicaria*, and *Allium angulosum.*

		Maximum	**Minimum**	**Median**
Voltage	*Carex remota*	628	197	420
	Lythrum salicaria	548	**190**	353
	Allium angulosum	**651**	254	**437**
Peak current	*Carex remota*	1.029	**0.278**	0.619
	Lythrum salicaria	1.475	0.371	0.729
	Allium angulosum	**1.500**	0.536	**1.247**
Current after 5 seconds	*Carex remota*	0.589	**0.160**	0.468
	Lythrum salicaria	0.823	0.235	0.542
	Allium angulosum	**1.542**	0.408	**0.790**
Power	*Carex remota*	775.223	**167.797**	424.228
	Lythrum salicaria	**1010.401**	188.661	517.446
	Allium angulosum	1009.756	294.213	**820.507**

For voltage, PMFCs with *Allium angulosum* exhibited higher values than those associated with the other two species. *Carex remota* and *Allium angulosum* showed comparable distributions; however, *Allium angulosum* displayed slightly higher median and maximum values, while minimum values were identical.

Regarding peak current, PMFCs with *Allium angulosum* again showed the highest values. In this case, *Allium angulosum* and *Lythrum salicaria* exhibited similar maximum values, whereas *Carex remota* consistently showed the lowest values.

For current measured after 5 seconds, PMFCs with *Allium angulosum* clearly outperformed the other species, with values that were markedly higher and not overlapping with those observed for *Carex remota* and *Lythrum salicaria*.

Power output followed a slightly different pattern. PMFCs with *Lythrum salicaria* reached the highest maximum power, although this value was very close to that observed for *Allium angulosum*. In contrast, the highest median power was recorded for *Allium angulosum*, while *Carex remota* exhibited the lowest power values overall.

The time-series analysis revealed distinct performance patterns among the three species for all monitored parameters (**Figure 4.7**). *Allium angulosum* consistently exhibited the highest electrical outputs throughout the initial phase of the experiment (May–July 2024). Peak values were frequently higher than those recorded for the other species, indicating a stronger early-season bioelectrochemical activity. After this initial period, all species showed a marked decline across all parameters, likely reflecting seasonal changes in temperature, plant physiological activity, and microbial dynamics. Despite this general decline, *Allium angulosum* maintained slightly higher and more stable values than *Carex remota* and *Lythrum salicaria* during the mid- and late-season intervals.

Lythrum salicaria showed intermediate performance, with moderate voltage (**Figure 4.7a**) and current (**Figure 4.7c** and **4.7d**) values throughout the experiment. Meanwhile, *Carex remota* generally produced the lowest electrical outputs, particularly in terms of peak current (**Figure 4.7c**) and power (**Figure 4.7b**), although occasional short-lived increases were observed.

Across all species, the temporal patterns of voltage, power, peak current, and current after 5 s displayed coherent trajectories: an initial peak during the first months, followed by a progressive reduction and stabilization toward the end of the monitoring period.

These results confirm that plant species differ in their ability to sustain PMFC performance over time and suggest that plant functional traits may play a key role in shaping bioelectrochemical output in outdoor PMFC systems.

Overall, the results demonstrate that PMFC electrical performance is influenced by plant species. Among the species tested, *Allium angulosum* consistently showed the best performance across most electrical parameters, indicating its greater suitability for outdoor PMFC applications.

Table 4.8 provide a summary of the electrodes conditions in each tested PMFCs group. Overall the aluminium anodes were found in similar proportions as Intact (44%) and Oxidised (52%), with only one Missing. In contrast, the copper cathode cables were found to be predominantly Oxidised across setups (>86%), with 11% Intacts and two cases Missing.

Table 4.8. Physical state of the Aluminum Foil Anode and of the Copper Cathode Cable at dismantling in each experimental setup of PMFCs supplied by *Carex remota*, *Lythrum salicaria* and *Allium angulosum* plant species.

		Carex remota	*Lythrum salicaria*	*Allium angulosum*
Aluminum Foil Anode	**Intact**	6	7	3
	Oxidised	6	5	8
	Missing	.	.	1
Copper Cathode Cable	**Intact**	2	.	2
	Oxidised	10	12	9
	Missing	.	.	1

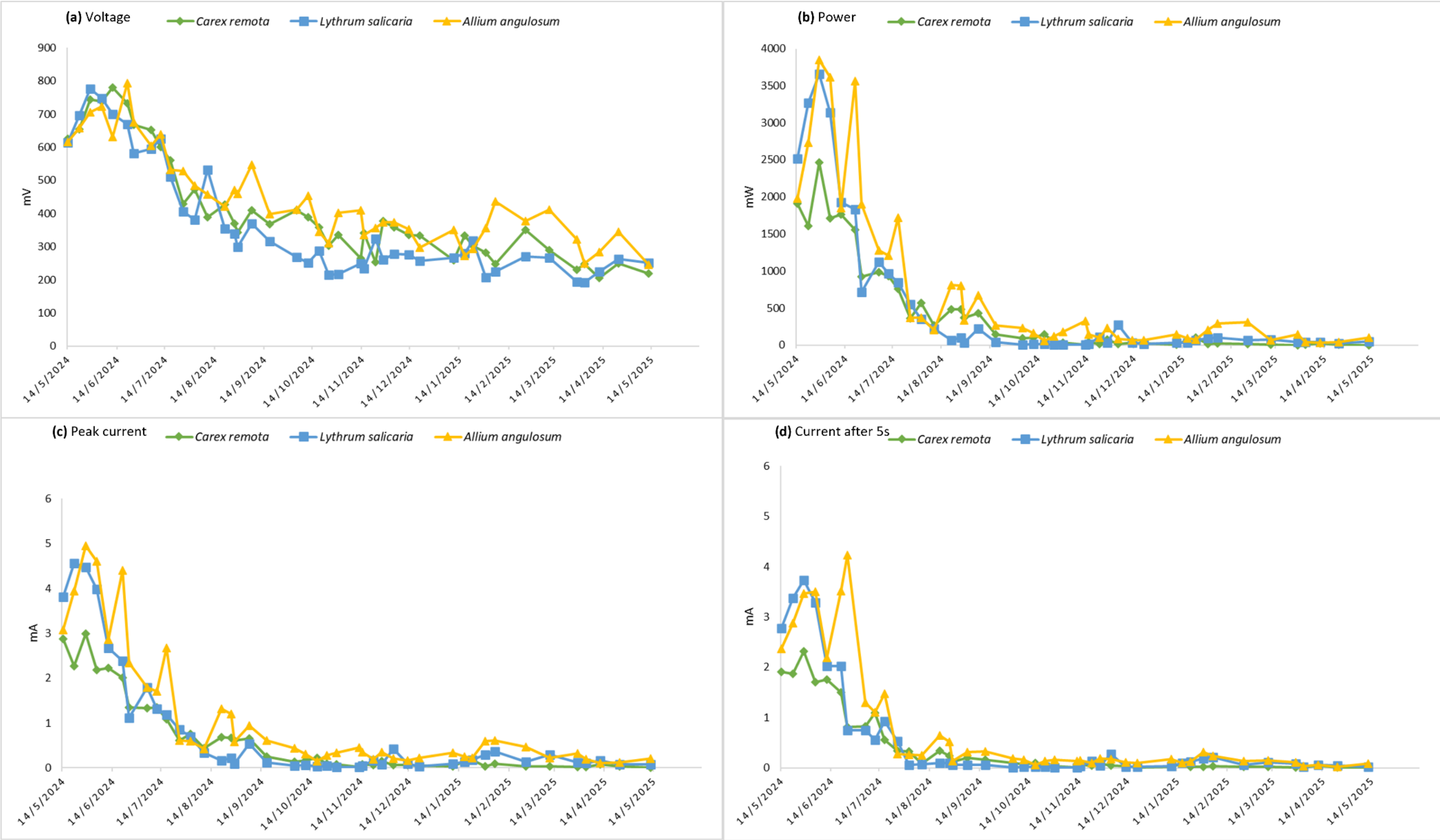

Figure 4.7. Comparison of group mean between PMFCs groups plant-fed by different species (*Carex remota*, *Lythrum salicarica*, *Allium angulosum*) from 14 May 2024 to 12 May 2025 for each variable: (**a**) open circuit voltage, (**b**) power, (**c**) peak current, (**d**) current after 5 s.

Figures 4.8-4.10 show graphical representations of the climatic data reported in **Table 4.5**, respectively Temperatures (°C), Rain (mm) and Average RH%.

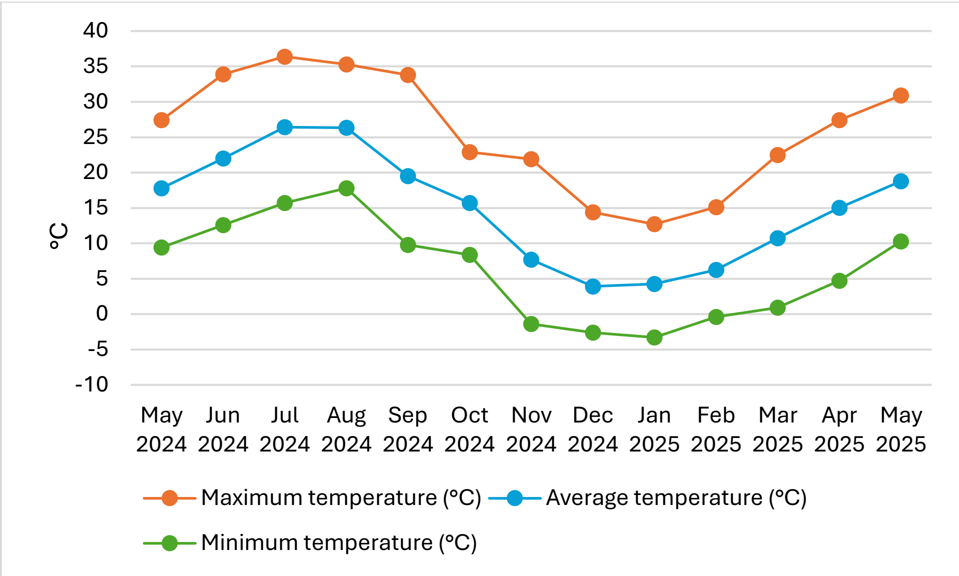

Figure 4.8. Graph showing the trend in monthly maximum, average and minimum temperatures (°C) from May 2024 to May 2025.

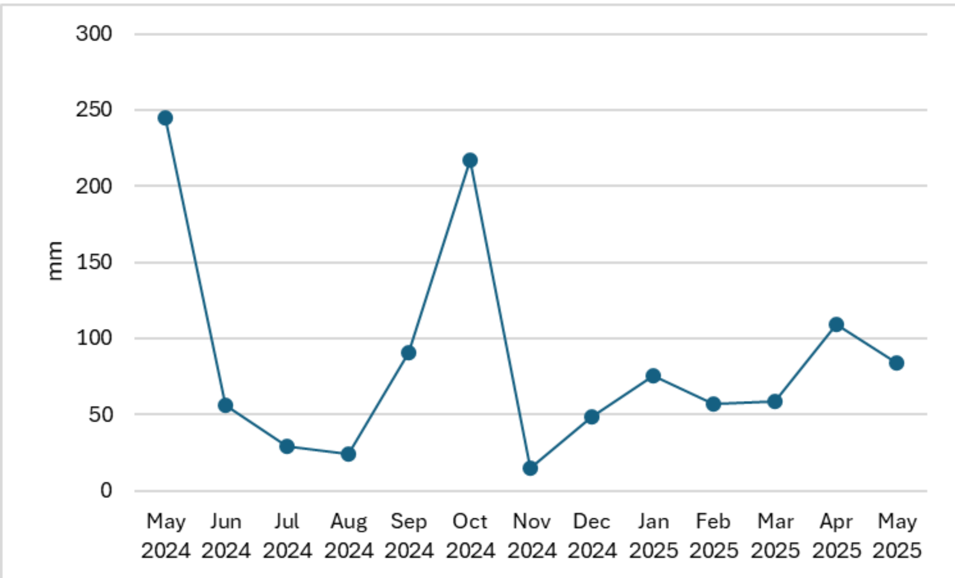

Figure 4.9. Graph showing the trend in monthly rain (mm) from May 2024 to May 2025.

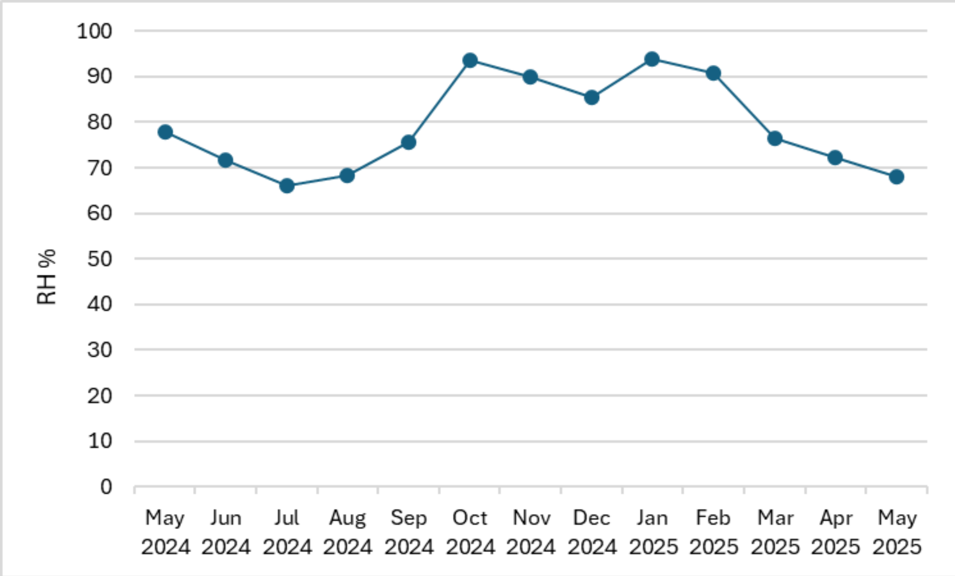

Figure 4.10. Graph showing the trend in monthly average Relative Humidit (%) from May 2024 to May 2025.

To evaluate potential monotonic correlation between the electrical parameters measured by the PMFCs and the climatic variables, Spearman's rank correlation coefficient (r_s) was calculated. For each month, the overall mean of all PMFC units (i.e., all sets supplied with leachate from the three plant species) was computed for voltage (mV) and power (mW) parameters. Current was excluded from the analysis, as it exhibited trends closely mirroring those of power, of which it is a component. Among termic variables (°C), only average temperature was considered. The results of the Spearman correlation analysis (r_s and p-value) are reported in **Table 4.9**.

A statistically significant moderate positive correlation was observed between voltage and average temperature (r_s = 0.55571), suggesting that voltage tends to increase as temperature increases. **Figure 4.11** displays the scatterplot of average temperature versus mean voltage values, highlighting this monotonic relationship.

Table 4.9. Summary of Spearman's correlation analysis results (r_s and *p*-value) between total monthly mean of voltage (mV) and power (mW) output of PMFCs and the corresponding monthly climatic variables: average temperature (°C), rain (mm) and average Relative Umidity (%). Significantly different results are highlighted.

	Monthly average temperature (°C)	Monthly rain (mm)	Monthly average RH (%)
Total monthly voltage mean of PMFCs (mV)	r_s = 0.55571 *p*-value = 0.048629	r_s = -0.12655 *p*-value = 0.68037	r_s = -0.18157 *p*-value = 0.55274
Total monthly power mean of PMFCs (mW)	r_s = 0.54396 *p*-value = 0,054647	r_s = -0.17582 *p*-value = 0,56558	r_s = -0,15934 *p*-value = 0,60309

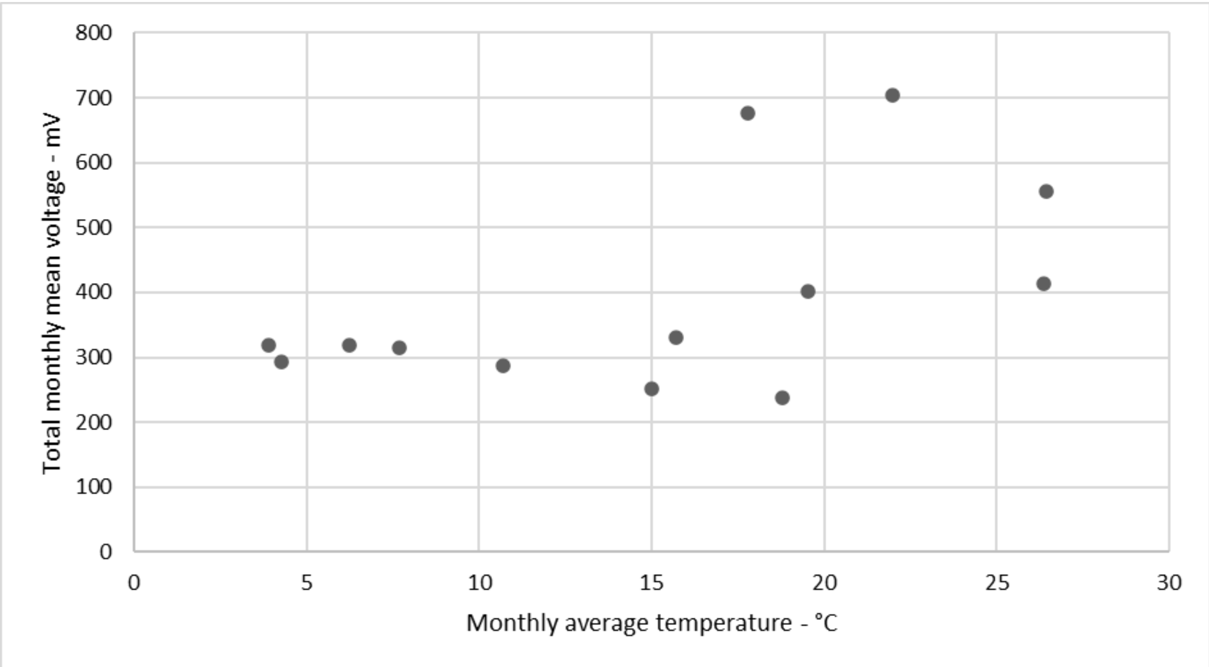

Figure 4.11. Scatterplot of monthly average temperature (°C) versus mean voltage (mV) generated by PMFCs, showing a statistically significant moderate positive monotonic relationship (Spearman's r_s = 0.56, p < 0.05).

Conclusions

Among the plant species analyzed, *Allium angulosum* showed the best outdoor electrical performance in PMFCs. This result is likely related to its botanical characteristics, particularly its root system architecture and life form, which appear to promote more favorable plant–microbe interactions in the rhizosphere. Overall, the findings suggest that it is reasonable to hypothesize that PMFC performance is significantly influenced by plant functional traits, including both life form and root architecture, in agreement with previous studies [14]. Other botanical traits could also play a role to explain the observed results, and are worthy of further investigation in this context.

Final electrode inspection suggests that preserving the integrity of the aluminium anode is more challenging in outdoor conditions, likely due to increased evaporation (where full immersion would otherwise maintain anoxia) and more variable microbial activity. In contrast, cathodes – operating under oxic conditions and directly exposed to water formation from bioelectrochemical reactions – are clearly prone to oxidation, potentially biasing the interpretation of bioelectrochemical performance. Within the proposed prototype, these limitations remain manageable, as maintenance and replacement of cathodic components are considerably simplified. Nonetheless, the use of non-oxidisable, highly conductive materials (e.g. stainless steel or graphite-based conductors), despite higher costs, should be considered a strategic investment to improve PMFC durability and reliability, ultimately supporting scalability.

However, the results also showed a limited operational lifespan under outdoor conditions. Based on the findings discussed in **Chapter 3**, this may be partly explained by the absence of a membrane in the MFC construction. Nonetheless, the reduced performance could also reflect seasonal climatic variability: the colder conditions of late autumn and winter may have suppressed microbial activity to a level from which the system was unable to recover, even when more favourable temperatures returned in spring.

These results highlight the importance of carefully selecting plant species for PMFC applications, especially under outdoor conditions. Beyond electrical performance, species selection should also account for ecological implications, as biodiversity represents a key component of sustainability. The use of invasive alien species in outdoor PMFC systems may compromise their overall sustainability, despite potential bioelectrochemical advantages.

In contrast, the use of native plant species offers multiple environmental benefits. Native plants are generally better adapted to local climatic and soil conditions, resulting in greater stability, resilience to local pests, and reduced requirements for pesticides, fertilizers, and irrigation. Their root systems often enhance drought tolerance and soil functioning, while their presence supports local ecosystems by providing habitat and resources for pollinators, birds, and other wildlife.

The integration of PMFCs into urbanized environments further strengthens the case for using native species. Increasing the richness, cover, or density of native plants in urban green spaces has been repeatedly associated with higher levels of animal biodiversity, suggesting that PMFC installations based on native vegetation could simultaneously contribute to renewable energy generation and urban biodiversity enhancement [22].

In conclusion, while non-native species may occasionally exhibit favorable electrical performance, their ecological risks must be carefully evaluated [14]. Sustainable outdoor PMFC applications should therefore prioritize native plant species that balance bioelectrochemical efficiency with biodiversity conservation and ecosystem sustainability.

References

[1] I. Rusyn, Y. Mittal, W. Apollon, Plant microbial fuel cells: An innovative path toward integrated food and energy production for a sustainable future, *Journal of Power Sources 656* (2025) 238068, https://doi.org/10.1016/j.jpowsour.2025.238068.

[2] S. R. Rahman, N. E. Eng, M. A. Ashraf, W. L. Pang, K. B. Tan, A. K. Singh, K. Y. Chan, Energy harvesting from living plant: A review on past research and way forward, *Energy Reports* 14 (2025): 268-281, https://doi.org/10.1016/j.egyr.2025.06.021.

[3] P. L. Chong, J. H. Chuah, C. O. Chow, P. K. Ng Plant microbial fuel cells: A comprehensive review of influential factors, innovative configurations, diverse applications, persistent challenges, and promising prospects, *International Journal of Green Energy*, 22(3) (2025) 599-648, https://doi.org/10.1080/15435075.2024.2421325.

[4] F.T. Kabutey, Q. Zhao, L. Wei, J. Ding, P. Antwi, F.K. Quashie, W. Wang, An overview of plant microbial fuel cells (PMFCs): configurations and applications, *Renew. Sustain. Energy Rev.* 110 (2019) 402–414, https://doi.org/10.1016/j.rser.2019.05.016.

[5] R. Nitisoravut, R. Regmi, Plant microbial fuel cells: a promising biosystems engineering, *Renew. Sustain. Energy Rev.* 76 (2017) 81–89, https://doi.org/10.1016/j.rser.2017.03.064.

[6] R. Regmi, Examining different classes of plants under various operating conditions for bioelectricity production. Plant microbial fuel cell [dissertation]. Thailand: Thammasat University (2017).
[7] J. Greenman, R. Thorn, N. Willey, I. Ieropoulos, Energy harvesting from plants using hybrid microbial fuel cells; potential applications and future exploitation, *Frontiers in Bioengineering and Biotechnology* 12 (2024), https://doi.org/10.3389/fbioe.2024.1276176
[8] S. Maddalwar, K.K. Nayak, M. Kumar, L. Singh, Plant microbial fuel cell: opportunities, challenges, and prospects, *Bioresour. Technol.* 341 (2021) 125772, https://doi.org/10.1016/j.biortech.2021.125772.
[9] R. Shaikh, A. Rizvi, M. Quraishi, S. Pandit, A.S. Mathuriya, P.K. Gupta, J. Singh, R. Prasad, Bioelectricity production using plant-microbial fuel cell: present state of art, *S. Afr. J. Bot.* 140 (2021) 393–408, https://doi.org/10.1016/j.sajb.2020.09.025.
[10] C. Raunkiær, The Life Forms of Plants and Statistical Plant Geography, Clarendon Press, Oxford (1934).
[11] R. Dewangan, R. Ghosh, M. Behera, A. Mandal, From waste to watts: performance assessment of upcycled aluminium electrodes in microbial fuel cells for treatment of domestic wastewater, *Sustainable Energy Technologies and Assessments* 83 (2025) 104676, https://doi.org/10.1016/j.seta.2025.104676.
[12] A. Andola, R. R. Pandey, H. Pandey, A. Prakash, R. K. Pandey, Waste-to-Energy Conversion via a Dual-Chamber Microbial Fuel Cell Using Recycled Aluminum Beverage Cans. *ACS Sustainable Resource Management* 179-188 (2025), https://doi.org/10.1021/acssusresmgt.5c00473?urlappend=%3Fref%3DPDF&jav=VoR&rel=cite-as.
[13] S. S. Mirza, M. M. Al-Ansari, M. Ali, S. Aslam, M. Akmal, L. Al-Humaid, A. Hussain, Towards sustainable wastewater treatment: Influence of iron, zinc and aluminum as anode in combination with salt bridge on microbial fuel cell performance, *Environmental research*, *209* (2022) 112781, https://doi.org/10.1016/j.envres.2022.112781.
[14] I. Brugellis, M. Grassi, P. Malcovati, S. Assini, Plant Microbial Fuel Cells in a botanical perspective: Nomenclatural constraints and new insights on plant traits potentially affecting bioelectrical performance, *Heliyon* 10(19) (2024), https://doi.org/10.1016/j.heliyon.2024.e38733.
[15] IPFI – index plantarum florae italicae. http://www.actaplantarum.org/, (2011), accessed 5 February 2026.

[16] S. Pignatti, R. Guarino, M. La Rosa, *Flora d'Italia* (2nd edition), Edagricole of New Business Media, Milan (2017).

[17] M. Giazzi, G. Peressutti, L. Cerri, M. Fumi, I. F. Riva, A. Chini, G. Ferrari, G. Cioni, G. Franch, G. Tartari, F. Galbiati, V. Condemi, A. Ceppi, Meteonetwork: an open crowdsourced weather data system, Atmosphere 13(6) (2022) 928, https://doi.org/10.3390/atmos13060928. Data obtained from the website https://www.meteonetwork.eu/it/weather-station/lmb346-stazione-meteorologica-di-zinasco-vecchio/archive (Accessed 16 February 2026).

[18] ARPA Lombardia. Catalogo di dati, metadati e banche dati 2024 [HYDSTRA - Banca dati delle serie temporali Idro-Nivo-Meteo per validazione e analisi dati – Stazione meteorologica 6699 di Pavia v. Folperti - Umidità relativa (%) dal 01/05/2024 al 31/12/2024], Unità Organizzativa ICT Sistemi Informativi e Transizione Digitale (2024), requested at https://www.arpalombardia.it/temi-ambientali/meteo-e-clima/form-richiesta-dati/ on 16 February 2026.

[19] ARPA Lombardia. Catalogo di dati, metadati e banche dati 2025 [HYDSTRA - Banca dati delle serie temporali Idro-Nivo-Meteo per validazione e analisi dati – Stazione meteorologica 6699 di Pavia v. Folperti - Umidità relativa (%) dal 01/01/2025 al 31/05/2025], Unità Organizzativa ICT Sistemi Informativi e Transizione Digitale (2025), requested at https://www.arpalombardia.it/temi-ambientali/meteo-e-clima/form-richiesta-dati/ on 16 February 2026.

[20] M. Turhan, B. Dai, D. Yildirim, Analytical MPPT solution using Thevenin approach for solar panels, in: Proc. Eurocon 2013, Zagreb, Croatia, 1–4 July 2013, 803–808.

[21] Ø. Hammer, D.A.T. Harper, P.D. Ryan, PAST: paleontological statistics software package for education and data analysis, *Palaeontol. Electron*. 4 (1) (2001) 9.

[22] K. Berthon, F. Thomas, S. Bekessy, The role of 'nativeness' in urban greening to support animal biodiversity, *Landscape and Urban Planning* 205 (2021) 103959, https://doi.org/10.1016/j.landurbplan.2020.103959.

Conclusions

This doctoral research demonstrates that the electrical performance of PMFCs is strongly influenced by a combination of biological, ecological, and engineering factors.

The literature review (**Chapter 1**) shows that PMFC performance is strongly shaped by plant life form and root system architecture. This work is the first to examine these relationships through a functional-trait lens. Hemicryptophytes and geophytes with adventitious (stoloniferous/rhizomatous) root systems appear particularly suitable for PMFC applications. Clear botanical identification — including full scientific names and authorship — is essential to ensure experimental reproducibility, as is the adoption of standardized metrics for reporting electrical performance.

Plant selection for PMFCs should also consider ecological implications, especially in outdoor applications. Biodiversity is a fundamental component of sustainability: even if PMFCs generate clean energy, their overall sustainability is undermined when invasive alien species are used.

Indoor experiments confirmed that system configuration plays a decisive role in determining PMFC electrical output.

Carbon pellet stratification had a marked impact on performance (**Chapter 2**): PMFCs with a single layer of carbon pellet consistently outperformed those with a double layer, showing higher voltage and power values as well as greater stability. This represents a promising result with practical implications, as the single-layer configuration is also more cost-effective and easier to assemble.

Regarding membrane inclusion within the cell stratification (**Chapter 3**) no statistically significant differences were detected. Nevertheless, PMFCs equipped with a membrane consistently showed higher values across all electrical parameters. This trend suggests that the presence of a membrane may enhance system performance—especially when combined with biological stimulation—although further investigation is needed to clarify its specific contribution.

Concerning electrodes condition at dismantling, the assessment revealed similar issues in the indoor (**Chapters 3**) compared with the outdoor environment (**Chapter 4**). The aluminium anode remained intact as long as anoxic conditions in the anodic chamber were maintained, trough proper and consistent irrigation, whilst outdoor conditions proved to be more unpredictable. The cathode, necessarily more exposed to degradation, may introduce bias when assessing performance, but this is an obstacle that can be overcome, given the design of the prototype presented, and the simplified maintenance requirements of the MFCs. Anyway non-oxidisable, highly conductive materials are worthy to be explored, as higher costs should be considered a strategic investment, with a view on scalability of PMFC technology and moving towars real worl applications.

The introduction of biological treatments highlighted complex interactions between nutrient availability, microbial metabolism, and electrochemical processes. While some treatments enhanced stability, others limited peak performance.

Unexpected outcomes were observed for the urea treatment (**Chapter 2**), suggesting the need to repeat the experiment using a less concentrated urea solution. In fact if in conventional agricultural practice, a moderate concentration of urea represents an efficient nitrogen source that promotes plant growth and vitality [1,2], an excessive concentration may lead to ammonia/ammonium toxicity, osmotic stress, and direct damage to root tissues [3]. Roots constitute the first site exposed to high local nitrogen concentrations following urea application, thus are particularly vulnerable. The excess of urea could cause variation in roots microbic communities, altered nutrient availability, and shift in ionic equilibrium in the rizosphere [2]. Under laboratory conditions, even greater care and caution are required, as urea remains confined within a self-contained system and is not subject to natural dispersion processes. These considerations highlight the importance of optimizing biological inputs and their application rates.

PMFCs treated with *Trichoderma asperellum* (**Chapter 3**) consistently outperformed the control systems, indicating that fungal inoculation is a valuable strategy for enhancing electrical activity and can be effectively employed as a biological performance booster. In particular, inoculation through the plant yielded stronger effects than direct inoculation into the cell, suggesting that plant–fungus interactions more effectively stimulate rhizosphere processes and electron transfer. This could be also due to the documented ability of the fungus to promote an increase in root biomass, and consequently the associated microbial activity. The combined plant inoculation and membrane configuration (TPM) achieved both higher electrical output and greater performance stability, underscoring the relevance of synergistic design choices.

Outdoor experimentation (**Chapter 4**) further demonstrated that PMFC performance is sensitive to plant species selection under real environmental conditions. Plant functional traits, particularly life form and root system architecture, emerge as worthwhile drivers of PMFC efficiency. Among the tested native species, *Allium angulosum* (bulbous, Geophyte) showed superior electrical performance, confirming that botanical traits are parameters to be taken into account for PMFC optimization. Several botanical traits may also have contributed to the observed results and therefore warrant further investigation, with a view to further exploring these aspects in the study of PMFCs. Importantly, the use of native species offers additional ecological benefits, including enhanced system resilience, reduced management requirements, and support for local biodiversity, reinforcing the sustainability of outdoor PMFC applications.

Although the whole study focuses on a limited set of electrochemical parameters, the findings refer to a completely new prototype and a novel setup. It is important to acknowledge that several environmental parameters – such as water quality characterization (e.g., COD, conductivity, pH, ORP, dissolved oxygen, and nitrogen speciation) – were not included in this study. These variables are typical in studies adopting a more conceptual research approach. However, the primary objective of this work was to evaluate the system from a product-oriented perspective, with a view toward future market deployment. In this context, the device is intended for use in real-life conditions by end users who may not have the means or expertise to monitor or control detailed environmental parameters. This is even more true when it comes to the lack of characterisation and activity assessment of the microbial component. Accordingly, the experimental design deliberately reflects a "real-world application" scenario. Similarly, some standard measurements commonly reported in the literature to comprehensively assess and benchmark microbial fuel cell performance – such as electrochemical impedance spectroscopy, polarization curves, and power density analyses – were not performed. As a consequence, direct comparison with results from other studies is more limited. Nevertheless, focusing on a reduced set of performance-oriented measurements enabled the implementation of a relatively high number of replicates, which were monitored on a weekly basis, thereby strengthening the robustness and reproducibility of the observed trends within the scope of this study. Several examples of operating PMFC prototypes supplying LED light strips and/or environmental monitoring sensors are provided in **Annex A**.

The aim was to assess the prototype's functionality under different conditions and establish an initial baseline for electrical performance. From an applied perspective, these findings indicate that optimizing PMFCs requires an integrated approach that combines biological additives, plant-mediated interactions, and appropriate physical configurations.

Overall, this work highlights the necessity of an interdisciplinary approach to PMFC development, integrating botany, plant ecology/physiology, microbiology, and electrochemical engineering. While PMFCs remain an emerging technology with limitations related to power density, scalability, and long-term durability, the findings of this research provide insights for improving system design and plant selection. By aligning bioelectrochemical performance with ecological sustainability, PMFCs hold promise as multifunctional systems capable of contributing to renewable energy production, environmental monitoring, and nature-based solutions for a more responsible and ecologically balanced progress.

References*

[1] S. Swify, R. Mažeika, J. Baltrusaitis, D. Drapanauskaitė, K. Barčauskaitė, Modified urea fertilizers and their effects on improving nitrogen use efficiency (NUE). *Sustainability*, *16*(1) (2023) 188, https://doi.org/10.3390/su16010188.

[2] M. Motasim, A. W. Samsuri, A. Nabayi, A. Akter, M. A. Haque, A. S. Abdul Sukor, A. M. Adibah, Urea application in soil: Processes, losses, and alternatives—A review. *Discover Agriculture*, *2*(1) (2024) 42, https://doi.org/10.1007/s44279-024-00060-z.

[3] W. L. Pan, I. J. Madsen, R. P. Bolton, L. Graves, T. Sistrunk, Ammonia/ammonium toxicity root symptoms induced by inorganic and organic fertilizers and placement. *Agronomy Journal*, *108*(6) (2016) 2485-2492, https://doi.org/10.2134/agronj2016.02.0122.

*These references are newly cited in this Conclusions section.

Data availability statement

The data supporting the findings of this thesis include proprietary information originally owned in part by Volta Plant Srl (University of Pavia spin-off company). Due to confidentiality restrictions and the nature of the datasets, the data are not publicly available in an open repository.

However, data may be made available by the author (corresponding author of the related publications) upon reasonable request, subject to a case-by-case evaluation of any persisting legal or technical constraints.

Appendix A

Novel Prototype Design, MFCs assembly, Demonstration Setups and Presentation of the Prototype at Events

This Appendix provides a technical description of the Novel PMFC prototype and MFC assembly. This is intended in a general way, in fact the specific configurations have been described in detail in the relevant chapters of this thesis, according to each experimental activity.

A chronological report is also provided, together with photographic documentation of optimized configurations developed for public demonstrations, events, and outdoor trials.

The minimum target values of bioelectrochemical energy needed by a PMFC to power the devices we tested were above 600 mV for tension and above 0.600 mA for current. Therefore, only MFCs meeting or exceeding these thresholds were used in the presented configurations.

Novel Prototype of PMFC and MFC construction

The new PMFC prototype was developed at the Flora, Vegetation and Ecosystem Services Laboratory of the University of Pavia (Scientific Coordinator Silvia Assini). The plant is hosted in an upper pot, while drainage water percolates into a lower container housing the MFC (**Figure A1**).

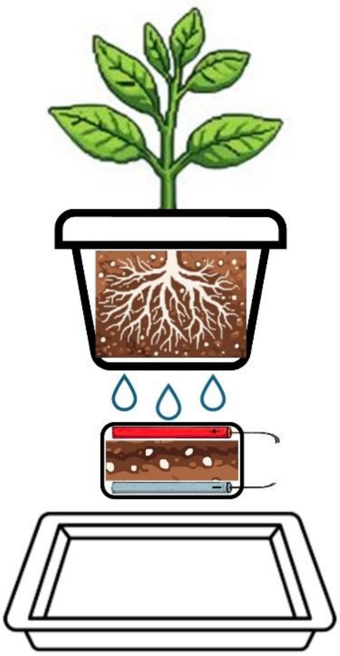

Figure A1. Schematic representation of the novel Plant Microbial Fuel Cell prototype.

Each MFC was composed by: a junction box, aluminum foil anode, soil, non wowen fabric (when required by the experimental configuration), carbon felt cathode, carbon pellet (when required by the experimental configuration) (**Figure A2**). A complete MFC is illustrated in **Figure A3**.

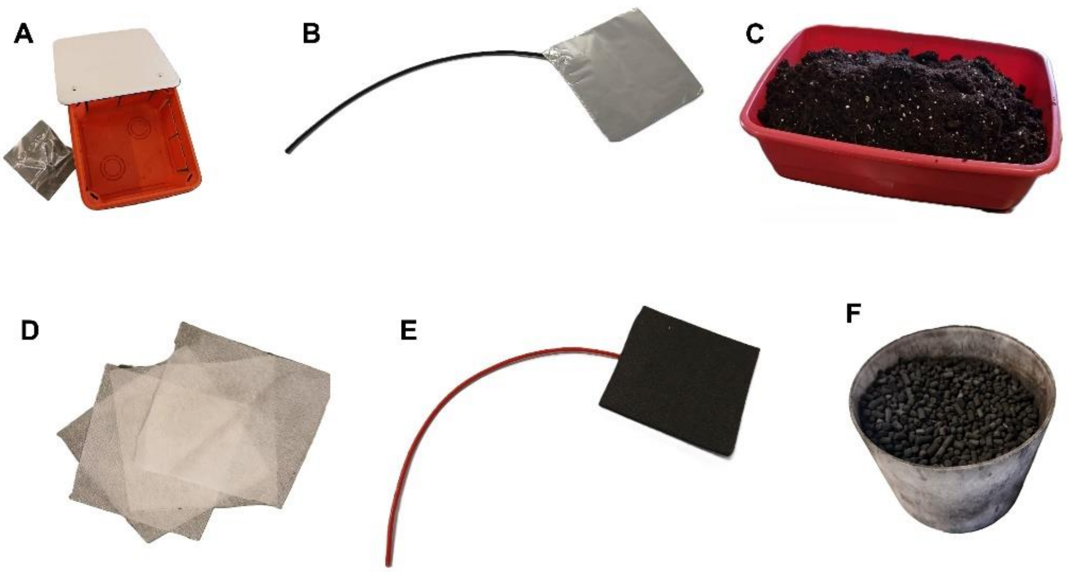

Figure A2. MFCs components: A = junction box, B = aluminum foil anode, C = all-purpose soil, D = non-woven fabric, E= carbon felt cathode, F= carbon pellets.

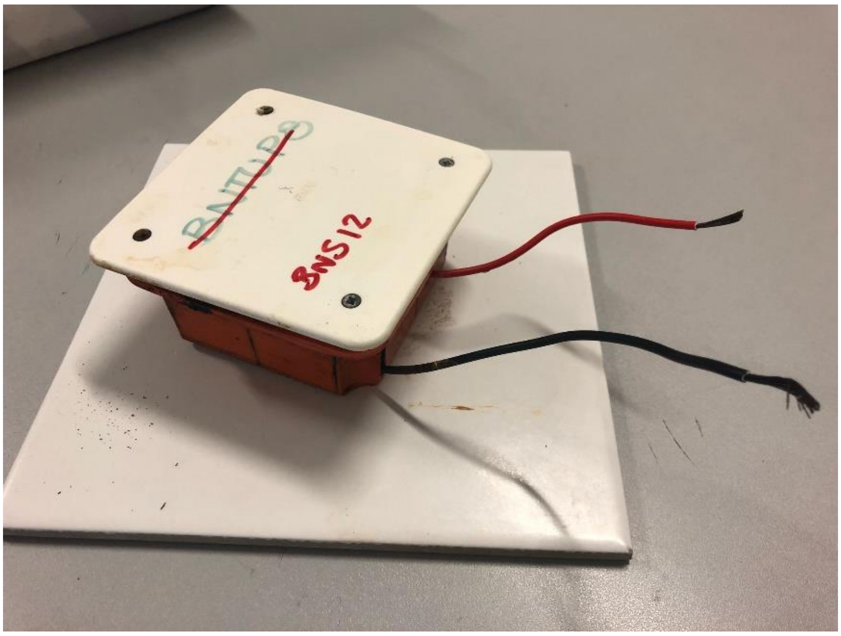

Figure A3. A complete MFC ready to be tested.

December 2022 - Indoor PMFC prototype powering LED light strips

The first indoor PMFC prototype was assembled to power LED light strips. The electrical circuit was soldered to a LED strip (**Figure A4**).

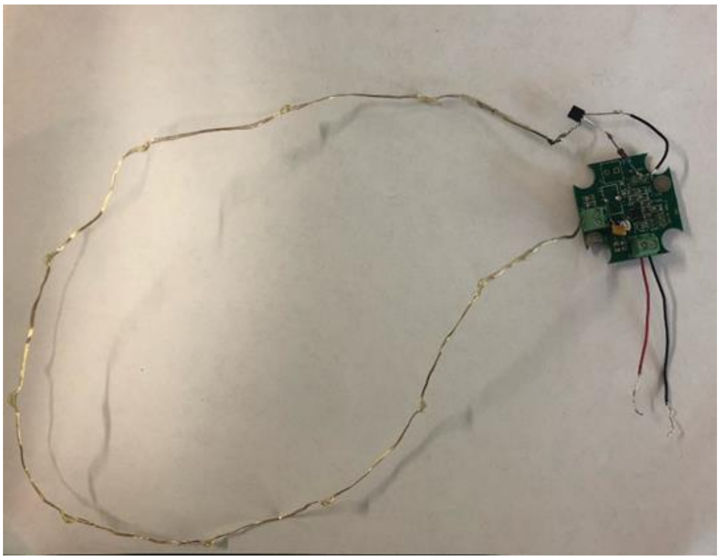

Figure A4. LED strip soldered to the circuit board.

MFCs that met the required electrical performance thresholds were integrated with the electronic component, resulting in functional prototypes (**Figure A5**). The plant species used were *Spathiphyllum lanceifolium* (Jacq.) Schott, *Peperomia caperata* Yunck., *Peperomia albovittata* C.DC.

Figure A5. First demonstration prototype of PMFCs powering LED light strips.

April 2023 - PMFC Prototype for Outdoor Testing

A first PMFC prototype for outdoor trials was assembled as a preliminary field-testing system. The external structure consisted of a square cultivation pot (22 × 22 × 26 cm) (**Fig. A6.a**), filled with coarse gravel (**Fig. A6.b**) to facilitate drainage.

a) **b)**

Figure A6. a) External cultivation pot; **b)** Internal coarse gravel layer.

An internal square pot (13 × 13 × 13 cm), housing the PMFC system (MFC and plant pot), was perforated on all four sides at approximately 2.5 cm from the base (**Figure A7.a**). This configuration allows water to be maintained at an appropriate level, ensuring anodic anoxic conditions. Two additional upper holes allowed the passage of the MFC electrode cables (**Figure A7.b**).

At this stage, the electronic component, consisting of a circuit board, with its wires, and the connected LED light, was assembled inside a junction box (8 × 8 × 4 cm) (**Figure A8.a**). The LED strip was soldered after positioning the circuit board inside the junction box and the wires were routed through the pre-drilled openings. The junction box was then closed and sealed using insulating and duct tape (**Figure A8.b**) to ensure protection against moisture and mechanical stress.

a) 

b) 

Figure A7. a) Internal pot perforated near the base; **b)** MFC with the electrodes cables passing through the holes of the internal pot, placed in the larger pot.

a) 

b) 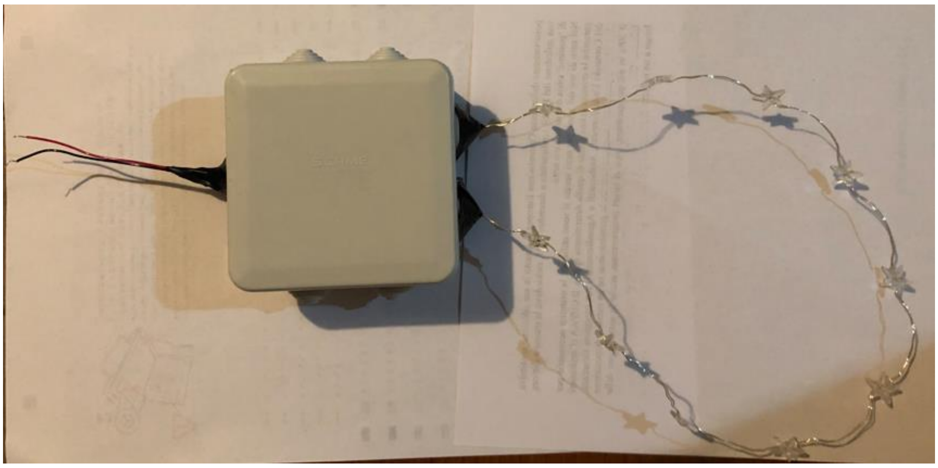

Figure A8. a) Circuit board inside the junction box: wires and LED strip coming out of the sides; **b)** closed and sealed with tape junction box, ready to be assembled to the prototype.

The circuit wires were connected to the MFC electrodes, and the electronic assembly was placed inside the external pot. The upper part of the system was sealed with duct tape (**Figure A9.a**) keeping only the LED strip on the outside. The system was then ready for burial and completed with a *Campanula portenschlagiana* Schult. plant on the top (**Figure A9.b**).

a) b)

Figure A9. a) Sealed system prior to burial; **b**) PMFC system installed in the field with *Campanula portenschlagiana*.

Overall, the prototype proved suitable for experimental use, particularly considering the simplicity and low cost of the materials employed.

A critical limitation concerns the LED strip, which, although effective in visually demonstrating the functionality of the system, it was very delicate in terms of electrical contacts. Consequently, once the system was sealed and buried, even minor malfunctions require full excavation for inspection and repair.

A potential improvement would be the implementation of a removable top-access compartment or a drawer specifically dedicated to housing the electronic components, allowing easier maintenance without dismantling the entire system.

September 24th 2023 - NODES Interactive Exhibition, Pavia Agrifood Day, Botanical Garden, University of Pavia.

The NODES Interactive Exhibition was hosted during Pavia Agrifood Day 2023 organised by the University of Pavia in the Botanical Garden. In this context, two PMFCs prototypes powering LED lights and one PMFC prototype powering a Sensirion SHT31 temperature and humidity sensor (connected to the MyAmbience app) were presented. Plant species used included *Cyclamen hederifolium* Aiton, *Peperomia albovittata*, *Epipremnum aureum* (Linden & André) G.S.Bunting (**Figure A10**). A digital multimeter was used to verify PMFCs energy delivery (**Figure A11**).

Figure A10. Demonstration at the Botanical Garden stand.

Figure A11. Monitoring energy output during sensor activation.

September 29th 2023 - European Night of Researchers – Sharper Night, University of Pavia.

In the context of the European Night of Researchers 2023, two PMFCs prototype powering LED lights with *Cyclamen hederifolium* plants, were presented.

To support the educational objectives of the event, a simple demonstration of the working principle of a voltaic cell was also provided, illustrating the basic mechanism underlying PMFC operation.

Participants assembled a Volta-type pile using copper coins and wetted aluminium foil. A digital multimeter was used to measure the output of the assembled system (**Figure A12**).

Figure A12. PMFC prototypes and Volta pile educational activity.

September 29th – October 2nd 2023 - *Autunno Pavese*, PalaExpo, Pavia.

The *Autunno Pavese* is a seasonal fair focused on local agri-food production, wine, and regional supply chains, involving producers, institutions, and the general public. In this context, two PMFC prototypes powering LED lights and one PMFC prototype powering a Sensirion SHT31 temperature and humidity sensor, connected to the MyAmbience app, were presented. Plant species used included *Cyclamen hederifolium* and *Epipremnum aureum* (**Figure A13**).

The sensor was connected to the PMFCs through a circuit (**Figure A14**) equipped with a capacitor, enabling it to be switched on (**Figure A15**) and remain lit for around 40 minutes.

Figure A13. PMFCs prototypes demonstration stand.

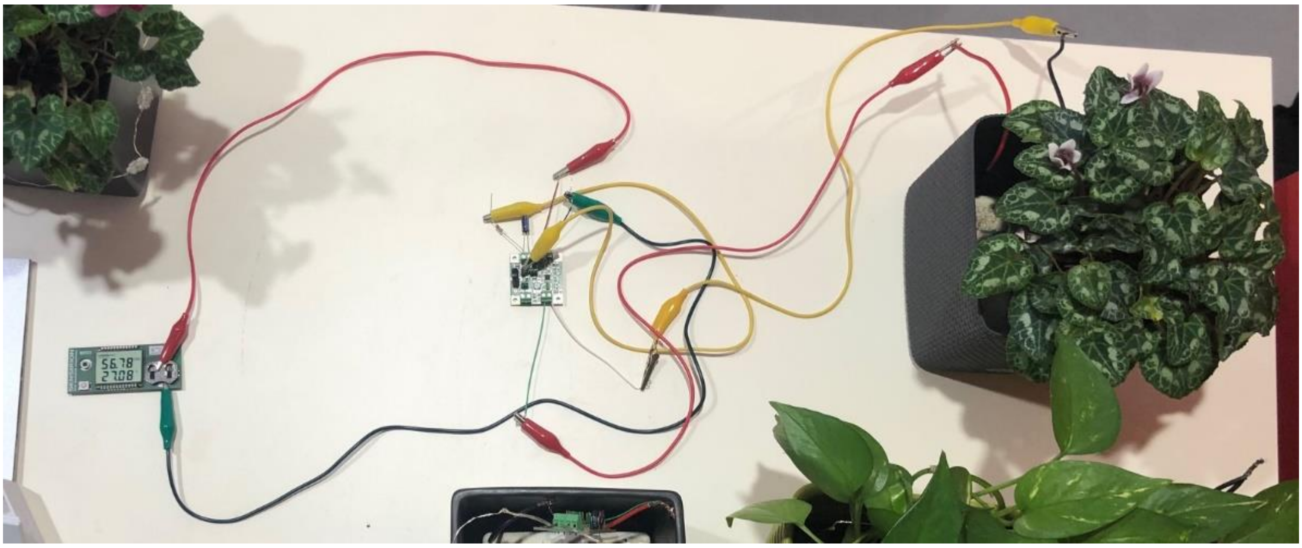

Figure A14. PMFC powering environmental sensor via the circuit system.

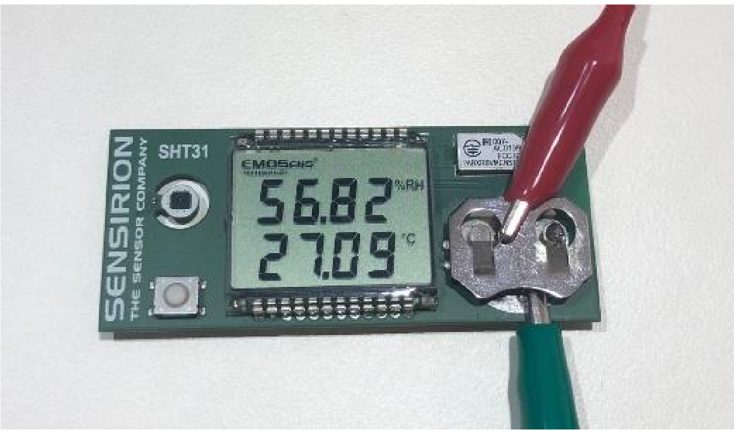

Figure A15. Sensirion SHT31 sensor operating under PMFC supply.

September 27th 2024 - European Night of Researchers - Sharper Night, University of Pavia.

Within the NODES project, during the European Night of Researchers 2024, a PMFC prototype powering simultaneously a temperature and humidity sensor and LED lights was presented (**Figure A16**). This configuration included two additional circuit systems compared to previous setups. The sensor was a Sensirion SHT4x, connected to the MyAmbience app. Plant species included *Cyclamen hederifolium* and *Carex oshimensis* "Evergold" (cultivar) (**Figure A17**).

Figure A16. Presentation within NODES project at Sharper Night 2024.

Figure A17. PMFC prototype powering LED lights and the environmental sensor simultaneously. The sensor is connected to the MyAmbience app, visible on the mobile screen.

February 2025 – Assembly of the Ultimate PMFC Prototype

Within the NODES funding framework, two 3D-printed prototypes were produced using bioplastic derived from coffee grounds and maize. The design was inspired by previous demonstration prototypes and optimized for indoor operation and improved aesthetics.

The prototype includes a base housing the MFC and collecting drainage water (**Figure A18**). Above it, there was the compartment housing the electronic components (**Figure A19**) subsequently sealed to ensure protection from leachate.

The system was designed to allow a single PMFC to power both a Sensirion SHT4x environmental sensor and an LED strip simultaneously. This was achieved through the integration of a switch circuit and a flasher circuit, alongside the existing boost circuit (**Figure A20**).

The plant pot was shaped like a twisted trapezium (**Figure A21**), and once placed on top of the outer cover cube, it will hang above the base of the prototype. The final configuration (**Figure A22**) allows a glimpse of the "drop" of percolating water falling onto the MFC to nourish it, and of the LED light, which will remain inside the cube; the sensor display should remain externally visible, for environmental monitoring. Plant species used was *Spathiphyllum lanceifolium*.

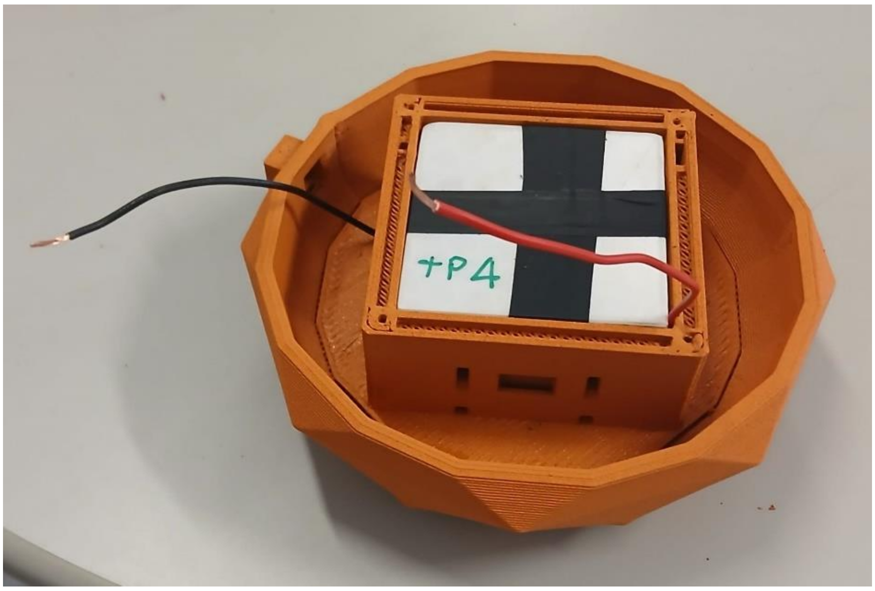

Figure A18. Prototype base housing a MFC. The design is inspired by geodesic geometry.

Figure A19. Compartment above the MFC, to be fitted with the electronic component.

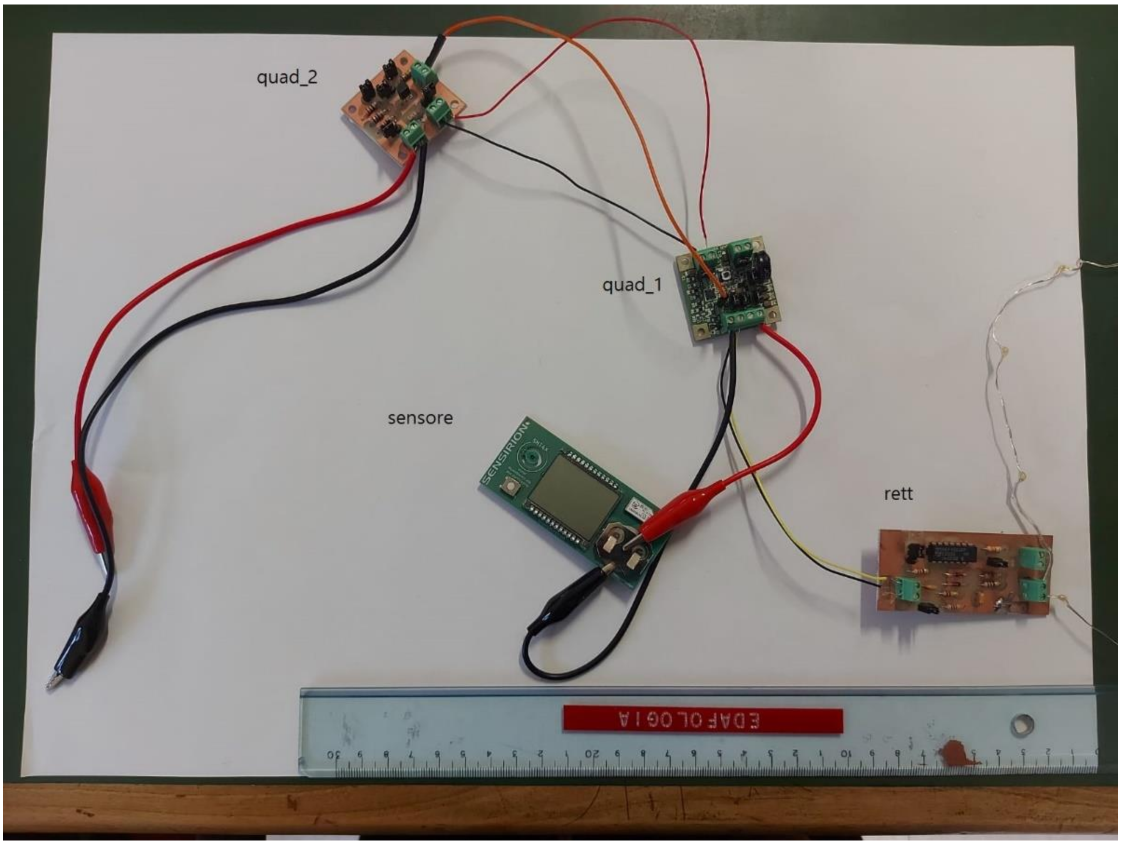

Figure A20. Electronic circuit components. From the left: quad_2 = boost circuit; quad_1 = switch circuit; sensore = sensor Sensirion SHT4x; rett = flasher circuit connected to the LED strip.

Figure A21. Twisted trapezoidal plant pot.

Figure A22. Ultimate PMFC prototype.

April 4th 2025 - NODES ROADSHOW, University of Pavia.

The NODES Roadshow is an event showcasing research, innovation, and projects developed within the NODES ecosystem. It connects universities, companies, and local stakeholders to promote collaboration.

Two PMFC prototypes were presented (**Figure A23**): the ultimate PMFC prototype with LED lighting and a previous PMFC version combining LED lighting and environmental monitoring with the Sensirion SHT4x sensor. Plant species used were *Spathiphyllum lanceifolium* and *Campanula portenschlagiana*.

The event provided an opportunity to demonstrate the potential of this technology to academics, stakeholders, businesses and governmental representatives (**Figures A24-A26**).

Figure A23. PMFC stand at NODES Roadshow Pavia 2025.

Figure A24. Illustrating PMFC operation to industry representatives.

Figure A25. Explaining how a PMFC works to the *Rector Emeritus* Francesco Svelto.

Figure A26. Showing the MyAmbience app (connected to the sensor supplied by the PMFC) to the Senator Gian Marco Centinaio.

Annex I

Photo credits, licences and links

Carex remota **L. photo credit – Table 4.1 (Chapter 4**, page 108)

Author: Krzysztof Ziarnek, Kenraiz, CC BY-SA 4.0 via Wikimedia Commons

Licence URL: https://creativecommons.org/licenses/by-sa/4.0 (accessed 5 February 2026)

Page URL: https://commons.wikimedia.org/wiki/File:Carex_remota_kz07.jpg (accessed 5 February 2026)

File URL: https://upload.wikimedia.org/wikipedia/commons/d/d1/Carex_remota_kz07.jpg (accessed 5 February 2026)

Lythrum salicaria **L. photo credit – Table 4.2 (Chapter 4**, page 108)

Author: H. Zell, CC BY-SA 3.0, via Wikimedia Commons

Licence URL: https://creativecommons.org/licenses/by-sa/3.0 (accessed 6 February 2026)

Page URL: https://commons.wikimedia.org/wiki/File:Lythrum_salicaria_001.JPG (accessed 6 February 2026)

File URL: https://upload.wikimedia.org/wikipedia/commons/f/fe/Lythrum_salicaria_001.JPG (accessed 6 February 2026)

Allium angulosum **L. photo credit – Table 4.3 (Chapter 4**, page 109)

Author: Magnus Manske, CC BY-SA 2.5, via Wikimedia Commons

Licence URL: https://creativecommons.org/licenses/by-sa/2.5 (accessed 6 February 2026)

Page URL:
https://commons.wikimedia.org/wiki/File:Allium_angulosum_(Alliaceae)_plant.JPG (accessed 6 February 2026)

File URL:
https://upload.wikimedia.org/wikipedia/commons/7/77/Allium_angulosum_%28Alliaceae%29_plant.JPG (accessed 6 February 2026)

Affiliation of coauthors

Silvia ASSINI
Department of Earth and Environmental Science, University of Pavia, Via Sant'Epifanio 14, 27100 Pavia, Italy.
Botanical Garden, University of Pavia, 27100 Pavia, Italy.
silviapaola.assini@unipv.it

Ilaria BRUGELLIS
Department of Earth and Environmental Science, University of Pavia, Via Sant'Epifanio 14, 27100 Pavia, Italy.
ilaria.brugellis01@universitadipavia.it

Cinzia CALVIO
Department of Biology and Biotechnology, University of Pavia, Via A. Ferrata 9, 27100 Pavia, Italy.
cinzia.calvio@unipv.it

Marco GRASSI
Department of Electrical Computer and Biomedical Engineering, University of Pavia, Via A. Ferrata 5, 27100 Pavia, Italy.
marco.grassi@unipv.it

Mariam MAHMOUD
mariam.mahmoud01@universitadipavia.it

Piero MALCOVATI
Department of Electrical Computer and Biomedical Engineering, University of Pavia, Via A. Ferrata 5, 27100 Pavia, Italy.
piero.malcovati@unipv.it

Solveig TOSI
National Biodiversity Future Center, Piazza Marina 61, 90133, Palermo, Italy.
Mycology Laboratory, Department of Earth and Environmental Sciences, University of Pavia, via Sant'Epifanio 14, 27100, Pavia, Italy
solveig.tosi@unipv.it

List of publications

Scientific articles on peer-reviewed journals related to this thesis

- **I. Brugellis**, M. Grassi, P. Malcovati, S. Assini, Plant Microbial Fuel Cells in a botanical perspective: Nomenclatural constraints and new insights on plant traits potentially affecting bioelectrical performance, Heliyon 10(19) (2024), https://doi.org/10.1016/j.heliyon.2024.e38733.
- **I. Brugellis**, M Grassi, P. Malcovati, S. Assini, Evaluating a New Prototype of Plant Microbial Fuel Cell: Is the Electrical Performance Affected by Carbon Pellet Layering and Urea Treatment?, Energies 2025 (18) (2025) 5320, https://doi.org/10.3390/en18195320.

Scientific articles on peer-reviewed journals not related to this thesis

- S. Assini, **I. Brugellis**, J. Nascimbene, M. Barcella, A. Gressani, G. Gheza, Dry grasslands of central-western Po Plain (Italy): implications under Council Directive 92/43/EEC, Plant Sociology, 61 (2024) 1-20, https://doi.org/10.3897/pls2024612/01.
- S. Assini, A. Gressani, M. Barcella, A. Bacchetta, **I. Brugellis**, G. Tarzariol, J. Nascimbene, G. Gheza, Employing plant translocations to restore open dry acidic habitats in European Continental lowlands: A case study in northern Italy, Journal for Nature Conservation 81 (2024) 126682, https://doi.org/10.1016/j.jnc.2024.126682.
- F. Bartolucci, G. Domina, M. Adorni, S. Assini, **I. Brugellis**, G. Buccomino, F. Carruggio, F. Conti, E. Costanzo, E. Del Guacchio, F. Falcinelli, F. Festi, L. Fontanabona, L. Forte, P. Fortini, G. Galasso, E. Genduso, L. Ghillani, G. Gottschlich, D. Iamonico, V.L.A. Laface, M. Lonati, F. Mascia, G. Mei, G. Nota, P. Palazzolo, G. Pazienza, G. Pellegrino, G. Potenza, L. Quaranta, E. Repetto, L. Rosati, F. Santi, G. Secci, G.N. Silletti, A. Stinca, G. Tavilla, V. Tomaselli, G. Tondi, L. Lastrucci, Notulae to the Italian native vascular flora: 16. Italian Botanist 16(1) (2023) 89-103, https://doi.org/10.3897/italianbotanist.16.114657.

Presentations at congresses

- **I. Brugellis**, M. Grassi, P. Malcovati, S. Assini, Enhancing the Potential of Plant Microbial Fuel Cells: The Influence of Botanical Characteristics on Bioelectrical Performance, in Abstract Book, The 3rd International Electronic Conference on Plant Sciences, Online, 15-17 January 2024, p. 147, Poster presentation, https://sciforum.net/paper/view/16787.
- **I. Brugellis**, M. Grassi, P. Malcovati, S. Assini, Deepening plant microbial fuel cells' roots: plant nomenclature, and how life forms and root architecture affect bioelectrical performances, in Abstract Book, *118° Congresso della Società Botanica Italiana* - IX International Plant Science Conference (IPSC) Pisa, 13 - 16 September 2023, p. 109, Poster presentation.

Proceedings of congresses

- G. Gheza, M. Barcella, **I. Brugellis**, A. Chiarucci, F. Della Rocca, L. Di Nuzzo, A. Gressani, F. Santi, C. Vallese, J. Nascimbene, S. Assini, Plants, cryptogams and insects reveal the effectiveness of the LIFE DRYLANDS project in restoring lowland acidic dry grasslands. 19th Eurasian Grassland Conference, Bolzano, 26 August – 1 September 2024 (Book of abstract), https://www.egc2024.it/en/program.
- M. Barcella, G. Gheza, J. Nascimbene, **I. Brugellis**, A. Gressani, C. Vallese, S. Assini, Restoration of dry-acidic Continental grasslands and heathlands in Natura 2000 sites in Piemonte and Lombardia: Preliminary results of the LIFE Drylands project. In: Book of Abstracts, 57th International Congress Italian Society of Vegetation Science (*Società Italiana di Scienza della Vegetazione*), University of Venice, Venezia, 6-7 June 2024, p. 4, https://www.scienzadellavegetazione.it/wp-content/uploads/2024/03/Book-of-Abstracts-57th-SISV-International-Congress.pdf.

Acknowledgements

I would like to express my sincere gratitude to Professor Silvia Assini, a trusting mentor whose guidance has been a fundamental point of reference for me. She consistently provided reassuring and concrete direction, even in the most complex moments, helping me transform difficulties into manageable steps through clear and effective guidance.

I would also like to thank Professor Marco Grassi, with whom it has been a true pleasure to collaborate. Through our work together, I had the opportunity to learn and explore topics that were entirely new to me, and from the very beginning we established a relationship grounded in mutual respect and strong cooperation.

My thanks go to Matteo Barcella and Alessia Gressani for the consistently enriching and inspiring conversations during breaks from work, and to everyone who has been part of the Laboratory of Flora, Vegetation and Ecosystem Services over the past three years.

I would like to thank my colleague Alice Fossati for her friendship, support, and the many meaningful moments we have shared over these three years; Professor Emanuela Martino, Valeria Cavalloro, and all the collaborators of the Extractions from Plant Matrices and Medicinal Plants Laboratory.

I would also like to thank Giulia Tarzariol, Professor Paola Nola, and all the members of the Dendrochronology and Dendroecology Laboratory, with whom I had the pleasure of collaborating during the tutoring activities for the *Botanica Generale* course.

My sincere thanks are equally due to Professor Solveig Tosi and the teams of the Laboratories Mushrooms for Agri-environment and Industry and Fungal Diversity and Systematics, with whom I collaborated fruitfully both in tutoring the *Botanica Sistematica* course and in carrying out an innovative experimental project that would otherwise not have been possible.

A particularly heartfelt acknowledgement goes to Raffaele Vitolo, Roberto Galleran, Costanza Marini, and all my colleagues from *Associazione Dottorandi Italiani* in Pavia and at the national level. The *Associazione Dottorandi Italiani* has been a profoundly meaningful and formative experience for me, placing me in direct contact with scholars from across disciplines and making me feel part of a large community of dedicated individuals who work not only to deepen their own fields of study, but above all to pursue shared goals within the complex socio-political context we are living in.

From the bottom of my heart, I thank my friends Viviana, Adele, Ambra and Marco.

Finally, I am deeply grateful to my entire family.